AD-A033 912 DAVID W TAYLOR NAVAL SHIP RESEARCH AND DEVELOPMENT CE--ETC F/G 20/4
THEORETICAL PREDICTION OF MOTION OF SMALL-WATERPLANE-AREA, TWIN--ETC(U)
DEC 76 C M LEE
UNCLASSIFIED DTNSRDC-76-0046 NL

1 OF 1
ADA033912

END
DATE FILMED
2 -77

UNCLASSIFIED

SECURITY CLASSIFICATION OF THIS PAGE (When Data Entered)

REPORT DOCUMENTATION PAGE

READ INSTRUCTIONS BEFORE COMPLETING FORM

1. REPORT NUMBER: DTNSRDC-76-0046
2. GOVT ACCESSION NO.
3. RECIPIENT'S CATALOG NUMBER
4. TITLE (and Subtitle): THEORETICAL PREDICTION OF MOTION OF SMALL-WATERPLANE-AREA, TWIN-HULL (SWATH) SHIPS IN WAVES
5. TYPE OF REPORT & PERIOD COVERED: F43412
6. PERFORMING ORG. REPORT NUMBER
7. AUTHOR(s): C. M. Lee
8. CONTRACT OR GRANT NUMBER(s): SF4341202
9. PERFORMING ORGANIZATION NAME AND ADDRESS: David W. Taylor Naval Ship Research and Development Center, Bethesda, Maryland 20084
10. PROGRAM ELEMENT, PROJECT, TASK AREA & WORK UNIT NUMBERS: (See reverse side)
11. CONTROLLING OFFICE NAME AND ADDRESS
12. REPORT DATE: December 1976
13. NUMBER OF PAGES: 90
14. MONITORING AGENCY NAME & ADDRESS (if different from Controlling Office): Research and development rept.
15. SECURITY CLASS. (of this report): UNCLASSIFIED
15a. DECLASSIFICATION/DOWNGRADING SCHEDULE

16. DISTRIBUTION STATEMENT (of this Report)

APPROVED FOR PUBLIC RELEASE: DISTRIBUTION UNLIMITED

88p.

17. DISTRIBUTION STATEMENT (of the abstract entered in Block 20, if different from Report)

18. SUPPLEMENTARY NOTES

19. KEY WORDS (Continue on reverse side if necessary and identify by block number)

Small-Waterplane-Area, Twin-Hull Ships
Ship Motion in Waves
Viscous Damping
Stabilizing Fins
Strip Theory

20. ABSTRACT (Continue on reverse side if necessary and identify by block number)

Linear equations of motion with the hydrodynamic coefficients approximated by strip method are used to obtain the motion of small-waterplane-area, twin-hull (SWATH) ships in regular and irregular waves. The couplings among different modes of motion are separated into three independent groups; surge, heave-pitch and sway-roll-yaw, and the resulting equations of motions are treated in the frequency domain.

(Continued on reverse side)

DD FORM 1 JAN 73 1473 EDITION OF 1 NOV 65 IS OBSOLETE
S/N 0102-014-6601

UNCLASSIFIED

SECURITY CLASSIFICATION OF THIS PAGE (When Data Entered)

387682 LB

(Block 10)

Task Area SF 43 412 02
Task 18247
Work Unit 1-1560-014

(Block 20 continued)

The hydrodynamic coefficients of predominantly nonviscous nature, added mass and wavemaking damping, are obtained by strip theory. The effects of wave diffraction, viscous damping, and stationary stabilizing fins are included in the equations of motion within the frame work of the linear frequency response of a body to waves. The assumptions involved in the evaluation of various hydrodynamic coefficients in the equation of motion are specified.

The validity of the theoretical prediction of motion is checked by correlating with the existing model experimental results, and the relevant discussions are made. In general, the theoretical prediction is found satisfactory except the case of near zero-encounter frequency which can occur when a ship cruises with certain speed in stern-quartering waves. A future effort for improvement of the theoretical prediction of SWATH ship motion in stern-quartering waves is recommended.

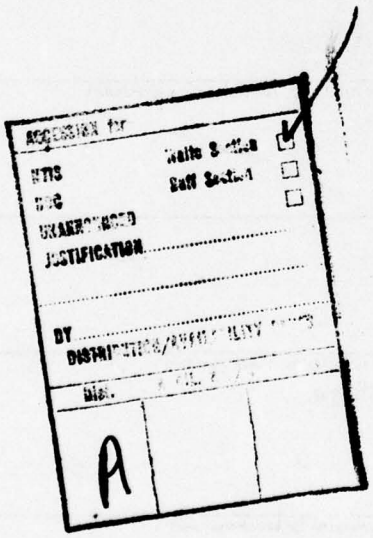

TABLE OF CONTENTS

LIST OF FIGURES

LIST OF TABLES

NOTATION

A	Amplitude of incident wave
A_i	Projected surface area of a pair of the ith fin
A_w	Waterplane area of ship
A_{ik}	Added mass coefficients in the ith mode due to the motion in the kth mode
a_o	Viscous lift coefficient
$a_{ii}(x)$	Sectional added mass in the ith mode
$a_{33_i}^{(f)}$	Heave added mass of a pair of the ith fins
$B_m(x)$	Maximum breadth of a cross section of one hull
B_{ik}	Damping coefficient in the ith mode due to the motion in the kth mode
$b(x)$	Horizontal distance between the midpoint of the beam of two hulls and the midpoint of the beam of one hull of a cross section
$b_{\ell i}$	Transverse distance from the x-axis to the midspan of the ith fin
$b_{ii}(x)$	Sectional damping in the ith mode
C_D	Cross-flow drag coefficient
$C_{Di}^{(f)}$	Cross-flow drag coefficient of the ith fin
C_{ik}	Restoring coefficient in the ith mode due to the motion in the ith mode
$C_{L\alpha i}$	Lift-curve slope per radian of the ith fin
$d(x)$	Draft of a cross section
$d_1(x)$	Depth of the maximum breadth point of a cross section
$d_2(x)$	$1/2\ d(x)$
$F_i^{(e)}$	Wave-exciting force (or moment) in the ith mode
$F_1^{(FK)}$	Froude-Krylov wave-exciting surge force
g	Gravitation acceleration
I_i	Mass moment of inertia about the ith mode axis for i = 4, 5, 6
Im_j	Imaginary part of complex function associated with j
I_{wi}	Waterplane area moment of inertia about the ith mode axis for i = 4, 5

$j = \sqrt{-1}$	Imaginary unit
$K_o = \frac{2\pi}{\lambda}$	Incident wave number (ω_o^2/g)
ℓ_i	x-coordinate of the quarter-chord point of the ith fin
M	Mass of ship
M_w	Waterplane area moment about the pitch axis
$m_i^{(f)}$	Mass of a pair of the ith fin
$\underline{N}$	Unit normal vector on the immersed contour in a cross section plane
$\underline{n}$	*Three dimensional unit normal vector pointing into the body surface*
(n_1, n_2, n_3)	Components of $\underline{n}$ in (x, y, z) directions
(n_4, n_5, n_6)	Components of $\underline{R} \times \underline{n}$ in (x, y, z) directions where $\underline{R}$ is the position vector
Oxyz	Right-handed cartesian coordinate system (see p. 5 for definition)
Re_j	Real part of complex function the imaginary part of which is associated with j
$S(\omega_o)$	Sea-energy spectrum
U	Forward velocity of ship
$\dot{y}_{1p(s)}(x)$	y-component of relative fluid velocity with respect to body at the one-half draft point on the port (starboard) side of hull at a cross section
$\dot{y}_{1o}$	$\lvert \dot{y}_{1p} \rvert + \lvert \dot{y}_{1s} \rvert$
$\dot{z}_{1p(s)}(x)$	z-component of relative fluid velocity with respect to body at the maximum breadth point of the port (starboard) side of hull at a cross section
$\dot{z}_{1o}$	$\lvert \dot{z}_{1p} \rvert + \lvert \dot{z}_{1s} \rvert$
$\dot{z}_{po(so)}$	z-component of relative fluid velocity with respect to a fin on the port (starboard) side
$\dot{z}_{rp(s)}(x)$	z-component of relative fluid velocity with respect to the body in roll motion at the maximum breadth point of the port (starboard) side of hull at a cross section
$\dot{z}_{ro}$	$\lvert \dot{z}_{rp} \rvert + \lvert \dot{z}_{rs} \rvert$
$\dot{z}_{po(so)}^{(R)}$	z-component of relative fluid velocity with respect to a fin on the port (starboard) side due to roll motion in waves
α	Trim angle

α_i	Phase angle of the ith mode motion with respect to the wave crest above the center of gravity of ship
β	Heading angle of incident wave with respect to the x-axis ($\beta = 0$ is the following wave and $\beta = \pi$ is the head wave)
ζ_o	Complex amplitude of incident waves
$\dot{\zeta}_{V(H)}$	Complex amplitude of vertical (horizontal) velocity of fluid induced by incident wave
η	Yaw angle
λ	Length of incident wave
$\xi_i(\dot{\xi}_i, \ddot{\xi}_i)$	Displacement (velocity, acceleration) of ship in the ith mode from its mean position; i = 1 for surge, 2 for sway, 3 for heave, 4 for roll, 5 for pitch, and 6 for yaw
ξ_{io}	Complex amplitude of ξ_i, i.e. ξ_i = Real part of $(\xi_{io} e^{-j\omega t})$, $\xi_{io} = \xi_{ic} + j\xi_{is}$
$\bar{\xi}_i^2 = \frac{\lvert \xi_{io} \rvert^2}{A^2}$	Response amplitude operator of the ith-mode displacement
ρ	Density of water
$\phi(x, y, z, t)$	Velocity potential function which represents the fluid disturbance due to wave and body motions
$\phi_I(x, y, z, t)$	Complex velocity potential for incident wave
$\phi_D(x, y, z, t)$	Complex velocity potential for diffracted wave
ϕ_i	Complex velocity potential for forced oscillation in the ith mode
ϕ_i'	Two-dimensional complex velocity potential for forced oscillation in the ith mode
ω	Wave-encountering frequency ($= \omega_o - K_o U \cos\beta$)
ω_o	Incident wave frequency in radians/second

ABSTRACT

Linear equations of motion with the hydrodynamic coefficients approximated by strip method are used to obtain the motion of small-waterplane-area, twin-hull (SWATH) ships in regular and irregular waves. The couplings among different modes of motion are separated into three independent groups, surge, heave-pitch and sway-roll-yaw, and the resulting equations of motions are treated in the frequency domain.

The hydrodynamic coefficients of predominantly nonviscous nature, added mass and wavemaking damping, are obtained by strip theory. The effects of wave diffraction, viscous damping, and stationary stabilizing fins are included in the equations of motion within the frame work of the linear frequency response of a body to waves. The assumption involved in the evaluation of various hydrodynamic coefficients in the equation of motion are specified.

The validity of the theoretical prediction of motion is checked by correlating with the existing model experimental results, and the relevant discussions are made. In general, the theoretical prediction is found satisfactory except the case of near zero-encounter frequency which can occur when a ship cruises with certain speed in stern-quartering waves. A future effort for improvement of the theoretical prediction of SWATH ship motion in stern-quartering waves is recommended.

ADMINISTRATIVE INFORMATION

This study was sponsored by the Naval Sea Systems Command as part of the High-Performance Vehicle Hydrodynamic Program of the Ship Performance Department, David W. Taylor Naval Ship Research and Development Center (DTNSRDC). Funding was provided under Task Area SF 43421202, Task 18247, Work Unit 1507-200.

INTRODUCTION

A small-waterplane-area, twin-hull (SWATH) ship consists of submerged twin hulls, an above-water hull, and connecting struts. Figure 1 is schematic of a typical SWATH configuration.

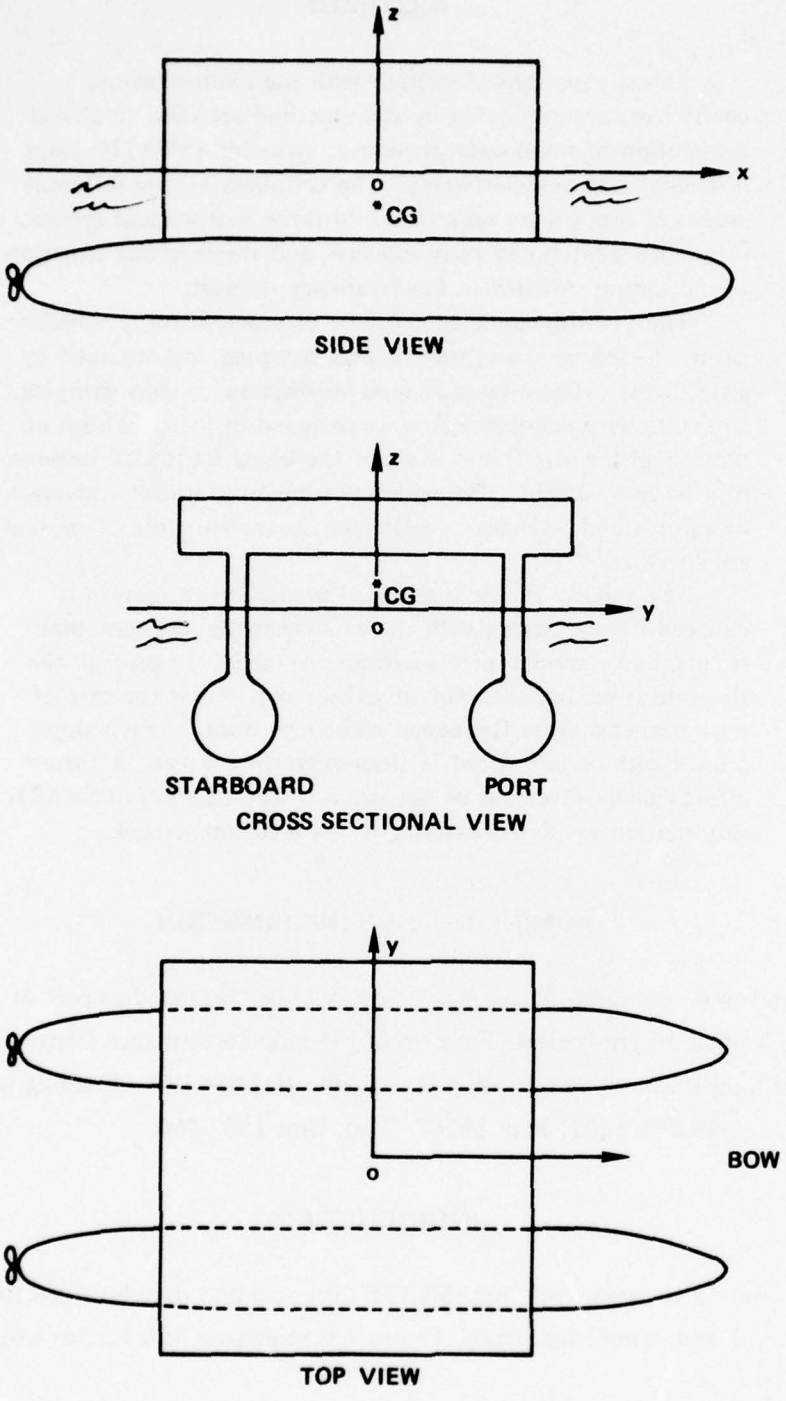

Figure 1 – Configuration of a SWATH Ship

The concept of the SWATH evolved through many years and its development is well documented.[1-3] One of the major advantages of the SWATH concept lies in its improved seakeeping quality compared to a monohull ship of equivalent displacement. The improvement is contributed mainly by the larger natural periods of heave and pitch modes due to the small waterplane area and by the smaller wave-exciting forces and moments due to the semi-submersible configuration.[4] The larger natural periods reduce the likelihood that resonant motions will be excited in moderate seas, and the smaller wave-exciting forces and moments not only reduce the motion but also provide a greater possibility for controlling its effects through the use of fins.

The overall assessment of a new hull concept versus existing ships is highly complicated and definitely beyond the scope of the present work. The aim here is to provide an analytical tool which can be utilized to assess certain aspects of the seakeeping qualities of SWATH ships and which may later be used to design specific hull forms.

Several analytical methods have been developed in various parts of the world in the past few years for predicting the motions of monohulls. Most of them use the so-called strip theory to evaluate the hydrodynamic coefficients associated with motion of ships. The strip theory is based on the assumption of two-dimensionality of fluid motion surrounding a cross section of a ship. A typical application of the strip theory is well described in Salvesen et al.[5]

Equations of motion and strip theory similar to those used in the cited reference 5 are employed here. However, the present work requires a considerable number of additional hydrodynamic coefficients which are normally absent in the equations of motion for monohull ships. Three distinct considerations should be included in the hydrodynamic coefficients for SWATH ships:

1. Hydrodynamic interactions between the two hulls.
2. The viscous damping effects. This cannot be neglected because for SWATH ships it is of the same order of magnitude as wavemaking damping. As expected for a lightly damped

---

[1] Lang, T.G. and D.T. Higdon, "S^3 Semi-Submerged Ship Concept and Dynamic Characteristics," AIAA/SNAME/USN Advanced Marine Vehicles Meeting, Annapolis, Maryland (Jul 1972).
A complete listing of references is given on pages 78–80.

[2] Leopold, R. et al., "The Low Water Plane Multi-Hull Principles, Status, and Plans," AIAA/SNAME/USN Advanced Marine Vehicles Meeting, Annapolis, Maryland (Jul 1972).

[3] Hawkins, S. and T. Sarchin, "The Small Waterplane-Area Twin Hull (SWATH) Program - A Status Report," AIAA/SNAME Advanced Marine Vehicles Meeting, San Diego, California (Jul 1974).

[4] Motora, S. and T. Koyama, "Wave-Excitationless Ship Forms," 6th Naval Hydrodynamic Symposium, Washington, D.C.; proceedings published by the Office of Naval Research, pp. 383-411 (1966).

[5] Salvesen, N. et al., "Ship Motion and Sea Loads," Trans. SNAME, Vol. 78 pp. 250-287 (1970).

system, neglect of viscous damping effects would yield unrealistically large motion amplitudes at the resonant frequencies.

3. Effect of stabilizing fins. A SWATH can become unstable in the vertical plane at and beyond a certain speed because of the small waterplane area. This is mainly caused by a destabilizing pitch moment, often referred to as the Munk moment, which is proportional to the square of the forward velocity of the body. Hence, stabilizing fins are necessary to augment the stability of the ship. The stabilizing fins can also provide much needed damping effects to the motion of a SWATH through the hydrodynamic lift generated by an angle of attack which results from the combination of the forward motion and the vertical motion of the fins. In order to satisfactorily compute the motions, the hydrodynamic effects contributed by the fins should be included in the equations of motion.

A theoretical prediction of motion and sea loads of twin-hull ships has been presented by Pien and Lee.[6] Since that time, significant improvements has been achieved in the prediction of SWATH ship motions. These mainly involve (1) a more adequate representation of the viscous damping in the equations of motion and (2) capability to predict the motion of a SWATH with stationary, horizontal fins.

The present report provides a detailed description of the theoretical analysis of the motion of SWATH ships in waves and the incorporation of that description into computer programs.[7] The first section of the report describes the equations of motion, their solutions, and the statistical averages of motion in irregular waves. The second section presents the derivation of the hydrodynamic coefficients. The third presents a correlation of theoretical results with model experimental results and pertinent discussions of these results.

Although comparisons of computed and measured values of the hydrodynamic coefficients and the motion suggest that the present motion prediction method is in general satisfactory, it is felt that further investigations should be pursued on such aspects as viscous damping effects, fin-body hydrodynamic interactions under a free surface, and prediction of motion in stern-quartering seas.

---

[6]Pien, P.C. and C.M. Lee, "Motion and Resistance of a Low-Waterplane Catamaran," 9th Naval Hydrodynamic Symposium, Paris, France, proceedings published by the Office of Naval Research, pp. 463-545 (1972).

[7]McCreight, K.K. and C.M. Lee, "Manual for Mono-Hull or Twin-Hull Ship Motion Prediction Computer Program," DTNSRDC Report SPD-686-02 (1976).

EQUATIONS OF MOTION AND SOLUTIONS

The formulation of the equations of motion will be limited to linear rigid body dynamic responses of the body to harmonic exciting forces or moments. The exciting forces and moments are assumed to be solely contributed by free-surface waves; to justify the linear response of the body, the wave slopes are assumed to be small. The ocean in which the ship is underway is infinitely deep and has no appreciable currents or winds which would invalidate the linear response assumption. With such an ocean environment, it can be safely assumed that the ship can maintain a constant mean speed and a straight mean course. The submerged portion of the ship hull is assumed to be sufficiently slender that the rate of lengthwise variation of the hydrodynamic pressures is small compared to the rate of the variation in the girthwise direction in a cross section of the ship.

The reference frame for which the equations of motion are to be formulated is a right-handed Cartesian coordinate system Oxyz which translates on the mean path of the ship with the ship speed. The origin is located on the undisturbed free surface, and the Oxy plane coincides with this surface. When the ship is at its mean position, the Oxz-plane contains the longitudinal plane of symmetry of the ship, the positive Ox-axis is directed toward the bow, and the positive Oz-axis is directed vertically upward. Figure 1 shows the coordinate system.

In general, the linearly coupled motion of a ship can be expressed in the form

$$\sum_{k=1}^{6} [(M_{ik} + A_{ik}) \ddot{\xi}_k + B_{ik} \dot{\xi}_k + C_{ik} \xi_k] = F_i^{(e)} e^{-j\omega t} \qquad (1)$$

Here i is 1 for surge, 2 for sway, 3 for heave, 4 for roll, 5 for pitch, and 6 for yaw; ξ_k is the linear or angular displacement of the ship from its mean position in the kth mode, $\ddot{\xi}_k$ and $\dot{\xi}_k$ are respectively the acceleration and velocity, M_{ik} is the mass matrix, A_{ik} is the added inertia, B_{ik} is the damping, C_{ik} is the restoring or spring constant, $F_i^{(e)}$ is the complex amplitude of the wave-exciting force, j is the imaginary unit associated only with a harmonic-time function, and ω is the wave-encounter frequency. The expression added mass (or inertia) which will be frequently employed in this report refers to the hydrodynamic coefficient associated with the acceleration of the body so that the product of the two provides a hydrodynamic equivalent of the inertia force or moment of the body. To be compatible with the complex expression on the right-hand side of Equation (1), the motion displacements ξ_k are assumed to be complex functions given by

$$\xi_k(t) = \xi_{ko} e^{-j\omega t} = (\xi_{kc} + j \xi_{ks}) e^{-j\omega t} \qquad (2)$$

where ξ_{kc} and ξ_{ks} are real functions and it is understood that whenever a product involved with $e^{-j\omega t}$ appears, only the real part of the product would be recognized, i.e.,

$$\xi_k(t) = \xi_{kc} \cos \omega t + \xi_{ks} \sin \omega t$$

The surge mode is assumed to be decoupled from the rest of the modes, and, furthermore, the added mass, damping, and diffracted wave force in the x-direction are assumed to be negligibly small. Thus, the equation of surge motion can be expressed by

$$M \ddot{\xi}_1 = F_1^{(FK)} e^{-j\omega t} \tag{3}$$

where

$$M = M_{ii},\ i = 1, 2, 3$$

is the mass of the body and appendages, if any. Substitution of Equation (2) into (3) yields

$$\xi_{1o} = \frac{F_1^{(FK)}}{-\omega^2 M} \tag{4}$$

where $F_1^{(FK)}$ is the Froude-Krylov part of the surge wave-exciting force.

Although simplifing assumptions were made to arrive at Equation (3), their validity may not be justified. Model experiments in stern-quartering and following waves have indicated that large surge motion in the order of the wave orbital motion can be induced simultaneously with large trim. It is quite plausible that coupling between the surge and pitch modes is not negligible when a SWATH ship undergoes large surge motion since the vertical center of gravity is located far above the main hull axis. This need to develop a more consistent hydrodynamic theory for SWATH ships in following waves is well recognized, but no such attempt will be made in this report.

The symmetry of the hull with respect to the longitudinal centerplane of a twin hull leads to decoupling of the vertical-plane modes from the horizontal-plane modes. Thus, the equations of motion can be divided into the following two groups:

Heave and pitch equations;

$$\begin{aligned}
(M + A_{33})\ddot{\xi}_3 + B_{33}\dot{\xi}_3 + C_{33}\xi_3 + A_{35}\ddot{\xi}_5 + B_{35}\dot{\xi}_5 + C_{35}\xi_5 &= F_3^{(e)} e^{-j\omega t} \\
(I_5 + A_{55})\ddot{\xi}_5 + B_{55}\dot{\xi}_5 + C_{55}\xi_5 + A_{53}\ddot{\xi}_3 + B_{53}\dot{\xi}_3 + C_{53}\xi_3 &= F_5^{(e)} e^{-j\omega t}
\end{aligned} \tag{5}$$

where I_5 (= M_{55}) is the mass moment of inertia about the y-axis.

Sway, roll, and yaw equations;

$$(M + A_{22})\ddot{\xi}_2 + B_{22}\dot{\xi}_2 + (A_{24} - Mz_o)\ddot{\xi}_4 + B_{24}\dot{\xi}_4 + A_{26}\ddot{\xi}_6 + B_{26}\dot{\xi}_6 = F_2^{(e)} e^{-j\omega t}$$

$$(I_4 + A_{44})\ddot{\xi}_4 + B_{44}\dot{\xi}_4 + C_{44}\xi_4 + (A_{42} - Mz_o)\ddot{\xi}_2 + B_{42}\dot{\xi}_2 + A_{46}\ddot{\xi}_6 + B_{46}\dot{\xi}_6 = F_4^{(e)} e^{-j\omega t}$$

$$(I_6 + A_{66})\ddot{\xi}_6 + B_{66}\dot{\xi}_6 + A_{62}\ddot{\xi}_2 + B_{62}\dot{\xi}_2 + A_{64}\ddot{\xi}_4 + B_{64}\dot{\xi}_4 = F_6^{(e)} e^{-j\omega t} \qquad (6)$$

where I_4 and I_6 are respectively the mass moment of inertia about the x- and z-axes, and z_o is the z-coordinate of the center of gravity of the ship.

The restoring coefficients contributed by the inherent buoyancy effect are easily obtained by

$$\begin{aligned} C_{33} &= \rho g A_w \\ C_{35} &= C_{53} = \rho g M_w \\ C_{44} &= \rho g I_{w4} - M g \overline{BG} \\ C_{55} &= \rho g I_{w5} - M g \overline{BG} \end{aligned} \qquad (7)$$

where ρ = density of water

g = gravitational acceleration

A_w = waterplane area

M_w = waterplane area moment about the y-axis

I_{w4} and I_{w5} = moment of inertia of the waterplane area about the x-axis and the y-axis, respectively

$\overline{BG}$ = vertical distance between the center of buoyancy and the center of gravity when the ship is at its mean position

As will be seen later, there are additional contributions to the restoring coefficients from the stabilizing fins.

Since Equations (5) and (6) are linear, the solutions of ξ_k are expected to be harmonic functions of time; hence the equations can be expressed as complex algebraic equations:

$$A_1 X_1 = B_1$$

$$A_2 X_2 = B_2$$

where

$$X_1 = \begin{bmatrix} \xi_{3o} \\ \xi_{5o} \end{bmatrix} \qquad X_2 = \begin{bmatrix} \xi_{2o} \\ \xi_{4o} \\ \xi_{6o} \end{bmatrix}$$

$$B_1 = \begin{bmatrix} F_3^{(e)} \\ F_5^{(e)} \end{bmatrix} \qquad B_2 = \begin{bmatrix} F_2^{(e)} \\ F_4^{(e)} \\ F_6^{(e)} \end{bmatrix}$$

$$A_1 = \begin{bmatrix} -\omega^2 (M + A_{33}) + C_{33} - j\omega B_{33} & -\omega^2 A_{35} + C_{35} - j\omega B_{35} \\ -\omega^2 A_{53} + C_{53} - j\omega B_{53} & -\omega^2 (I_5 + A_{55}) + C_{55} - j\omega B_{55} \end{bmatrix}$$

$$A_2 = \begin{bmatrix} -\omega^2 (M + A_{22}) - j\omega B_{22} & -\omega^2 (A_{24} - Mz_o) - j\omega B_{24} & -\omega^2 A_{26} - j\omega B_{26} \\ -\omega^2 (A_{42} - Mz_o) - j\omega B_{42} & -\omega^2 (I_4 + A_{44}) + C_{44} - j\omega B_{44} & -\omega^2 A_{46} - j\omega B_{46} \\ -\omega^2 A_{62} - j\omega B_{62} & -\omega^2 A_{64} - j\omega B_{64} & -\omega^2 (I_6 + A_{66}) - j\omega B_{66} \end{bmatrix}$$

An inversion of the matrices provides the amplitudes of the motion by

$$\bar{\xi}_k = | \xi_{ko} | = [\xi_{kc}^2 + \xi_{ks}^2]^{1/2} \tag{8}$$

and the phase angles with respect to the wave crest above the coordinate origin by

$$\alpha_k = \tan^{-1} [-\xi_{ks}/\xi_{kc}] \tag{9}$$

for k = 2, 3, 4, 5, 6.

The velocity and acceleration of the motion are obtained by simply multiplying the complex amplitudes of the displacements by $-j\omega$ and $-\omega^2$, respectively. The surge amplitude $\bar{\xi}_1$ and phase α_1 can be obtained similarly from Equation (4).

The complex amplitudes of the absolute and relative vertical motion of a point (x, y, z) on the ship are given for the absolute vertical motion by

$$\xi_v^{(A)} = \xi_{3o} + y\,\xi_{4o} - x\,\xi_{5o} \tag{10}$$

and for the relative motion by

$$\xi_v^{(R)} = \xi_v^{(A)} - \zeta_o \tag{11}$$

where ζ_o is the complex amplitude of the incoming wave given by

$$\zeta_o = A\, e^{j K_o (x \cos\beta - y \sin\beta)} \tag{12}$$

Here A is the wave amplitude, K_o the wave number defined by $K_o = 2\pi/\lambda = \omega_o^2/g$, λ the wavelength, ω_o the wave frequency, and β the wave heading angle with respect to the x-axis in the counterclockwise direction from the x-axis (= 0 deg represents the wave heading from the stern to the bow). Strickly speaking, Equation (11) is an approximation since we have neglected deformations of the wave elevation along the body caused by the diffraction of waves by the body surface and by the waves generated by the body motion.

The complex amplitude of absolute transverse motion of a point on the ship is given by

$$\xi_H^{(A)} = \xi_{2o} + x\,\xi_{6o} - z\,\xi_{4o} \tag{13}$$

In the foregoing, the frequency-response of the various motion amplitudes and phases were given. The complex amplitudes of any motion quantity divided by the amplitude of the waves are often called transfer functions or frequency-response functions. In principle, the time history of the system response to any random signal can be obtained for a linear system by a convolution integral of the product of the signal and the inverse Fourier transform of the transfer function. A correct approach to ship motion in the time domain, however, is not so straightforward as described in the foregoing; this has been pointed out by Cummins.[8] As is well recognized, a unique representation of the time history of sea waves is impossible; hence representation of sea waves has been made through energy spectra from which various statistical averages of the wave conditions can be obtained.

St. Denis and Pierson[9] were the first to introduce an application of sea energy spectra in conjunction with the transfer function to obtain various statistical averages of ship responses. Since then, statistical averages have been used almost as a standard tool for the investigation of ship motion in irregular waves. The major underlying assumptions for the concept are that the relationship between the wave excitation and ship response is linear, that wave and ship motion are stationary and normal random processes with zero mean, and that the spectral density functions of waves and ship motion are narrow banded. If a sea-energy spectral density function which has the dimensional units of $[L^2T]$ is denoted by $S(\omega_o)$, the variance of a motion quantity, say, $\overline{\xi}_k$, can be obtained by

---

[8]Cummins, W.E., "The Impulse Response Function and Ship Motions," Schiffstechnik, Vol. 9, pp. 101-109 (1962); reprinted as DTMB Report 1661.

[9]St. Denis, M. and W.J. Pierson, "On the Motion of Ships in Confused Seas," Trans. SNAME, Vol. 61, pp. 280-357 (1953).

$$E = \int_0^\infty (\bar{\xi}_k/A)^2 \, S(\omega_o) \, d\omega_o$$

As can be seen in the next section, the wave-exciting forces $F_k^{(e)}$, k = 1, ... 6, are linearly proportional to the incoming wave amplitude; hence if the wave amplitude is taken as a unit value, the resulting motion amplitudes obtained from the solutions of the equations of motion are already factored by the wave amplitude. In the following, all transfer functions are understood to be normalized by the wave amplitude unless otherwise specified. Thus, Equation (13) will be written as

$$E = \int_0^\infty (\bar{\xi}_k)^2 \, S(\omega_o) \, d\omega_o \qquad (14)$$

where $(\bar{\xi}_k)^2$ is often called the response amplitude operator (RAO).

Of the few mathematical expressions for sea spectra, the most frequently used by ship motion investigators are the so-called Pierson-Moskowitz spectrum[10] and the Bretschneider spectrum.[11] More recently the trend is to use actually measured sea spectra in order to examine the motion of a ship in a wide variety of sea conditions.[12] For example, Miles[13] has provided a stratified sample of 323 sea spectra based on measurements obtained at Station India in the North Atlantic. Proper weighting factors for the frequency of occurrence for each of the spectra given in Miles[13] can be determined from the useful wave statistics compiled by Hogben and Lumb.[14] It follows, then, that the probability can be determined that a ship operating in the North Atlantic will exceed certain seaworthiness characteristics, e.g., vertical acceleration, slamming and deck wetness per hour, etc. Since these predictions are made under the assumption of the Rayleigh probability distribution function, it is tacitly assumed that distribution of the motion amplitudes follows the Rayleigh function and this may not be quite true in some cases.

---

[10] Pierson, W.J. and L. Moskowitz, "A Proposed Spectral Form for Fully Developed Wind Seas, Based on the Similarity Theory of S.A. Kitaigarodskii," J. Geophys. Res., Vol. 69, No. 24, pp. 5181-5190 (1964).

[11] Bretschneider, C.L., "Wave Variability and Wave Spectra for Wind-Generated Gravity Waves," Beach Erosion Board, U.S. Army Corps of Engineers TM 118 (1959).

[12] Hadler, J.B. et al., "Ocean Catamaran Seakeeping Design, Based on the Experience of USNS HAYES," Trans. SNAME, Vol. 82, pp. 126-161 (1974).

[13] Miles, M., "Wave Spectra Estimated from a Stratified Sample of 323 North Atlantic Wave Records," National Research Council, Division of Mechanical Engineering Report LTR-SH-118 (1971).

[14] Hogben, N. and F.E. Lumb, "Ocean Wave Statistics," H.M. Stationery Office, London (1967).

The variance for the velocity and the acceleration of the kth mode motion can be easily obtained by

$$E_v = \int_0^\infty (\omega \bar{\xi}_k)^2 \, S(\omega_o) \, d\omega_o$$

$$E_a = \int_0^\infty (\omega^2 \bar{\xi}_k)^2 \, S(\omega_o) \, d\omega_o \qquad (15)$$

Both the Pierson-Moskowitz spectrum and the Bretschneider spectrum can be expressed in the form

$$S(\omega_o) = \frac{C_1}{\omega_o^5} \exp(-C_2/\omega_o^4) \qquad (16)$$

where

$$C_1 = \begin{cases} 0.78 & \text{- Pierson-Moskowitz} \\ \dfrac{487.06 H_s^2}{T_o^4} & \text{- Bretschneider} \end{cases}$$

in which H_s is the significant waveheight in metres, T_o is the modal period in seconds, and

$$C_2 = \begin{cases} 3.12/H_s^2 & \text{- Pierson-Moskowitz} \\ 1948.24/T_o^2 & \text{- Bretschneider} \end{cases}$$

In the application of these empirical formulas, caution is necessary in taking the integral limit to infinity since, as can be seen from Equation (16), $\omega^4 S(\omega_o) \to 1/\omega_o$ as $\omega \to \infty$; hence the integral behaves like a logarithmic function with an infinite argument e.g., since the RAO of relative vertical motion approaches unity as ω_o goes to infinity, the spectrum of the acceleration of relative motion at high frequencies would behave like $1/\omega_o$. Since Equation (16) is an empirical formula based on the recorded ocean waves which usually yield uncertain data at high frequencies because of the filtering process, the high-frequency end of the formula is not reliable as Pierson points out (see pages 86-89 of Reference 15). Thus, for the prediction of motion of ships with lengths greater than 30 m, the high frequency limit in the integration should be replaced by something like 3.0 rad/sec which corresponds to about a 6-m gravity wavelength in deep water.

[15] Pierson, W.J., "The Theory and Applications of Ocean Wave Measuring Systems at and below the Sea Surfaces, on the Land from Aircraft, and from Space Craft," NASA Contractors Report NASA CR-2646 (1976).

Various often used statistical averages can be expressed in the form

$$\text{Average Amplitude} = C\sqrt{E_o} \tag{17}$$

Here E_o is the variance of a particular motion amplitude. C = 1.253 provides the average, C = 2.0 provides the one-third highest average or significant average and C = 2.546 provides the one-tenth highest average.

From the Rayleigh law of probability distribution, the probable number of slams sustained per n sec by the main hull bottom or the cross-deck bottom of a SWATH ship at a given location can be given by

$$N_s = \frac{n}{2\pi}\sqrt{\frac{E_v^{(R)}}{E^{(R)}}}\exp\left(-\frac{C_o^2}{2E^{(R)}} - \frac{V_T^2}{2E_v^{(R)}}\right) \tag{18}$$

The superscript (R) denotes the relative motion of the location of interest, C_o is the vertical distance from the calm waterline to either the main hull bottom or the cross-deck bottom in the same dimensional unit used for $\sqrt{E^{(R)}}$, and V_T is the threshold velocity that incites slamming. The value of V_T can differ from case to case and should be given in the same dimensional unit as $\sqrt{E_v^{(R)}}$. In many cases the values of V_T are unknown, and if V_T is set to zero, Equation (18) then gives either the number of hull bottom emergences or water contacts of the cross-deck bottom per n sec. If we set $V_T = 0$ and take C_o to be the deck height, then Equation (18) provides the probable number of occurrences of deck wetness per n sec.

For a design or operational criterion, it is also of interest to know the probable extreme value a ship may encounter in given sea environments. Ochi[16] has shown that the extreme value in amplitude expected in n observations γ_n can be expressed by

$$\gamma_n(\delta) = \sqrt{2\ell_n\left(\frac{3600T}{2\pi\delta}\sqrt{\frac{E_v}{E}}\right)}\sqrt{E}$$

for small δ

where T is the time in hours during which an extreme sea environment may persist, and δ is given a value of 0.01 if the design goal calls for a 99-percent assurance that the extreme amplitude γ_n will not be exceeded. For $\delta = 1$, γ_n represents the "most probable extreme value" in amplitude. For a large number of observations, the probability that the extreme value will exceed γ_n is 63.2 percent.

[16]Ochi, M.K., "On Prediction of Extreme Values," J. Ship Res., Vol. 17, No. 1, pp. 29-37 (1973).

EVALUATION OF HYDRODYNAMIC COEFFICIENTS

The hydrodynamic coefficients in the equations of motion will be divided into three groups. The first consists of those coefficients which can be obtained under the assumption of potential flow, the second consists of those coefficients mainly associated with the viscous nature of the fluid, and the third is associated with the hydrodynamic lift generated by the stationary fins.

The derivation of these coefficients involves application of various assumptions and approximations, and rigorous justifications are lacking for some of them. This section attempts to describe as well as possible the underlying assumptions involved in deriving each coefficient. There are still unsolved problems to be looked into before more satisfactory justifications can be offered for deriving some of the coefficients, especially those in the second and third groups.

COEFFICIENTS OBTAINED UNDER POTENTIAL-FLOW ASSUMPTION

The added mass coefficients A_{ij}, the damping coefficients contributed by the motion-generated outgoing waves B_{ij}, and the wave-exciting forces $F_i^{(e)}$ for i, j = 1, 2, 3, 4, 5, 6 belong to this group. The basic solution is obtained under an assumption of two-dimensional potential flow at each cross section of the ship. The boundary-value problem is solved for the velocity potential functions for infinitely long, semisubmerged, horizontal twin cylinders having cross sections identical to the cross section of a SWATH undergoing heave, sway, or roll oscillation. This is done by the method of source distribution which is described in detail by Lee et al.[17] for heave oscillation; an extension of the method was made later for sway and roll oscillations. The validity of the two-dimensional solution was checked and comparisons between the theoretical and experimental results presented[17] for rectangular, circular, and triangular twin cylinders.

Application of the source distribution method to oscillating twin cylinders results in two distinct singular solutions at certain discrete frequencies of oscillation. One stems from the mathematical failure associated with the solution of the Fredholm-type integral equations in the course of determining the source strengths,[18] and the other stems from the physical reality that standing waves are trapped between the two cylinders at certain frequencies of oscillation given approximately by

---

[17] Lee, C.M. et al., "Added Mass and Damping Coefficients of Heaving Twin Cylinders in a Free Surface," NSRDC Report 3695 (1971).

[18] John, F., "On the Motion of Floating Bodies: II. Simple Harmonic Motions," Commun. Pure Appl. Math., Vol. 13, pp. 45-101 (1950).

$$\omega = \sqrt{\frac{g n \pi}{(b/a - 1)}} \quad \text{for } n = 1, 2, \ldots$$

where b is one-half the distance between the centerline of each cylinder and a is the half-beam of the individual cylinder at the waterline.

The former type of singular solutions can be removed by extending the source distribution onto the waterline inside the cylinders and imposing either wall condition or the condition of vanishing velocity potential on the inner waterline. The validity of this method can be demonstrated by numerical results[6, 19] and yet no vigorous mathematical proof has been established for the existence and the uniqueness of the solution obtainable by this method. There appears to be no way to remove the latter type of singular solutions except by a full three-dimensional solution. In practice, the range of frequencies of interest for motions of ships of lengths greater than 200 ft lies below the frequencies at which the singular behavior of the two-dimensional solution occurs. However, caution is necessary when the loading on a ship due to waves is computed, since the peak loading may occur in a higher frequency range.

To obtain the three-dimensional coefficients, the sectional hydrodynamic coefficients of the two-dimensional solution are integrated lengthwise. For the case of a ship without forward speed, the strip approximation described in the foregoing may still be an acceptable approximation in a practical sense; however, it appears that for a ship with forward speed, the lengthwise flow disturbances generated by the forward speed may immediately invalidate the two-dimensional flow assumption at each cross section. The long controversy on this particular point still continues.

Ogilvie and Tuck[20] presented a more consistent and rational theory for forward speed effects on the hydrodynamic coefficients which are derived on the basis of strip theory.

Faltinsen[21] demonstrated a better correlation of the theoretical results obtained from the Ogilive and Tuck theory[20] with experimental results for a few of the hydrodynamic coefficients which can be strongly influenced by forward speed of a ship. There is no doubt that computations of these coefficients according to Ogilvie and Tuck are much more tedious and expensive than computations according to conventional strip theory.[5] Yet, conclusive

[19] Ohmatsu, S., "On the Irregular Frequencies in the Theory of Oscillating Bodies in a Free Surface," Ship Research Institute of Japan Report 48 (1975).

[20] Ogilvie, T.F. and E.O. Tuck, "Rational Strip Theory of Ship Motions; Part I," University of Michigan, College of Engineering Report 013 (1969).

[21] Faltinsen, O., "Numerical Investigation of the Ogilivie-Tuck Formulas for Added Mass and Damping Coefficients," J. Ship Res., Vol. 18, pp. 73-84 (1974).

evidence does not seem to exist that this new theory will necessarily improve the prediction of ship motion.*

Although, as pointed out by Ogilvie and Tuck, some argument may be made regarding the consistency of the perturbation expansion, conventional strip theory will be used in this report. Details of the development of the theory are given in Appendix A and only the final expressions obtained there will be given here.

Let the velocity potential function $\Phi(x, y, z, t)$ whose gradient represents the velocity field in the fluid region disturbed by incoming waves and motion of a ship be expressed in the form

$$\Phi = -U x + \phi_s(x, y, z) + (\phi_I(x, y, z) + \phi_D + \sum_{i=1}^{6} \xi_{io}\, \phi_i)\, e^{-j\omega t}$$

Here ϕ_s is the steady wave-resistance potential, ϕ_I and ϕ_D are respectively the complex potentials representing the incoming and diffracted waves, ϕ_i is the complex potential representing the fluid disturbance by the ship motion in the ith mode, and ξ_{io} is the complex amplitude of the displacement in the ith mode. Then, the hydrodynamic coefficients can be given by

$$A_{ik} = \mathrm{Re}_j \left[-\frac{\rho}{\omega^2} \int_L dx \int_{C(x)} \left\{ \phi'_{iN}(y, z; x) + \frac{2U}{j\omega} \phi'_{3N}\, \delta_{i5} - \frac{2U}{j\omega} \phi'_{2N}\, \delta_{i6} \right\} \phi'_k\, d\ell \right] \quad (20)$$

$$B_{ik} = \mathrm{Im}_j \left[-\frac{\rho}{\omega} \int_L dx \int_{C(x)} \left\{ \phi'_{iN}(y, z; x) + \frac{2U}{j\omega} \phi'_{3N}\, \delta_{i5} - \frac{2U}{j\omega} \phi'_{2N}\, \delta_{i6} \right\} \phi'_k\, d\ell \right] \quad (21)$$

for i, j = 2, 3, 4, 5, 6 (see Equations (76) and (77) in Appendix A).

In Equations (20) and (21), Re_j and Im_j mean the real and the imaginary part of what follows; $\int_L$ is the lengthwise integral; $\int_{C(x)}$ is the integral along the immersed contour of the section located at x when the ship is at its mean position; δ_{ik} is the Kronecker delta function; ϕ'_i is the two-dimensional representation of ϕ_i (strip assumption); and subscript N denotes the normal derivative in the y-z plane, the positive sense of the two-dimensional unit normal vector $\underline{N}$ being pointing into the body. For later use, the sectional added mass $a_{ii}(x)$ and the wavemaking damping $b_{ii}(x)$ are defined by

*Since as their first effort, Ogilvie and Tuck[20] covered only the coefficients on the left-hand side of the equations of motions (see Equation (5)), motion computation cannot be performed unless a consistent theory is also developed to cover the wave-exciting terms.

$$a_{ii}(x) = Re_j \left[-\frac{\rho}{\omega^2} \int_{C(x)} \phi'_{iN} \phi'_i \, d\ell \right] \tag{22}$$

$$b_{ii}(x) = Im_j \left[-\frac{\rho}{\omega} \int_{C(x)} \phi'_{iN} \phi'_i \, d\ell \right] \tag{23}$$

for i = 2, 3 and 4.

The wave-exciting terms are expressed by

$$F_1^{(e)} = j\omega_o \rho \int_L dx \int_{C(x)} n_1 \phi_I \, d\ell \tag{24}$$

$$F_i^{(e)} = \rho \int_L dx \int_{C(x)} \left[j\omega_o N_i + \left(\phi'_i + \frac{2U}{j\omega} \phi'_3 \delta_{i5} - \frac{2U}{j\omega} \phi'_2 \delta_{i6} \right) \frac{\partial}{\partial N} \right] \phi_I \, d\ell \tag{25}$$

for i = 2, 3, 4, 5, 6. Here n_1 is the x-component of the unit normal vector on the ship surface pointing into the body, N_i is the ith component of the two-dimensional unit normal vector such that N_2 and N_3 are the y- and z-components,

$$N_4 = y N_3 - z N_2$$

$$N_5 = -x N_3$$

$$N_6 = x N_2$$

and ϕ_I is given by

$$\phi_I = -\frac{jgA}{\omega_o} \exp (K_o z + j K_o x \cos\beta - j K_o y \sin\beta) \tag{26}$$

and

$$\phi_{IN} = K_o (-j N_2 \sin\beta + N_3) \phi_I$$

in which the notations are as defined under Equation (12).

If the hull geometry is given by z = h(y; x) the definition of the components of the unit normal vector can be given as

$$n_1 = \frac{1}{N} \left(h_y \frac{dy(x)}{dx} - \frac{dz(x)}{dx} \right)^*$$

*For the main hull of a SWATH ship having the form of body of revolution, we can obtain n_1 by $R'(x)/(1 + R'^2)^{1/2}$ where R(x) is the radius of the cross section of one hull and $R'(x) = dR/dx$.

$$N_2 = -\frac{h_y}{N}$$

$$N_3 = \frac{1}{N}$$

$$N_4 = \frac{1}{N}(y + z\,h_y)$$

$$N_5 = -\frac{x}{N}$$

$$N_6 = -\frac{x\,h_y}{N}$$

where $N = \sqrt{1 + h_y^2}$. If the offsets of the hull are given at several waterlines at each station of a ship, the hull derivatives dy/dx and dz/dx may be obtained numerically by use of the three-point Lagrangian interpolation rule along the same waterline. As can be seen in Figure 2, if we know the tangent angle α at a given point of a cross section contour, then at a given point of a cross section contour, we have

$$h_y = \tan \alpha$$

Hence

$$N = \frac{1}{\cos \alpha},\ N_2 = -\sin \alpha \text{ and } N_3 = \cos \alpha$$

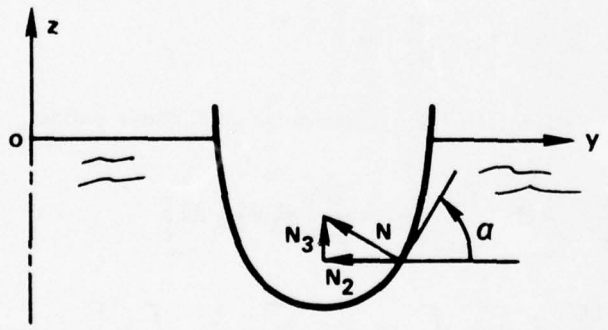

Figure 2 – Unit Normal Vector in the Plane of a Cross Section

Table 1 shows the expressions for the hydrodynamic coefficients given in terms of Equations (20) through (26). Note that the forward speed effect on the hydrodynamic coefficients appears distinctly as multiplication factors to some coefficients. However, the sectional hydrodynamic quantities a_{ii} and b_{ii} for i = 2, 3, and 4 are functions of the geometry of the cross section as well as the encounter frequency, and since the encounter frequency is a function of the forward speed, the forward-speed effects are also implicitly imbedded in other hydrodynamic coefficients.

To facilitate reader's understanding, the derivation of A_{53} and B_{66} will be illustrated in the following. From Equation (20)

$$A_{53} = \mathrm{Re}_j \left[-\frac{\rho}{\omega^2} \int_L dx \int_{C(x)} \left(\phi'_{5N} + \frac{2U}{j\omega} \phi'_{3N} \right) \phi'_3 \, d\ell \right]$$

From Equation (68) in Appendix A,

$$N_3 = -\frac{\phi'_{3N}}{j\omega}$$

$$\phi'_{5N} = -j\omega N_5 + U N_3$$

From the slender-body assumption,

$$N_5 = -x N_3$$

Hence

$$\phi'_{5N} = j\omega \left(x + \frac{U}{j\omega} \right) N_3 = -\left(x + \frac{U}{j\omega} \right) \phi'_{3N}$$

and

$$\phi'_5 = -\left(x + \frac{U}{j\omega} \right) \phi'_3$$

Substitution of this relation into the expression of A_{53} above yields

$$A_{53} = \mathrm{Re}_j \left[-\frac{\rho}{\omega^2} \int_L dx \int_{C(x)} \left(-x + \frac{U}{j\omega} \right) \phi'_3 \, \phi'_{3N} \, d\ell \right]$$

$$= -\int x \, dx \left[-\frac{\rho}{\omega^2} \mathrm{Re}_j \int_{C(x)} \phi'_3 \, \phi'_{3N} \, d\ell \right] + \frac{U}{\omega^2} \int_L dx \left[-\frac{\rho}{\omega} \mathrm{Im}_j \int_{C(x)} \phi'_3 \, \phi'_{3N} \, d\ell \right]$$

TABLE 1 – HYDRODYNAMIC COEFFICIENTS OBTAINED UNDER POTENTIAL-FLOW ASSUMPTION

$$A_{22} = \int_L a_{22}(x)\,dx$$

$$B_{22} = \int b_{22}\,dx$$

$$A_{24} = \int a_{24}\,dx$$

$$B_{24} = \int b_{24}\,dx$$

$$A_{26} = \int x\,a_{22}\,dx + \frac{U}{\omega^2} B_{22}$$

$$B_{26} = \int x\,b_{22}\,dx - U A_{22}$$

$$A_{33} = \int a_{33}\,dx$$

$$B_{33} = \int b_{33}\,dx$$

$$A_{55} = \int x^2\,a_{33}\,dx + \frac{U^2}{\omega^2} A_{33}$$

$$B_{55} = \int x^2\,b_{33}\,dx + \frac{U^2}{\omega^2} B_{33}$$

$$A_{53} = -\int x\,a_{33}\,dx + \frac{U}{\omega^2} B_{33}$$

$$B_{53} = -\int x\,b_{33}\,dx - U A_{33}$$

$$A_{66} = \int x^2\,a_{22}\,dx + \frac{U^2}{\omega^2} A_{22}$$

$$A_{35} = -\int x\,a_{33}\,dx - \frac{U}{\omega^2} B_{33}$$

$$B_{35} = -\int x\,b_{33}\,dx + U A_{33}$$

$$A_{44} = \int a_{44}\,dx$$

$$B_{44} = \int b_{44}\,dx$$

$$A_{42} = A_{24} = \int a_{24}\,dx$$

$$B_{42} = B_{24} = \int b_{24}\,dx$$

$$A_{46} = \int x\,a_{24}\,dx + \frac{U}{\omega^2} B_{24}$$

$$B_{46} = \int x\,b_{24}\,dx - U A_{42}$$

$$B_{66} = \int x^2\,b_{22}\,dx + \frac{U^2}{\omega^2} B_{22}$$

$$A_{62} = \int x\,a_{22}\,dx - \frac{U}{\omega^2} B_{22}$$

$$B_{62} = \int x\,b_{22}\,dx + U A_{22}$$

$$A_{64} = \int x\,a_{24}\,dx - \frac{U}{\omega^2} B_{24}$$

$$B_{64} = \int x\,b_{24}\,dx + U A_{24}$$

TABLE 1 (Continued)

$$F_1^{(e)} = \rho g A \int_L dx\, e^{j K_o x \cos\beta} n_1 \int_{C(x)} (-j N_2 \sin\beta + N_3)\, e^{K_o (z - jy \sin\beta)}\, d\ell$$

$$F_2^{(e)} = \frac{-j\rho g A}{\omega_o} \int_L dx\, e^{j K_o x \cos\beta} \int_{C(x)} \left\{ j\omega_o N_2 + K_o (-j N_2 \sin\beta + N_3)\, \phi_2' \right\} e^{K_o (z - jy \sin\beta)}\, d\ell$$

$$F_3^{(e)} = \frac{-j\rho g A}{\omega_o} \int_L dx\, e^{j K_o x \cos\beta} \int_{C(x)} \left\{ j\omega_o N_3 + K_o (-j N_2 \sin\beta + N_3)\, \phi_3' \right\} e^{K_o (z - jy \sin\beta)}\, d\ell$$

$$F_4^{(e)} = \frac{-j\rho g A}{\omega_o} \int_L dx\, e^{j K_o x \cos\beta} \int_{C(x)} \left\{ j\omega_o (y N_3 - z N_2) + K_o (-j N_2 \sin\beta + N_3)\, \phi_4' \right\} e^{K_o (z - jy \sin\beta)}\, d\ell$$

$$F_5^{(e)} = \frac{-j\rho g A}{\omega_o} \int_L dx\, e^{j K_o x \cos\beta} \int_{C(x)} \left\{ -j\omega_o x N_3 + K_o (-j N_2 \sin\beta + N_3) \cdot \left(\frac{U}{j\omega} - x \right) \phi_3' \right\} e^{K_o (z - jy \sin\beta)}\, d\ell$$

$$F_6^{(e)} = \frac{-j\rho g A}{\omega_o} \int_L dx\, e^{j K_o x \cos\beta} \int_{C(x)} \left\{ j\omega_o x N_2 - K_o (-j N_2 \sin\beta + N_3) \cdot \left(\frac{U}{j\omega} - x \right) \phi_2' \right\} e^{K_o (z - jy \sin\beta)}\, d\ell$$

The definitions given by Equations (22) and (23) can be used to write

$$A_{53} = -\int_L x\, a_{33}(x)\, dx + \frac{U}{\omega^2}\int_L b_{33}(x)\, dx$$

$$= -\int_L x\, a_{33}\, dx + \frac{U}{\omega^2} B_{33}$$

Procedures similar to the foregoing together with the relations

$$N_2 = -\phi'_{2N}/(j\omega),\ N_6 = x\, N_2,\ \text{and}\ \phi'_6 = \left(x + \frac{U}{j\omega}\right)\phi'_2$$

can be used to derive

$$B_{66} = \mathrm{Im_j}\left[-\frac{\rho}{\omega}\int_L dx \int_{C(x)} \left(\phi'_{6N} - \frac{2U}{j\omega}\phi'_{2N}\right)\phi'_6\, d\ell\right]$$

$$= \mathrm{Im_j}\left[-\frac{\rho}{\omega}\int_L dx \int_{C(x)} \left(-j\omega N_6 - U N_2 - \frac{2U}{j\omega}\phi'_{2N}\right)\phi'_6\, d\ell\right]$$

$$= \mathrm{Im_j}\left[-\frac{\rho}{\omega}\int_L dx \int_{C(x)} \left\{\left(x + \frac{U}{j\omega}\right)(-j\omega N_2) - \frac{2U}{j\omega}\phi'_{2N}\right\}\left(x + \frac{U}{j\omega}\right)\phi'_2\, d\ell\right]$$

$$= \mathrm{Im_j}\left[-\frac{\rho}{\omega}\int_L dx \int_{C(x)} \left(x - \frac{U}{j\omega}\right)\left(x + \frac{U}{j\omega}\right)\phi'_2\,\phi'_{2N}\, d\ell\right]$$

$$= \int_L \left(x^2 + \frac{U^2}{\omega^2}\right) dx \left[-\frac{\rho}{\omega}\mathrm{Im_j}\int_{C(x)} \phi'_2\,\phi'_{2N}\, d\ell\right]$$

$$= \int_L x^2\, b_{22}(x)\, dx + \frac{U^2}{\omega^2} B_{22}$$

VISCOUS DAMPING COEFFICIENTS

Hydrodynamic coefficients derived under the potential-flow assumption (as shown in the preceding section) have been found to provide satisfactory motion predictions for most conventional-type ships wherein wavemaking damping predominated. However, as in the case of predicting roll motion of a surface ship, when wavemaking damping is no longer the dominant contributing factor to the overall damping, the damping contributed by the viscous effects of the fluid has to be taken into account.

The semisubmersible SWATH configuration does not generate large surface waves when it oscillates in the vertical-plane modes. This means that the wavemaking damping of SWATH ships in the vertical-plane modes (i.e., heave, pitch, and surge) is relatively small compared with that of conventional ships. When the viscous effects contributing to the damping are neglected, the computed motion amplitude in the neighborhood of resonance is similar to that of a typical underdamped linear system, i.e., a narrowly tuned, high spiked motion at the resonant frequency. Figure 3 shows such behavior for a SWATH configuration proceeding in regular head waves when computed with the potential-flow hydrodynamic coefficients alone. Model Experimental results are included in the figure to indicate the errors caused when the predictions underestimate damping coefficients. The need for a more reasonable evaluation of damping coefficients is obvious; however, discouragingly, there is very little one can do to improve the evaluation theoretically.

Encouraged by the remarks made in Pien and Lee,[6] Kim[22] tried to include the forward-speed effect more rigorously, and used a thin-ship approach in his evaluation of damping coefficients. Figure 4 compares his results with those obtained by the strip theory (described in the preceding section) and by experimental results for a SWATH model designated as SWATH 1 (previously called Modcat 1). Kim's results do not differ significantly from the experimental results, yet when the motion based on these damping coefficients was computed, the unrealistically large motion that characterized Figure 3 were still present. This implies that even experimentally obtained damping coefficients are not sufficient to yield reasonable motion predictions. Thus we are led to conclude that forced-oscillation experiments of a model with small amplitude of motion do not yield realistic values of damping for a model that undergoes large motion near reasonance.

If the foregoing conclusion is correct, the damping must be nonlinear with respect to the motion amplitude when it exceeds a certain magnitude.* Figure 5 presents unpublished experimental results obtained at DTNSRDC by Wahab by vertically oscillating a two-dimensional cylinder with a bulbous bow cross section at zero speed. The theoretical results shown in the figure were obtained by using the source distribution method developed by Frank for single cylindrical forms.[23] Here, a large discrepancy between the potential-flow theory and experiment is obvious, unlike the case for a three-dimensional body shown in Figure 4.

[22]Kim, Ki-Han, "Determination of Damping Coefficients of SWATH Catamaran Using Thin Ship Theory," Mass. Inst. Technol. Dept. Ocean Eng. Report 75-4 (1975).

*A linearity check for the damping coefficient with respect to the motion amplitudes was made in the experiment as shown in Figure 4.

[23]Frank, W., "Oscillation of Cylinders in or below the Free Surface of Deep Fluids," NSRDC Report 2375 (1967).

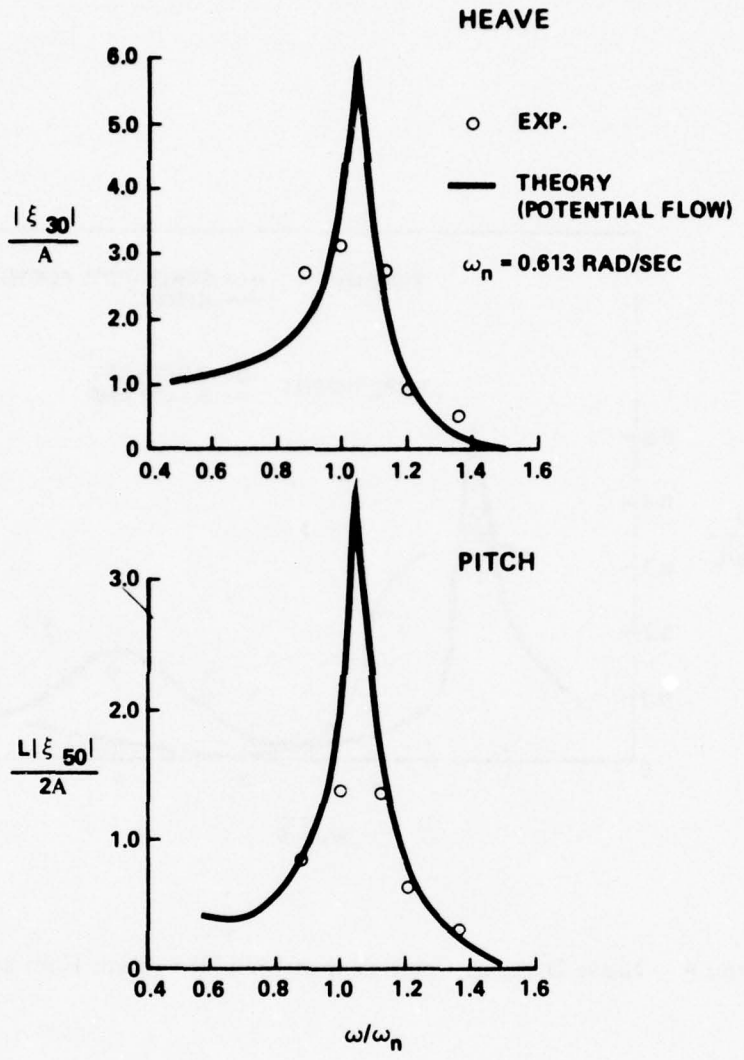

Figure 3 – Heave and Pitch Motion of SWATH 4 in Regular Head Waves at 20 Knots Without Viscous Damping

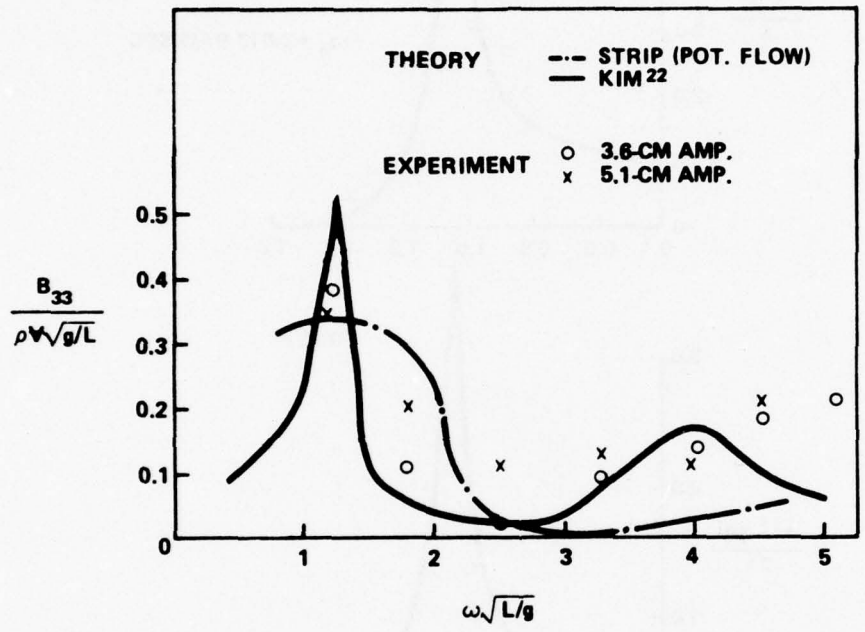

Figure 4 – Heave Damping Coefficient of SWATH I (Twin Hull) at Fn = 0.2

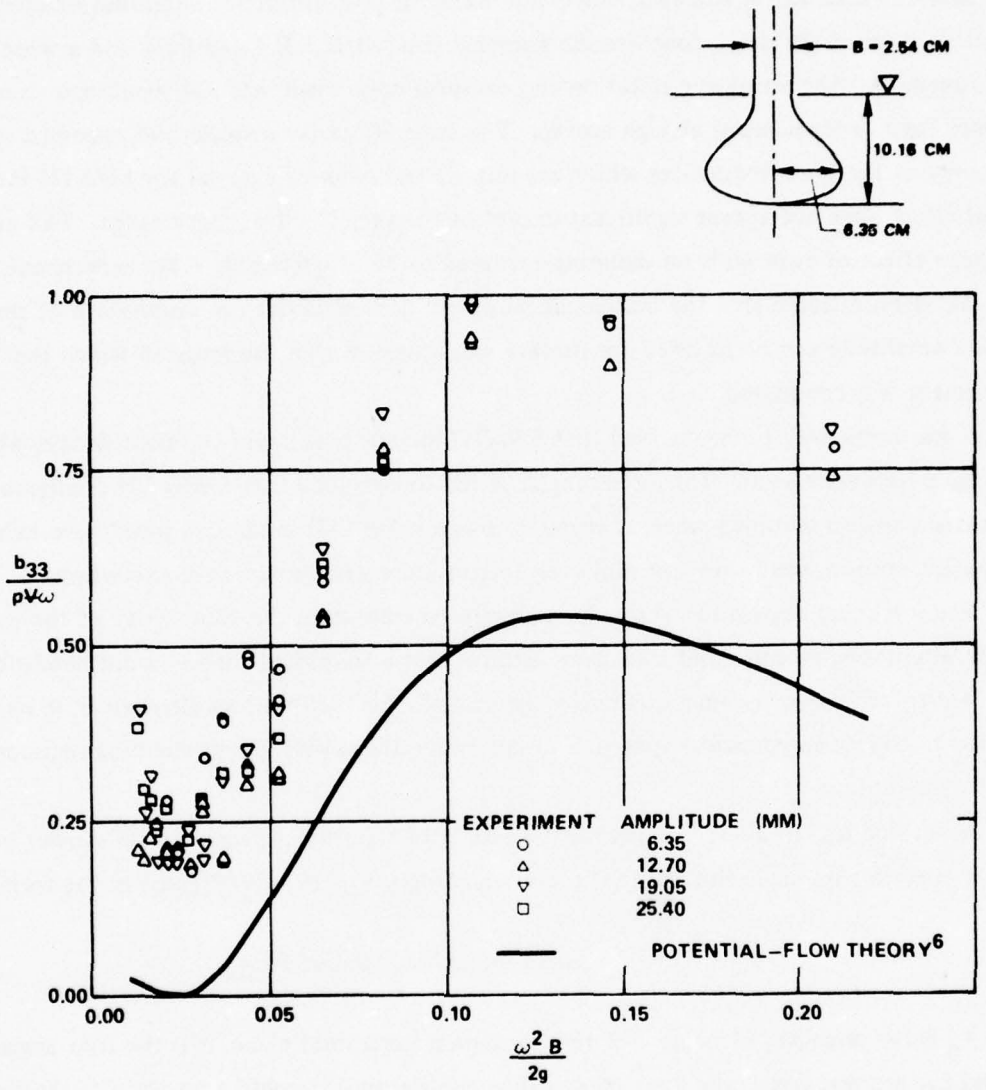

Figure 5 – Heave Damping Coefficient of a Bulbous Bow Section

A forced heave-oscillating experiment with a SWATH model (some results of which are shown in Figure 4) was conducted at DTNSRDC by Stahl (as yet unpublished) under various conditions. The forced-vertical oscillation test were made with the models of a single hull of two different scale ratios and twin hulls, with three to four different amplitudes of oscillations to within 0.16 of the draft, four Froude numbers (Fn = 0, 0.2, 0.4 and 0.6), and a wide range of frequencies. The nonlinear effect on the damping coefficient was not significant except perhaps for low frequencies at high speeds. The scale effect for a single hull appeared significant only at the high frequencies which are outside the range of interest for SWATH ships. Speed effect does not appear significant except in the very low frequency range. The mutual blockage effect of twin hulls on damping appeared to be insignificant. This experiment, in fact, has demonstrated that the mathematical model derived under the assumption of small motion amplitude can be justified for motion amplitudes within the range in which the experiment was conducted.

It has frequently been observed that SWATH models have rapid transient decays when they have forward speeds. Thus, one might be led to conclude that a SWATH configuration possesses a critical damping when at speed. However, SWATH models at speed have exhibited a resonant motion when they are subjected to continuous harmonic wave excitations.

The foregoing description is intended merely to emphasize the complexity of the problem we are attempting to solve and thus demonstrates that a simplified theory could hardly be expected to provide more than qualitative agreement. Left without an alternative, it was decided to follow an empirical approach to determine the supplemental damping required to predict the motion.

According to Thwaites,[24] experimental results of side forces generated on slender bodies with moderate trim angle showed that the vertical force F_v can be expressed in the form

$$F_v = \frac{1}{2}\rho U^2 A_p \sin\alpha\,|\sin\alpha|\,(a_o\,|\cot\alpha| + C_D) \tag{27}$$

Here A_p is the projected plane area of the body on a horizontal plane, α is the trim angle, and a_o and C_D are real constants; a_o is often called the viscous-lift coefficient and C_D the cross-flow drag coefficient. The value of a_o found from the experiments on airship models with circular or polygonal cross sections was about 0.07 while C_D seemed to lie beween 0.4 and 0.7. An experiment by Allen and Perkins[25] showed that C_D increases as the slenderness ratio increases.

[24] Thwaites, B. (Editor), "Incompressible Aerodynamics," Oxford University Press, pp. 405-421 (1960).

[25] Allen, H.J. and E.E. Perkins, "A Study of Effects of Viscousity on Flow over Slender Inclined Bodies of Revolution," NACA Report 1048 (1951).

For a harmonically oscillating body in the vertical-plane modes in regular waves with a constant forward speed, the foregoing expression will be assumed to take the form

$$F_v = \frac{1}{2}\rho A_p (U^2 a_o \alpha + C_D w|w|)$$

where w is the relative fluid velocity with respect to the body and given by

$$w = \dot{\xi}_3 - x\dot{\xi}_5 + y\dot{\xi}_4 - \dot{\zeta}_v(x, \pm b(x), -d_1(x)) = U(\alpha - \xi_5)$$

The angle of incidence of flow at a cross section of the body at x can be expressed as

$$\alpha = \xi_5 + (\dot{\xi}_3 - x\dot{\xi}_5 + y\dot{\xi}_4 - \dot{\zeta}_v(x, \pm b(x), -d_1(x))/U \tag{28}$$

where $\dot{\zeta}_v$ = vertical velocity of the fluid induced by the incoming wave

$b(x)$ = transverse distance from the x-axis to the midpoint of the beam of one hull

$d_1(x)$ = depth to the maximum-breadth point at a cross section

The expression given above tacitly assumes that α is small and the diffraction of the incident wave can be neglected. It should be noted that the term $y\dot{\xi}_4$ will not contribute to the vertical force because of the symmetry of ship geometry with respect to the centerplane.

If the body is undergoing motion in the horizontal-plane modes, the angle of flow incidence at the mean depth of the cross section of x can be expressed as

$$\eta = -\xi_6 + (\dot{\xi}_2 + x\dot{\xi}_6 + d_2(x)\dot{\xi}_4 - \dot{\zeta}_H(x, \pm b(x), -d_2(x))/U \tag{29}$$

where $d_2(x)$ is one-half the draft at the cross section at x and $\dot{\zeta}_H(x, y, z)$ is the transverse velocity of the fluid induced by the incoming wave.

Now, similar to the potential-flow case, the strip concept will be introduced to Equation (27) together with the assumption of small α and no viscous interactions between the two hulls. The vertical force induced on the twin hulls can then be obtained by

$$F_v = \frac{\rho}{2} U^2 \int_L B_m(x) \sum_{i=1}^{2} (a_o \alpha_i(x) + C_D(\alpha_i - \xi_5)|\alpha_i - \xi_5|)\, dx$$

where $B_m(x)$ is the maximum beam of the submerged cross section of one hull at x and α_1 and α_2 are respectively the angle of incidence on the port and starboard hulls. With the following new notation defined by

$$\dot{z}_1 = \dot{z}_{1s} + \dot{z}_{1p},$$

$$\dot{z}_{1s} = \dot{\xi}_3 - x\dot{\xi}_5 - \dot{\zeta}_v(x, -b(x), -d_1(x))$$

and

$$\dot{z}_{1p} = \dot{\xi}_3 - x\,\dot{\xi}_5 - \dot{\zeta}_v(x, b(x), -d_1(x))$$

F_v can be written as

$$F_v = \frac{\rho}{2}\int_L B_m(x)\,[2\,a_o\,U^2\,\xi_5 + a_o\,U\,\dot{z}_1 + C_D\,(\dot{z}_{1s}\,|\dot{z}_{1s}| + \dot{z}_{1p}\,|\dot{z}_{1p}|]\,dx \qquad (30)$$

Similarly, the horizontal force F_H can be expressed as

$$F_H = \frac{\rho}{2}U^2\int_L d(x)\sum_{i=1}^{2}(a_o\,\eta_i(x) + C_D\,(\eta_i + \xi_6)\,|\eta_i + \xi_6|)\,dx$$

$$= \frac{\rho}{2}\int_L d\,[-2\,a_o\,U^2\,\xi_6 + a_o\,U\,\dot{y}_1 + C_D\,(\dot{y}_{1s}\,|\dot{y}_{1s}| + \dot{y}_{1p}\,|\dot{y}_{1p}|)]\,dx \qquad (31)$$

where $d(x)$ is the draft of the cross section at x,

$$\dot{y}_1 = \dot{y}_{1s} + \dot{y}_{1p}$$

$$\dot{y}_{1s} = \dot{\xi}_2 + x\,\dot{\xi}_6 + d_2(x)\,\dot{\xi}_4 - \dot{\zeta}_H(x, -b(x), -d_2(x))$$

$$\dot{y}_{1p} = \dot{\xi}_2 + x\,\dot{\xi}_6 + d_2\,\dot{\xi}_4 - \dot{\zeta}_H(x, b(x), -d_2(x))$$

In Equations (30) and (31), a_o and C_D are assumed to be constant over the length of the ship.

The moments contributed by the flow incident angles can similarly be given for roll moment by

$$M_R = \frac{\rho}{2}\int_L B_m(x)\,b(x)\,[a_o\,U\,\dot{z}_r + C_D\,(\dot{z}_{rs}\,|\dot{z}_{rs}| + \dot{z}_{rp}\,|\dot{z}_{rp}|)]\,dx$$

$$+\frac{\rho}{2}\int_L d(x)\,d_2(x)\,[-2\,a_o\,U^2\,\xi_6 + a_o\,U\,\dot{y}_1 + C_D\,(\dot{y}_{1s}\,|\dot{y}_{1s}| + \dot{y}_{1p}\,|\dot{y}_{1p}|)]\,dx \qquad (32)$$

where

$$\dot{z}_r = \dot{z}_{rs} + \dot{z}_{rp}$$

$$\dot{z}_{rs} = b(x)\,\dot{\xi}_4 + \dot{\zeta}_v(x, -b(x), -d_1(x))$$

$$\dot{z}_{rp} = b(x)\,\dot{\xi}_4 - \dot{\zeta}_v(x, b(x), -d_1(x))$$

For pitch moment, the equation is

$$M_P = -\frac{\rho}{2}\int_L x\, B_m(x)\,[2a_o U^2 \xi_5 + a_o U \dot{z} + C_D(\dot{z}_{1s}|\dot{z}_{1s}| + \dot{z}_{1p}|\dot{z}_{1p}|)]\,dx \qquad (33)$$

and for yaw moment:

$$M_Y = \frac{\rho}{2}\int_L x\, d(x)\,[-2a_o U^2 \xi_6 + a_o U \dot{y}_1 + C_D(\dot{y}_{1s}|\dot{y}_{1s}| + \dot{y}_{1p}|\dot{y}_{1p}|)]\,dx \qquad (34)$$

The fluid velocity induced by the incoming wave is obtained from Equation (26) by

$$\dot{\zeta}_v(x, y, z, t) = \frac{\partial \phi_I}{\partial z} e^{-j\omega t}$$

$$= e^{-j\omega t}\frac{\partial}{\partial z}\left(-\frac{jgA}{\omega_o}\exp(K_o z + jK_o x\cos\beta - jK_o y\sin\beta)\right)$$

$$= -j\omega_o A\exp(K_o z + jK_o x\cos\beta - jK_o y\sin\beta)\, e^{-j\omega t} \qquad (35)$$

and

$$\dot{\zeta}_H(x, y, z, t) = \frac{\partial \phi_I}{\partial y} e^{-j\omega t}$$

$$= -\omega_o A\exp(K_o z + jK_o x\cos\beta - jK_o y\sin\beta)\, e^{-j\omega t} \qquad (36)$$

The cross-flow drag terms in the foregoing expressions are nonlinear; hence they cannot be directly introducted into the linear equations of motion. By the rule of Fourier, it can be shown that

$$\cos\theta\,|\cos\theta| = \frac{\int_o^{2\pi}\cos\theta\,|\cos\theta|\cos n\theta\, d\theta}{\int_o^{2\pi}\cos^2 n\theta\, d\theta}\cos n\theta$$

$$= A_o + A_1\cos\theta + A_2\cos 2\theta + \ldots$$

where

$$A_o = 0$$

$$A_n = 0 \text{ for n even}$$

$$A_n = (-1)\frac{n+1}{2}\frac{8}{n(n^2-4)\pi} \text{ for n odd}$$

$$A_1 = \frac{8}{3\pi}, A_3 = \frac{8}{15\pi}, \ldots$$

Thus, for any harmonic motion given by $x = x_o \cos \omega t$, an approximation of

$$\dot{x}\,|\dot{x}| \simeq \frac{8}{3\pi}\,\omega\, x_o\, \dot{x} \tag{37}$$

can be established. This approximation is often called the equilinearization method, and it is used frequently for a dynamic system with weakly nonlinear behavior.

Substitution of the cross-flow drag terms in the foregoing equations for the forces and moments by the equilinearized form requires *a prior* knowledge of the amplitude of motion such as x_o in Equation (37). In the present work, the amplitude of motion is obtained by solving the equations of motion without the cross-flow damping terms; the equations of motion are then resolved with the equilinearized damping terms, and the process is repeated until a reasonable convergence on the motion amplitude is obtained.

The viscous damping coefficients and the wave-exciting coefficients can be derived from the foregoing expressions of the forces and moments generated by the viscous effects. These coefficients are expressed with an asterisk attached to the notation and are shown in Table 2. The definitions of the new notation used in Table 2 are given by

$$\dot{z}_{1o} = |\dot{z}_{1s}| + |\dot{z}_{1p}|$$

$$\dot{y}_{1o} = |\dot{y}_{1s}| + |\dot{y}_{1p}|$$

and

$$\dot{z}_{ro} = |\dot{z}_{rs}| + |\dot{z}_{rp}|$$

The restoring coefficients such as C^*_{26}, C^*_{46}, and C^*_{66} cannot be incorporated in Equation (16) since such restoring terms are not present. Thus, they will be lumped with the added inertia term by equating $C^*_{26} = -A^*_{26}/\omega^2$, $C^*_{46} = -A^*_{46}/\omega^2$, and $C^*_{66} = -A^*_{66}/\omega^2$. As long as the equations of motion in linear form are solved in the frequency domain, such an exchange of the terms between the inertial and restoring coefficients with the factor $(-\omega^2)$ will not alter the solutions. However, this exchange of the terms should not be made in the time-domain analysis of the motion and in the stability analysis of the ship.

TABLE 2 – VISCOUS DAMPING COEFFICIENTS

$$B^*_{22} = \rho a_o U \int_L d(x)\, dx + \rho \frac{4}{3\pi} C_D \int_L \dot{y}_{1o}(x)\, d(x)\, dx$$

$$B^*_{24} = \rho a_o U \int d\, d_2\, dx + \rho \frac{4}{3\pi} C_D \int \dot{y}_{1o}\, d\, d_2\, dx$$

$$B^*_{26} = \rho a_o U \int x\, d\, dx + \rho \frac{4}{3\pi} C_D \int \dot{y}_{1o}\, x\, d\, dx$$

$$C^*_{26} = -A^*_{26}/\omega^2 = -\rho a_o U^2 \int d\, dx$$

$$B^*_{33} = \rho a_o U \int B_m\, dx + \rho \frac{4}{3\pi} C_D \int \dot{z}_{1o}\, B_m\, dx$$

$$B^*_{35} = -\rho a_o U \int x\, B_m\, dx - \rho \frac{4}{3\pi} C_D \int x\, \dot{z}_{1o}\, B_m\, dx$$

$$C^*_{35} = \rho a_o U^2 \int B_m\, dx$$

$$B^*_{44} = \rho a_o U \int b^2\, B_m\, dx + \rho \frac{4}{3\pi} C_D \int \dot{z}_{To}\, b^2\, B_m\, dx$$

$$+ \rho a_o U \int d\, d_2^2\, dx + \rho \frac{4}{3\pi} C_D \int \dot{y}_{1o}\, d\, d_2^2\, dx$$

$$B^*_{42} = \rho a_o U \int d\, d_2\, dx + \rho \frac{4}{3\pi} C_D \int \dot{y}_{1o}\, d\, d_2\, dx$$

$$B^*_{46} = \rho a_o U \int x\, d\, d_2\, dx + \rho \frac{4}{3\pi} C_D \int \dot{y}_{1o}\, x\, d\, d_2\, dx$$

$$C^*_{46} = -A^*_{46}/\omega^2 = -\rho a_o U^2 \int d\, d_2\, dx$$

$$B^*_{55} = \rho a_o U \int x^2\, B_m\, dx + \rho \frac{4}{3\pi} C_D \int \dot{z}_{1o}\, x^2\, B_m\, dx$$

TABLE 2 (Continued)

$$B_{53}^{*} = -\rho a_o U \int x B_m \, dx - \rho \frac{4}{3\pi} C_D \int \dot{z}_{1o} x B_m \, dx$$

$$C_{55}^{*} = -\rho a_o U^2 \int x B_m \, dx$$

$$B_{66}^{*} = \rho a_o U \int x^2 d \, dx + \rho \frac{4}{3\pi} C_D \int \dot{y}_{1o} x^2 d \, dx$$

$$B_{62}^{*} = \rho a_o U \int x d \, dx + \rho \frac{4}{3\pi} C_D \int \dot{y}_{1o} x d \, dx$$

$$B_{64}^{*} = \rho a_o U \int x d d_2 \, dx + \rho \frac{4}{3\pi} C_D \int \dot{y}_{1o} x d d_2 \, dx$$

$$C_{66}^{*} = -A_{66}^{*}/\omega^2 = -\rho a_o U^2 \int x d \, dx$$

$$F_2^{*} = -\rho \omega_o A a_o U \int d e^{K_o(-d_2 + j x \cos\beta)} \cos(K_o b(x) \sin\beta) \, dx$$

$$-\rho \frac{4}{3\pi} \omega_o A C_D \int d e^{K_o(-d_2 + j x \cos\beta)} (e^{j K_o b \sin\beta} |\dot{y}_{1s}| + e^{-j K_o b \sin\beta} |\dot{y}_{1p}|) \, dx$$

$$F_3^{*} = -j\rho \omega_o A a_o U \int B_m e^{K_o(-d_1 + j x \cos\beta)} \cos(K_o b \sin\beta) \, dx$$

$$-j\rho \frac{4}{3\pi} \omega_o A C_D \int B_m e^{K_o(-d_1 + j x \cos\beta)} (e^{j K_o b \sin\beta} |\dot{z}_{1s}| + e^{-j K_o b \sin\beta} |\dot{z}_{1p}|) \, dx$$

$$F_4^{*} = -\rho \omega_o A a_o U \int B_m b e^{K_o(-d_1 + j x \cos\beta)} \sin(K_o b \sin\beta) \, dx$$

$$+j\rho \frac{4}{3\pi} \omega_o A C_D \int B_m b e^{K_o(-d_1 + j x \cos\beta)} (e^{j K_o b \sin\beta} |\dot{z}_{1s}| - e^{-j K_o b \sin\beta} |\dot{z}_{1p}|) \, dx$$

$$F_5^{*} = j\rho \omega_o A a_o U \int x B_m e^{K_o(-d_1 + j x \cos\beta)} \cos(K_o b \sin\beta) \, dx$$

TABLE 2 (Continued)

$$+ j\rho \frac{4}{3\pi} \omega_o A C_D \int x B_m e^{K_o(-d_1 + jx\cos\beta)} (e^{jK_o b \sin\beta} |\dot{z}_{1s}| + e^{-jK_o b \sin\beta} |\dot{z}_{1p}|) dx$$

$$F_6^* = -\rho \omega_o A a_o U \int x d e^{K_o(-d_2 + jx\cos\beta)} \cos(K_o b \sin\beta) dx$$

$$-\rho \frac{4}{3\pi} \omega_o A C_D \int x d e^{K_o(-d_2 + jx\cos\beta)} (e^{jK_o b \sin\beta} |\dot{y}_{1s}| + e^{-jK_o b \sin\beta} |\dot{y}_{1p}|) dx$$

FIN-GENERATED LIFT COEFFICIENTS

As mentioned earlier, a SWATH configuration can become unstable in the vertical-plane modes at high speeds due to an inherently small waterplane area. Both theoretical[26] and experimental[27] investigations showed that small horizontal fins fixed on the inboard sides of the hull at certain longitudinal positions significantly improve the stability and considerably reduce the peak motion amplitude.

The reduction of the peak-motion amplitude for heave, pitch, and roll modes was more significant when the stabilizing fins were placed both forward and aft of the longitudinal center of gravity. For stability, the aft fins should be larger than the forward fins. The main factor contributing to the reduction of the peak-motion amplitude stems from the damping effects of the fins. It will be shown later that the angle of attack on the fins is proportional to the vertical velocity of the fins when the ship has a forward speed.

Fins, being a lifting surface, generate a lift when subjected to an angle of attack. For fins attached to a SWATH ship, the angle of attack on the fins can be generated by the trim and the relative fluid velocity with respect to the fins in the horizontal and vertical directions. The trim angle can easily be found if the pitch angle of the body is known, but to find the relative fluid velocity components involves the motion of the fins with respect to the fluid motion caused by the incoming and diffracted waves and the forward speed of the ship. It is therefore a tremendously difficult task to perform an accurate evaluation of the lift generated by the fins. To name a few hydrodynamic effects to be considered, there are body-fin inter-

[26] Lee, C.M. and M. Martin, "Determination of Size of Stabilizing Fins for Small Waterplane Area, Twin-Hull Ships," DTNSRDC Report 4495 (1974).

[27] Kallio, J.A. and J.J. Ricci, "Seaworthiness Characteristics of a Small Waterplane Area Twin-Hull (SWATH IV) Part II," DTNSRDC Report SPD 620-02 (1976).

actions, the blockage effect of the other hull, unsteady effect, boundary-layer effect, downwash and upwash effects between the fore-and-aft fins and from the fins on the other hull, the free-surface effect on the fins, and so forth. It is an almost impossible task to take into account the aforementioned effects satisfactorily, hence the following assumptions will be made to keep the analysis in a tractable form. Except for the body-fin effect based on the investigation performed by Pitts, Nielsen, and Kaattari,[28] all other effects will be neglected. Justification for neglecting some of the effects may be made, but most of the justification will be based on heuristic physical arguments, and will be omitted in this report except for the investigation shown in Appendix B.

Let the center of pressure of a thin foil of span S and chord C be located at $x = \ell$. The lift L on the foil with a small angle of attack can be expressed by

$$L(t) = \frac{\rho}{2} U^2 A^{(f)} C_{L\alpha} \alpha(t) \tag{38}$$

where $A^{(f)}$ is the plane area of the foil and $C_{L\alpha}$ the lift-curve slope. The $C_{L\alpha}$ will be assumed to be the sum of the two effects which can be expressed as

$$C_{L\alpha} = (K_{W(B)} + K_{B(W)})(C_{L\alpha})_W \tag{39}$$

where

$$K_{W(B)} = \frac{(C_{L\alpha})_{W(B)}}{(C_{L\alpha})_W}$$

$$K_{B(W)} = \frac{(C_{L\alpha})_{B(W)}}{(C_{L\alpha})_W}$$

in which the subscript W represents the case of the foil alone, B(W) the case of the lift on the body induced by the foil, and W(B) the case of the lift on the wing induced by the body. According to slender body theory,[29,30] $K_{W(B)}$ and $K_{B(W)}$ can be expressed in terms of the ratio of the radius of the body r at which the fin is attached and the transverse distance from the body axis to the tip of the fin r_o, i.e.,

[28]Pitts, W.C., J.N. Nielsen and G.E. Kaattari, "Lift and Center of Pressure of Wing-Body-Tail Combinations at Subsonic, Transonic, and Supersonic Speeds," NACA Report 1307 (1959).

[29]Spreiter, J.R., "The Aerodynamic Forces on Slender Plane- and Cruciform-Wing and Body Combinations," NACA Report 962 (1950).

[30]Morikawa G., "Supersonic Wing-Body Lift," J. Aeron. Sci., Vol. 18, No. 4, pp. 217-228 (1951).

$$K_{W(B)} = \frac{2}{\pi(1-\delta)^2}\left[(1+\delta^4)\left\{\frac{1}{2}\tan^{-1}\frac{1}{2}\left(\frac{1}{\delta}-\delta\right)+\frac{\pi}{4}\right\}\right.$$

$$\left.-\delta^2\left\{\left(\frac{1}{\delta}-\delta\right)+2\tan^{-1}\delta\right\}\right] \tag{40}$$

$$K_{B(W)} = \frac{1}{(1-\delta^2)}\left[(1-\delta^2)^2-\frac{2}{\pi}\left[(1+\delta^4)\left\{\frac{1}{2}\tan^{-1}\frac{1}{2}\left(\frac{1}{\delta}-\delta\right)+\frac{\pi}{4}\right\}\right.\right.$$

$$\left.\left.-\delta^2\left\{\left(\frac{1}{\delta}-\delta\right)+2\tan^{-1}\delta\right\}\right]\right] \tag{41}$$

where $\delta = r/r_o$. The foregoing two functions are plotted in Figure 6.

An empirical formula derived by Whicker and Fehlner[31] for low aspect ratio wings will be used for the evaluation of $(C_{L\alpha})_W$. The expression for the wings of zero sweep angle is given by

$$(C_{L\alpha})_W = \frac{1.8\,\pi\,A_e}{1.8+\sqrt{A_e^2+4}} \text{ per radian} \tag{42}$$

Rather than taking twice the value of the geometric aspect ratio as did Whicker and Fehlner, we choose the effective aspect ratio in this report as

$$A_e = \left(r_o - \frac{r^2}{r_o}\right)/C \tag{43}$$

where C is the average chord of the fin.

The numerator of the above equation corresponds to the distance between a point vortex located at the tip of the wing and its reflected image inside a circle. The foregoing approach is mainly designed to make an engineering approximation rather than seeking a rigorous rational approach. For more rigorous approaches, see the extensive review given in Ashley and Rodden.[32] Since the fins are attached to an oscillating body, the unsteady effect on the lifting characteristics may be important. However, it can be found from Lawrence and Gerber[33] that the unsteady effect on $(C_{L\alpha})_W$ is negligible for wings of aspect ratio less than 1.5.

[31] Whicker, L.F. and L.F. Fehlner, "Free-Stream Characteristics of a Family of Low-Aspect-Ratio, All-Movable Control Surfaces for Application to Ship Design," David Taylor Model Basin Report 933 (1958).

[32] Ashley, H. and W.P. Rodden, "Wing-Body Aerodynamic Interaction," Ann. Rev. Fluid Mech., Vol. 4 (1972).

[33] Lawrence, H.R. and E.H. Gerber, "The Aerodynamic Forces on Low Aspect Ratio Wings Oscillating in an Incompressible Flow," J. Aeron. Sci., Vol. 19, No. 11, pp. 769-781 (1952).

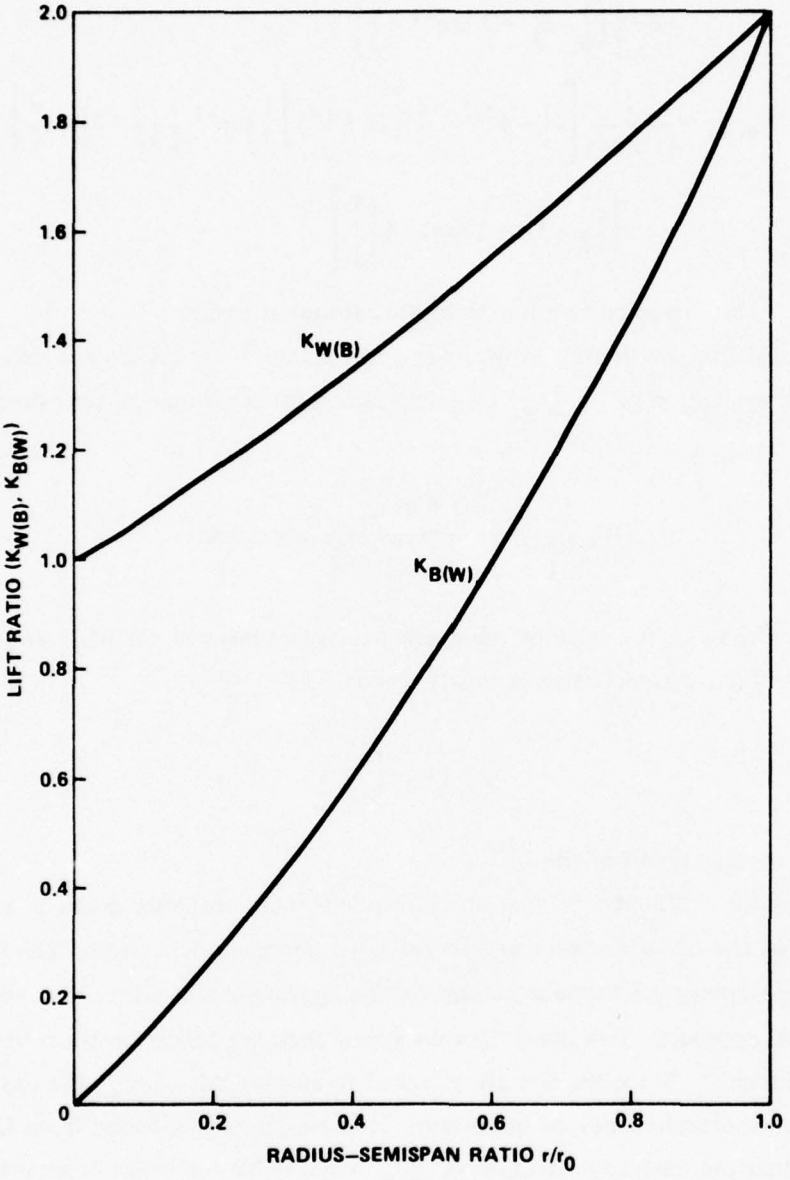

Figure 6 – Values of Lift Ratios Based on Slender-Body Theory
(From Pitts et al.[28])

The angle of attack on a fin at the center of pressure located at $(\ell, b_1, -d_1(\ell))$ can be obtained under the assumption of a small angle of attack by

$$\alpha(t) = \xi_5(t) + \frac{(\dot{\xi}_3(t) - \ell\,\dot{\xi}_5(t) + b_1\,\dot{\xi}_4(t) - \dot{\zeta}_v(\ell, b_1, -d_1, t))}{U} \tag{44}$$

where the wave-induced vertical velocity $\dot{\zeta}_v$ is defined in Equation (35). The center of pressure of a fin will be assumed to be located at the midspan and quarter-chord from the leading edge. Here again, the wave-diffraction effects by the body and the fins are neglected.

When a foil oscillates vertically, a cross-flow drag and virtual inertia force result. The cross-flow drag D(t) can be expressed as

$$D(t) = \frac{\rho}{2} A^{(f)} C_D^{(f)} (\dot{\xi}_3 - \ell\,\dot{\xi}_5 + b_1\,\dot{\xi}_4 - \dot{\zeta}_v) \,|\, \dot{\xi}_3 - \ell\,\dot{\xi}_5 + b_1\,\dot{\xi}_4 - \dot{\zeta}_v \,| \tag{45}$$

where $C_D^{(f)}$ is the cross-flow drag coefficient of the foil, and the virtual inertia force I(t) can be expressed as

$$I(t) = (m^{(f)} + a_{33}^{(f)})(\ddot{\xi}_3 - \ell\,\ddot{\xi}_5 + b_1\,\ddot{\xi}_4) \tag{46}$$

Unless the mass of the fin is specified, it will be approximated by taking the fin section as a neutrally buoyant ellipse as $m^{(f)} = \rho\,\pi/4\ SCt$ where S is the span and t is the maximum thickness of the fin. The added mass will be approximated by $a_{33}^{(f)} = \rho S\,\pi/4\ C^2$. For N number of fins for each hull, the heave force $F_v^{(f)}$, pitch moment $M_p^{(f)}$, and roll moment $M_R^{(f)}$ contributed by 2N fins can be obtained from the foregoing results as shown below.

$$\begin{aligned} F_v^{(f)} &= I(t) + L(t) + D(t) \\ &= \sum_{i=1}^{N} \Bigg[(m_i^{(f)} + a_{33i}^{(f)})(\ddot{\xi}_3 - \ell_i\,\ddot{\xi}_5) \\ &\quad + \frac{\rho}{2} U^2 A_i^{(f)} C_{L\alpha_i} \left\{ 2\xi_5 + 2\frac{\dot{\xi}_3 - \ell_i\,\dot{\xi}_5}{U} - \frac{\dot{\zeta}_v(b_{1i}) + \dot{\zeta}_v(-b_{1i})}{U} \right\} \\ &\quad + \frac{\rho}{2} A_i^{(f)} C_{Di}^{(f)} \Big\{ (\dot{\xi}_3 - \ell_i\,\dot{\xi}_5 - \dot{\zeta}_v(b_{1i})) \,|\, \dot{\xi}_3 - \ell_i\,\dot{\xi}_5 - \dot{\zeta}_v(b_{1i}) \,| \\ &\quad + (\dot{\xi}_3 - \ell_i\,\dot{\xi}_5 - \dot{\zeta}_v(-b_{1i})) \,|\, \dot{\xi}_3 - \ell_i\,\dot{\xi}_5 - \dot{\zeta}_v(-b_{1i}) \,| \Big\} \Bigg] \end{aligned} \tag{47}$$

where the abbreviation $\dot{\zeta}_v(b_{1i})$ stands for $\dot{\zeta}_v(\ell_i, b_{1i}, -d_{1i})$ and the lift-curve slope for the ith fin $C_{L\alpha i}$ is obtained from Equation (39).

It can be noticed in the above equation that the roll-contributed lift and drag do not appear because these forces on the fins are located opposite to one another and will be canceled. Strictly speaking, however, the vertical velocity contributed by the roll motion should have been included within the absolute signs in Equation (47). Since the introduction of the roll motion in the vertical-plane modes complicates the computational procedure, it will be tacitly assumed that the roll effect on $F_V^{(f)}$ is negligible. The pitch moment is obtained by

$$M_P^{(f)} = -\sum_{i=1}^{N} \ell_i f_i \tag{48}$$

where f_i is the expression given within the brackets after the summation sign in Equation (47). The roll moment is obtained by

$$\begin{aligned} M_R^{(f)} = \sum_{i=1}^{N} \Bigg[& b_{1i}^2 \left(m_i^{(f)} + a_{33i}^{(f)}\right) \ddot{\xi}_4 \\ & + \frac{\rho}{2} U A_i^{(f)} C_{L\alpha i} \left\{ b_{1i}(2 b_{1i} \dot{\xi}_4 - \dot{\zeta}_v(b_{1i}) + \dot{\zeta}_v(-b_{1i})) \right\} \\ & + \frac{\rho}{2} A_i^{(f)} C_{Di}^{(f)} \Big\{ b_{1i}(b_{1i} \dot{\xi}_4 - \dot{\zeta}_v(b_{1i})) \, | b_{1i} \dot{\xi}_4 - \dot{\zeta}_v(b_{1i}) | \\ & + b_{1i}(b_{1i} \dot{\xi}_4 + \dot{\zeta}_v(-b_{1i})) \, | b_{1i} \dot{\xi}_4 + \dot{\zeta}_v(-b_{1i}) | \Big\} \Bigg] \end{aligned} \tag{49}$$

Table 3 indicates hydrodynamic coefficients associated with the stabilizing fins. The superscript (f) is used to denote these coefficients. Equilinearization for viscous damping, as shown in Equation (37), is also made. The relative fluid vertical velocity amplitude at the ith fin on the starboard side hull $\dot{z}_{so}$ and on the port side hull $\dot{z}_{po}$ are defined by

$$\dot{z}_{so} = | \dot{\xi}_3 - \ell_i \dot{\xi}_5 - \dot{\zeta}_v(\ell_i, - b_{1i}, - d_{1i}) | \tag{50}$$

$$\dot{z}_{po} = | \dot{\xi}_3 - \ell_i \dot{\xi}_5 - \dot{\zeta}_v(\ell_i, b_{1i}, - d_{1i}) | \tag{51}$$

and the relative velocity amplitude due to the roll motion is also similarly defined by

$$\dot{z}_{so}^{(R)} = | b_{1i} \dot{\xi}_4 + \dot{\zeta}_v(\ell_i, - b_{1i}, - d_{1i}) | \tag{52}$$

$$\dot{z}_{po}^{(R)} = | b_{1i} \dot{\xi}_4 - \dot{\zeta}_v(\ell_i, b_{1i}, - d_{1i}) | \tag{53}$$

TABLE 3 – HYDRODYNAMIC COEFFICIENTS OF STABILIZING FINS

$$A_{33}^{(f)} = \sum_{i=1}^{N} (m_i^{(f)} + a_{33i}^{(f)})$$

$$A_{35}^{(f)} = - \Sigma \, \ell_i \, (m_i^{(f)} + a_{33i}^{(f)}$$

$$B_{33}^{(f)} = \rho \, \Sigma \, A_i^{(f)} \left\{ U \, C_{L\alpha i} + \frac{4}{3\pi} \, C_{Di}^{(f)} \, (\dot{z}_{so} + \dot{z}_{po}) \right\}$$

$$B_{35}^{(f)} = \rho \, \Sigma \, \ell_i \, A_i^{(f)} \left\{ U \, C_{L\alpha i} + \frac{4}{3\pi} \, C_{Di}^{(f)} \, (\dot{z}_{so} + \dot{z}_{po}) \right\}$$

$$C_{35}^{(f)} = \rho \, U^2 \, \Sigma \, A_i^{(f)} \, C_{L\alpha i}$$

$$A_{44}^{(f)} = \Sigma \, b_{1i}^2 \, (m_i^{(f)} + a_{33i}^{(f)})$$

$$B_{44}^{(f)} = \rho \, \Sigma \, b_{1i}^2 \, A_i^{(f)} \left\{ U \, C_{L\alpha i} + \frac{4}{3\pi} \, C_{Di}^{(f)} \, (\dot{z}_{so}^{(R)} + \dot{z}_{po}^{(R)}) \right\}$$

$$A_{55}^{(f)} = \Sigma \, \ell_i^2 \, (m_i^{(f)} + a_{33i}^{(f)})$$

$$A_{53}^{(f)} = A_{35}^{(f)}$$

$$B_{55}^{(f)} = \rho \, \Sigma \, \ell_i^2 \, A_i^{(f)} \left\{ U \, C_{L\alpha i} + \frac{4}{3\pi} \, C_{Di}^{(f)} \, (\dot{z}_{so} + \dot{z}_{po}) \right\}$$

$$B_{53}^{(f)} = B_{35}^{(f)}$$

$$C_{55}^{(f)} = - \rho \, U^2 \, \Sigma \, \ell_i \, A_i^{(f)} \, C_{L\alpha i}$$

$$F_3^{(f)} = - \rho \, \omega_o \, A \, U \, \Sigma \, A_i^{(f)} \, C_{L\alpha i} \, e^{K_o(-d_{1i} + j \ell_i \cos\beta)} \cos (K_o \, b_{1i} \sin\beta)$$

$$- j \rho \, \frac{4}{3\pi} \, \omega_o \, A \, \Sigma \, A_i^{(f)} \, C_{Di}^{(f)} \, e^{K_o(-d_{1i} + j \ell_i \cos\beta)}$$

$$(\dot{z}_{so} \, e^{j K_o \, b_{1i} \sin\beta} + \dot{z}_{po} \, e^{-j K_o \, b_{1i} \sin\beta})$$

$$F_4^{(f)} = - \rho \, \omega_o \, A \, U \, \Sigma \, b_{1i} \, A_i^{(f)} \, C_{L\alpha i} \, e^{K_o(-d_{1i} + j \ell_i \cos\beta)} \sin (K_o \, b_{1i} \sin\beta)$$

$$+ j \rho \, \frac{4}{3\pi} \, \omega_o \, A \, \Sigma \, b_{1i} \, A_i^{(f)} \, C_{Di}^{(f)} \, e^{K_o(-d_{1i} + j \ell_i \cos\beta)}$$

$$(\dot{z}_{so}^{(R)} \, e^{j K_o \, b_{1i} \sin\beta} - \dot{z}_{po}^{(R)} \, e^{-j K_o \, b_{1i} \sin\beta})$$

TABLE 3 – (Continued)

$$F_5^{(f)} = j\rho\,\omega_o\,A\,U\,\Sigma\,\ell_i\,A_i^{(f)}\,C_{L\alpha i}\,e^{K_o(-d_{1i}+j\ell_i\cos\beta)}\cos(K_o\,b_{1i}\sin\beta)$$

$$+ j\rho\,\frac{4}{3\pi}\,\omega_o\,A\,\Sigma\,\ell_i\,A_i^{(f)}\,C_{Di}^{(f)}\,e^{K_o(-d_{1i}+j\ell_i\cos\beta)}$$

$$(\dot{z}_{so}\,e^{jK_o\,b_{1i}\sin\beta} + \dot{z}_{po}\,e^{-jK_o\,b_{1i}\sin\beta})$$

The hydrodynamic coefficients of a SWATH ship with stabilizing fins are the sum of the effects of the potential flow, viscosity, and fins; the final expressions for the hydrodynamic coefficients to be used in the equations of motion ((5) and (6)) can be obtained by summing the coefficients in Tables 1 through 3 and are shown in Table 4. An exception to the straightforward summation is made for B_{35}, B_{53}, and A_{55} in which A_{33} is taken as the sum of the heave added mass of the bare hull and the fins.

TABLE 4 – TOTAL HYDRODYNAMIC COEFFICIENTS

$$A_{1k} = B_{1k} = 0 \quad \text{for } k = 1, 2, \cdots, 6$$

$$A_{22} = \int_L a_{22}(x)\,dx$$

$$B_{22} = \int b_{22}\,dx + \rho\,a_o\,U\int_L d\,dx + \rho\,\frac{4}{3\pi}\,C_D\int \dot{y}_{1o}\,d\,dx$$

$$A_{24} = \int a_{24}\,dx$$

$$B_{24} = \int b_{24}\,dx + \rho\,a_o\,U\int d\,d_2\,dx + \rho\,\frac{4}{3\pi}\,C_D\int \dot{y}_{1o}\,d\,d_2\,dx$$

$$A_{26} = \int x\,a_{22}\,dx + \frac{U}{\omega^2}\int b_{22}\,dx + \frac{\rho\,a_o\,U^2}{\omega^2}\int d\,dx$$

TABLE 4 – (Continued)

$$B_{26} = \int x\, b_{22}\, dx - U \int a_{22}\, dx + \rho\, a_o\, U \int x\, d\, dx + \rho\, \frac{4}{3\pi}\, C_D \int \dot{y}_{1o}\, x\, d\, dx$$

$$A_{33} = \int a_{33}\, dx + \sum_{i=1}^{N} (m_i^{(f)} + a_{33}^{(f)})$$

$$B_{33} = \int b_{33}\, dx + \rho\, a_o\, U \int B_m\, dx + \rho\, \frac{4}{3\pi}\, C_D \int \dot{z}_{1o}\, B_m\, dx + \rho \sum_{i=1}^{N} A_i^{(f)} \left\{ U\, C_{L\alpha i} + \frac{4}{3\pi}\, C_{Di}^{(f)}\, (\dot{z}_{so} + \dot{z}_{po}) \right\}$$

$$C_{33} = \rho\, g\, A_w$$

$$A_{35} = -\int x\, a_{33}\, dx - \frac{U}{\omega^2} \int b_{33}\, dx - \sum_{i=1}^{N} \ell_i (m_i^{(f)} + a_{33i}^{(f)})$$

$$B_{35} = -\int x\, b_{33}\, dx + U\, A_{33} - \rho\, a_o\, U \int x\, B_m\, dx - \rho\, \frac{4}{3\pi}\, C_D \int \dot{z}_{1o}\, x\, B_m\, dx - \rho \sum_{i=1}^{N} \ell_i\, A_i^{(f)} \left\{ U\, C_{L\alpha i} + \frac{4}{3\pi}\, C_{Di}^{(f)}\, (\dot{z}_{so} + \dot{z}_{po}) \right\}$$

$$C_{35} = \rho\, g\, M_w + \rho\, a_o\, U^2 \int B_m\, dx + \rho\, U^2 \sum_{i=1}^{N} A_i^{(f)}\, C_{L\alpha i}$$

$$A_{44} = \int a_{44}\, dx + \sum_{i=1}^{N} b_{1i}^{\,2}\, (m_i^{(f)} + a_{33i}^{(f)})$$

$$B_{44} = \int b_{44}\, dx + \rho\, a_o\, U \int b^2\, B_m\, dx + \rho\, \frac{4}{3\pi}\, C_D \int \dot{z}_{ro}\, b^2\, B_m\, dx + \rho \sum_{i=1}^{N} b_{1i}^{\,2}\, A_i^{(f)} \left\{ U\, C_{L\alpha i} + \frac{4}{3\pi}\, C_{Di}^{(f)}\, (\dot{z}_{so}^{(R)} + \dot{z}_{po}^{(R)}) \right\} + \rho\, a_o\, U \int d\, d_2^{\,2}\, dx + \rho\, \frac{4}{3\pi}\, C_D \int \dot{y}_{1o}\, d\, d_2^{\,2}\, dx$$

TABLE 4 (Continued)

$$C_{44} = \rho g I_{w4} - M g \overline{BG}$$

$$A_{42} = \int a_{24}\, dx$$

$$B_{42} = \int b_{24}\, dx + \rho a_o U \int d\, d_2\, dx + \rho \frac{4}{3\pi} C_D \int \dot{y}_{1o}\, d\, d_2\, dx$$

$$A_{46} = \int x\, a_{24}\, dx + \frac{U}{\omega^2} \int b_{24}\, dx + \rho \frac{U^2}{\omega^2} a_o \int d\, d_2\, dx$$

$$B_{46} = \int x\, b_{24}\, dx - U \int a_{24}\, dx + \rho a_o U \int x\, d\, d_2\, dx + \rho \frac{4}{3\pi} C_D \int \dot{y}_{1o}\, x\, d\, d_2\, dx$$

$$A_{55} = \int x^2\, a_{33}\, dx + \frac{U^2}{\omega^2} A_{33} + \sum_{i=1}^{N} \ell_i^2 \left(m_i^{(f)} + a_{33_i}^{(f)}\right)$$

$$B_{55} = \int x^2\, b_{33}\, dx + \frac{U^2}{\omega^2} \int b_{33}\, dx + \rho a_o U \int x^2\, B_m\, dx + \rho \frac{4}{3\pi} C_D \int \dot{z}_{1o}\, x^2\, B_m\, dx$$

$$+ \rho \sum_{i=1}^{N} \ell_i^2\, A_i^{(f)} \left\{ U C_{L\alpha i} + \frac{4}{3\pi} C_{Di}^{(f)} \left(\dot{z}_{so} + \dot{z}_{po}\right) \right\}$$

$$C_{55} = \rho g I_{w5} - M g \overline{BG} - \rho a_o U^2 \int x\, B_m\, dx - \rho U^2 \sum_{i=1}^{N} \ell_i\, A_i^{(f)}\, C_{L\alpha i}$$

$$A_{53} = -\int x\, a_{33}\, dx + \frac{U}{\omega^2} \int b_{33}\, dx - \sum_{i=1}^{N} \ell_i \left(m_i^{(f)} + a_{33_i}^{(f)}\right)$$

$$B_{53} = -\int x\, b_{33}\, dx - U A_{33} - \rho a_o U \int x\, B_m\, dx - \rho \frac{4}{3\pi} C_D \int \dot{z}_{1o}\, x\, B_m\, dx$$

$$- \rho \sum_{i=1}^{N} \ell_i\, A_i^{(f)} \left\{ U C_{L\alpha i} + \frac{4}{3\pi} C_{Di}^{(f)} \left(\dot{z}_{so} + \dot{z}_{po}\right) \right\}$$

$$C_{53} = \rho g M_w$$

TABLE 4 (Continued)

$$A_{66} = \int x^2 a_{22}\, dx + \frac{U^2}{\omega^2} \int a_{22}\, dx + \rho \frac{U^2}{\omega^2} a_o \int x\, d\, dx$$

$$B_{66} = \int x^2 b_{22}\, dx + \frac{U^2}{\omega^2} \int b_{22}\, dx + \rho\, a_o\, U \int x^2\, d\, dx + \rho \frac{4}{3\pi} C_D \int \dot{y}_{1o}\, x^2\, d\, dx$$

$$A_{62} = \int x\, a_{22}\, dx - \frac{U}{\omega^2} \int b_{22}\, dx$$

$$B_{62} = \int x\, b_{22}\, dx + U \int a_{22}\, dx + \rho\, a_o\, U \int x\, d\, d_2\, dx + \rho \frac{4}{3\pi} C_D \int \dot{y}_{1o}\, x\, d\, dx$$

$$A_{64} = \int x\, a_{24}\, dx - \frac{U}{\omega^2} \int b_{24}\, dx$$

$$B_{64} = \int x\, b_{24}\, dx + U \int a_{24}\, dx + \rho\, a_o\, U \int x\, d\, d_2\, dx + \rho \frac{4}{3\pi} C_D \int \dot{y}_{1o}\, x\, d\, d_2\, dx$$

$$F_1^{(e)} = \rho\, g\, A \int_L dx\, e^{jK_o x \cos\beta}\, n_1 \int_{C(x)} (-jN_2 \sin\beta + N_3)\, e^{K_o(z - jy\sin\beta)}\, d\ell$$

$$F_2^{(e)} = -\frac{j\rho\, g\, A}{\omega_o} \int_L dx\, e^{jK_o x\cos\beta} \int_{C(x)} \left\{ j\omega_o N_2 + K_o(-jN_2\sin\beta + N_3)\,\phi_2' \right\} e^{K_o(z - jy\sin\beta)}\, d\ell$$

$$- \rho\, \omega_o\, A\, a_o\, U \int_L dx\, d\, e^{K_o(-d_2(x) + jx\cos\beta)} \cos\left(K_o\, b(x)\sin\beta\right)$$

$$- \rho \frac{4}{3\pi} \omega_o\, A\, C_D \int_L dx\, d\, e^{K_o(-d_2 + jx\cos\beta)} \left(e^{jK_o\, b\sin\beta} \left|\dot{y}_{1s}\right| + e^{-jK_o\, b\sin\beta} \left|\dot{y}_{1p}\right|\right)$$

$$F_3^{(e)} = \frac{-j\rho\, g\, A}{\omega_o} \int_L dx\, e^{jK_o x\cos\beta} \int_{C(x)} \left\{ j\omega_o N_3 + K_o(-jN_2\sin\beta + N_3)\,\phi_3' \right\} e^{K_o(z - jy\sin\beta)}\, d\ell$$

$$- j\rho\, \omega_o\, A\, a_o\, U \int_L dx\, B_m(x)\, e^{K_o(-d_1(x) + jx\cos\beta)} \cos\left(K_o\, b(x)\sin\beta\right)$$

$$- j\rho \frac{4}{3\pi} \omega_o\, A\, C_D \int_L dx\, Bm\, e^{K_o(-d_1 + jx\cos\beta)} \left(e^{jK_o\, b\sin\beta} \left|\dot{z}_{1s}\right| + e^{-jK_o\, b\sin\beta} \left|\dot{z}_{1p}\right|\right)$$

TABLE 4 (Continued)

$$- j\rho\omega_o A U \sum_i A_i^{(f)} C_{L\alpha i} e^{K_o(-d_{1i} + j\ell_i \cos\beta)} \cos(K_o b_{1i} \sin\beta)$$

$$- j\rho \frac{4}{3\pi} \omega_o A \sum A_i^{(f)} C_{Di}^{(f)} e^{K_o(-d_{1i} + j\ell_i \cos\beta)} (\dot{z}_{so} e^{jK_o b_{1i} \sin\beta} + \dot{z}_{po} e^{-jK_o b_{1i} \sin\beta})$$

$$F_4^{(e)} = -\frac{j\rho g A}{\omega_o} \int_L dx\, e^{jK_o x \cos\beta} \int_{C(x)} \left\{ j\omega_o (y N_3 - z N_2) \right.$$

$$\left. + K_o (-j N_2 \sin\beta + N_3) \phi_4' \right\} e^{K_o(z - jy \sin\beta)} d\ell$$

$$- \rho\omega_o A a_o U \int_L dx\, B_m(x)\, b(x)\, e^{K_o(-d_1(x) + jx \cos\beta)} \sin(K_o b \sin\beta)$$

$$+ j\rho \frac{4}{3\pi} \omega_o A C_D \int_L dx\, B_m\, b\, e^{K_o(-d_1 + jx \cos\beta)} (|\dot{z}_{1s}| e^{jK_o b \sin\beta} - |\dot{z}_{1p}| e^{-jK_o b \sin\beta})$$

$$- \rho\omega_o A a_o U \int_L dx\, d(x)\, d_2(x)\, e^{K_o(-d_2 + jx \cos\beta)} \cos(K_o b(x) \sin\beta)$$

$$- \rho \frac{4}{3\pi} \omega_o A C_D \int_L dx\, d\, d_2\, e^{K_o(-d_2 + jx \cos\beta)} (|\dot{y}_{1s}| e^{jK_o b \sin\beta} + |\dot{y}_{1p}| e^{-jK_o b \sin\beta})$$

$$- \rho\omega_o A U \sum b_{1i} A_i^{(f)} C_{L\alpha i} e^{K_o(-d_{1i} + j\ell_i \cos\beta)} \cos(K_o b_{1i} \sin\beta)$$

$$+ j\rho \frac{4}{3\pi} \omega_o A \sum b_{1i} A_i^{(f)} C_{Di}^{(f)} e^{K_o(-d_{1i} + j\ell_i \cos\beta)}$$

$$(\dot{z}_{so}^{(R)} e^{jK_o b_{1i} \sin\beta} - \dot{z}_{po}^{(R)} e^{-jK_o b_{1i} \sin\beta})$$

$$F_5^{(e)} = -\frac{j\rho g A}{\omega_o} \int dx\, e^{jK_o x \cos\beta} \int \left\{ -j\omega_o x N_3 \right.$$

$$\left. + K_o(-j N_2 \sin\beta + N_3) \left(\frac{U}{j\omega} - x \right) \phi_3' \right\} e^{K_o(z - jy \sin\beta)} d\ell$$

$$+ j\rho\omega_o A a_o U \int dx\, x\, B_m(x) e^{K_o(-d_1(x) + jx \cos\beta)} \cos(K_o b(x) \sin\beta)$$

TABLE 4 (Continued)

$$+ j\rho \frac{4}{3\pi} \omega_o A C_D \int dx\, x\, B_m\, e^{K_o(-d_1 + jx\cos\beta)} \left(|\dot{z}_{1s}|\, e^{jK_o b \sin\beta} + |\dot{z}_{1p}|\, e^{-jK_o b \sin\beta} \right)$$

$$+ j\rho\, \omega_o A U \Sigma\, \ell_i A_i^{(f)} C_{L\alpha i}\, e^{K_o(-d_{1i} + j\ell_i \cos\beta)} \cos\left(K_o b_{1i} \sin\beta\right)$$

$$+ j\rho \frac{4}{3\pi} \omega_o A\, \Sigma\, \ell_i A_j^{(f)} C_{Di}^{(f)}\, e^{K_o(-d_{1i} + j\ell_i \cos\beta)} \left(\dot{z}_{so}\, e^{jK_o b_{1i} \sin\beta} + \dot{z}_{po}\, e^{-jK_o b_{1i} \sin\beta} \right)$$

$$F_6^{(e)} = -\frac{j\rho g A}{\omega_o} \int dx\, e^{jK_o x \cos\beta} \int \left\{ j\omega_o x N_2 - K_o(-jN_2 \sin\beta + N_3) \right.$$

$$\left. \left(\frac{U}{j\omega} - x \right) \phi_2' \right\} e^{K_o(z - jy\sin\beta)}\, d\ell$$

$$- \rho\, \omega_o A\, a_o U \int dx\, x\, d(x)\, e^{K_o(-d_2(x) + jx\cos\beta)} \cos\left(K_o b(x) \sin\beta\right)$$

$$- \rho \frac{4}{3\pi} \omega_o A C_D \int dx\, x\, d\, e^{K_o(-d_2 + jx\cos\beta)} \left(|\dot{y}_{1s}|\, e^{jK_o b \sin\beta} + |\dot{y}_{1p}|\, e^{-jK_o b \sin\beta} \right)$$

RESULTS AND DISCUSSION

Model experimental results available at DTNSRDC are now utilized to verify the validity of the theoretically predicted values. The comparisons are made for two-dimensional hydrodynamic coefficients of twin cylinders of semisubmersible cross section as well as for three-dimensional hydrodynamic coefficients of the single hull of a SWATH model and of complete twin hulls with and without fins. The motion of two SWATH models, SWATH 4 and SWATH 6A, in regular waves are also compared.

The particular dimensions of the SWATH models used to obtain experimental data are shown in Table 5 along with the sizes and locations of the stabilizing fins attached to SWATH 6A.

More complete descriptions of the experiments for the models shown in Table 5 have already been published.[27, 34, *]

Since the main backbone of the strip theory is based on two-dimensional hydrodynamic coefficients, it is important to check the validity of the two-dimensional hydrodynamic calculations.

At an early stage in the SWATH program, a forced oscillation of twin cylindrical bodies of semisubmerged cross section was conducted at the Center by D.M. Gerzina. The forced oscillation was made independently in heave, sway, and roll mode. The dimensions of the cross section of the model and the experimental results are presented in Figures 7-9. The theoretical curves presented in these figures were obtained by the method of source distribution.[23] Two or three amplitudes of oscillation were used in the experiment to check the linearity of the results. The amplitudes shown in Figure 9 are the vertical strokes of the pivoted arms used to generate the roll oscillation. The notation a (= 10.15 cm) is the radius of one hull, ω is the circular frequency of oscillation, S_A is the submerged sectional area of the two hulls, and b (= 30.48 cm) is one-half the distance between the centerline of each hull.

The distinct discontinuities apparent at certain frequencies in the figures are due to the trapped mode of standing waves between the two bodies. Although it appears that heave oscillation did not include discontinuities in the hydrodynamic coefficients, it would occur at the higher frequencies. The sway and heave added mass coefficients (a_{22} and a_{33}) obtained theoretically and experimentally correlate fairly well. The discrepancy observed in Figure 9

[34] Lee, C.M. and L.O. Murray, "Experimental Investigation of Hydrodynamic Coefficients of a Small Waterplane Area, Twin-Hull Model (SWATH 6A)," DTNSRDC Report (in preparation).

*Reported informally for SWATH 1 by R. Stahl.

TABLE 5 – PARTICULARS OF THE SWATH MODELS USED TO OBTAIN DTNSRDC EXPERIMENTAL DATA
(Dimensions are full scale)

Parameter	SWATH 1	SWATH 4	SWATH 6A
Displacement, long tons in s.w.	28543	4115	2802
Length at the Waterline, m	134	69.1	52.5
Length of Main Hull, m	158.5	87.7	73.2
Beam of Each Hull at the Waterline, m	5.2	2.4	2.2
Hull Spacing between the Centerlines, m	42.1	22.9	22.9
Draft at the Midship, m	17.3	9.1	8.1
Bridging Structure Clearance from Waterline, m		5.2	6.1
Maximum Diameter of Main Hull, m	9.4	5.5	4.6
Longitudinal Center of Gravity Aft of Main Hull Nose, m	77.5	42.3	35.5
Vertical Center of Gravity above Baseline, m	15.3	9.6	10.4
Transverse $\overline{GM}$, m	–	2.4	2.9
Longitudinal $\overline{GM}$, m	–	11.1	6.8
Radius of Gyration For Pitch	32.8	20.8	16.9
Radius of Gyration For Roll	–	–	10.2
Waterplane Area, m	1272.7	251.3	193.9
Model Scale Ratio	1/40.94	1/20.4	1/22.5

SWATH 6A Fins (Rectangular Planform):

	Chord m	Span m	Location* m
Fore Fin	2.59	3.11	17.15
Aft Fin	4.48	5.36	62.24

*Distance from the main hull nose to the quarter-chord point.

for the roll added inertia a_{44} is construed as resulting from experimental errors due to difficulty in generating pure roll oscillation. The sway and roll damping coefficients (b_{22} and b_{44}) showed considerable discrepancies between theory and experiment. The theoretical values of damping coefficients were not expected to correlate well with the experimental results because of the limitation of the potential-flow assumption, especially for the roll damping

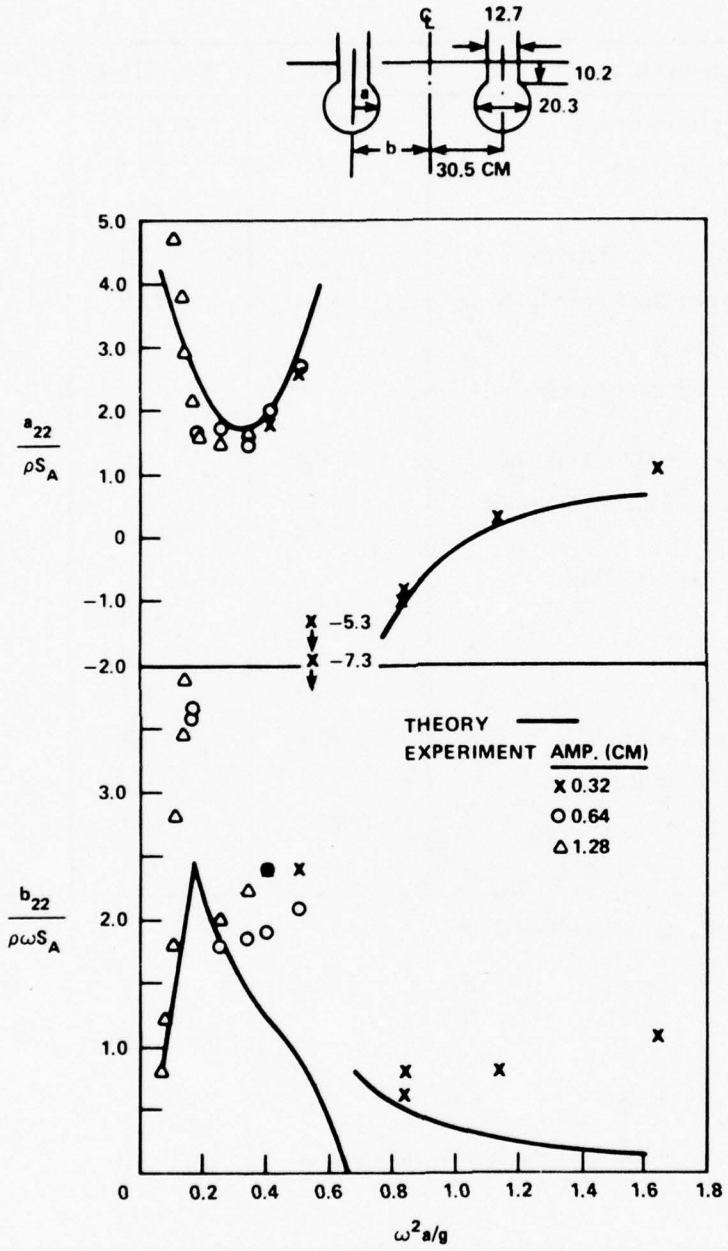

Figure 7 – Sway Added Mass and Damping Coefficients of Semisubmersible Twin Cylinders

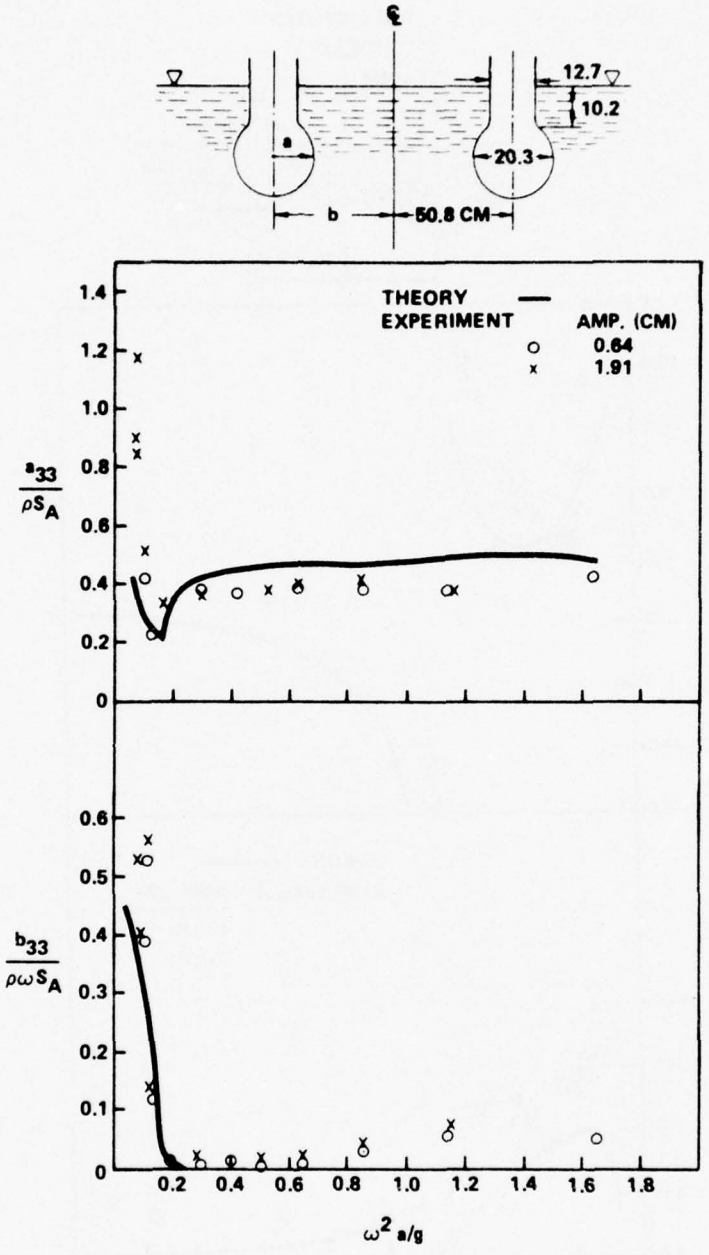

Figure 8 – Heave Added Mass and Damping Coefficients of Semisubmersible Twin Cylinders

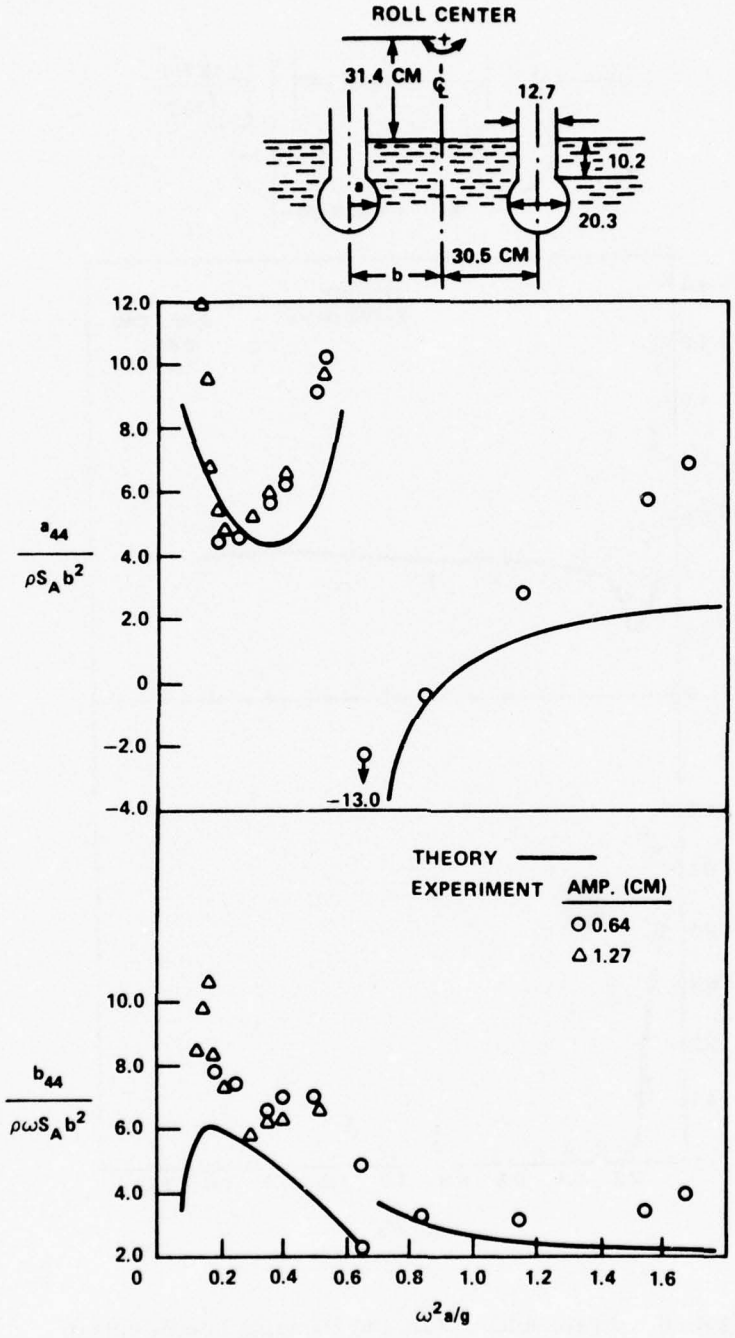

Figure 9 – Roll Added Inertia and Damping Coefficients of Semisubmersible Twin Cylinders

coefficient. The heave damping coefficient (b_{33}) in Figure 8 showed good agreement between theory and experiment, except for higher frequencies. Similar experimental results for b_{33} in a single cylinder of bulbous cross section in low frequencies showed a distinct discrepancy with theoretical values, as shown in Figure 5 in which the dividing factor for b_{33} was the same as S_A. The twin cylinders can be expected to exhibit a discrepancy similar to that observed for the single cylinder in the small frequency region. In fact, this will be demonstrated later when the three-dimensional heave damping coefficient is discussed. Unfortunately, the frequency range chosen in the experiment for the twin semisubmersible cylinders was rather high from the viewpoint of SWATH motion. The horizontal scales in Figure 7 - 9 are equivalent to

$$2\pi a/\lambda \ (= \omega^2 a/g)$$

where λ is the wave length.

For $\omega^2 a/g = 0.2$,

$$\lambda = 10\pi a$$

which is about the magnitude of one ship length of a SWATH ship. As can be seen later in the comparisons of motions, the SWATH ships hitherto examined were barely excited by a wave of such short length.

Comparisons of three-dimensional hydrodynamic coefficients are shown in Figures 10 through 12. Figure 10 compares the theoretical and experimental values of heave added mass coefficient A_{33} and damping coefficient B_{33} of SWATH 1. Both demihull and twin-hull results are presented for A_{33}. It is interesting to note that the demihull theory appears to fit the twin-hull experimental results well. The dip exhibited by the twin-hull theory may appear suspicious; however, such a dip in A_{33} has been confirmed for a conventional catamaran by another experiment.[6] The dip in A_{33} for a twin-hull ship is considered to be caused by a mutual blockage effect between the two hulls. Comparison of the theoretically predicted dip in A_{33} for a SWATH shape cannot be made at present due to the lack of available experimental results. The theoretical values of A_{33} for $\omega\sqrt{L/g} < 2.0$ appeared to be lower than the experimental values.

As demonstrated earlier in Figures 3 and 4, the damping coefficients involved in the vertical-plane modes play a sensitive role in the prediction of heave and pitch motion. As pointed out, the damping coefficients obtained under potential-flow theory for small-amplitude oscillation yield overestimated peak amplitudes of the motion at the resonant frequency compared to the magnitude measured in motion experiments in regular waves. The wave amplitudes used in the motion experiments were such that the ratio of the wavelength to the

amplitude was usually greater than 100; this can normally be considered to be adequate for application in the development of a linear boundary-value problem involving a free surface. Unfortunately, this turned out to be untrue in the prediction of SWATH motion at the resonant frequencies.

Figure 10 presents three theoretical values of heave damping coefficients, one for the demihull and the other two for the twin hulls. One of these two was obtained under the potential-flow assumption which is expressed in Table 1 as B_{33} and the other included the so-called cross-flow effects, denoted by B^*_{33} in Table 2. Theoretical values for the demihull seemed to agree well with the experimental results for both the demihull and twin hulls obtained under small amplitudes of oscillation. However, the demihull theory appeared to underpredict damping in the small frequency region, $\omega\sqrt{L/g} < 2.0$, for large-amplitude oscillation. Note that even the largest amplitude of oscillation (5.1 cm) corresponds to only about one-tenth the draft of the model. At the resonant frequency the heave amplitude of a SWATH model without fins can reach about three times the wave amplitude, or about 15 cm for the SWATH 1 model at zero speed if the ratio of the wavelength to amplitude is assumed to be 100. Thus, the amplitude of 5.1 cm does not reflect the peak amplitude of oscillation of a SWATH model in waves. As can be seen in Figure 10, the heave damping coefficients obtained by the strip theory under the potential-flow assumptions were considerably lower than the experimental values in the high frequency range. The chained curve which represents the present theory including the cross-flow effects seems to fit the experimental results better at high frequencies.

It is of more interest to us to examine the damping coefficients of a SWATH ship when it has a forward speed. Furthermore, as mentioned earlier, SWATH ships should have stabilizing fins for stability in high-speed operations. The stabilizing fins can contribute significant damping in heave, pitch, and roll modes in high-speed range. Figure 11 compares the heave and pitch damping coefficients obtained by the present theory and experiments. Three hull conditions were examined: the bare hull, the hull with aft fins, and the hull with fins fore and aft. Table 5 indicates sizes and locations of the fins used in the experiment. The fins were attached on the inboard side of each hull and were stationary. The theoretical results shown were obtained by the expressions given in Table 4. The values of coefficients chosen were as follows: $a_o = 0.07$, $C_D = 0.5$, $C_{L\alpha}$ for the fore fin = 4.38, and $C_{L\alpha}$ for the aft fin = 3.2. The $C_{L\alpha}$ values were obtained by using Equations (39), (42), (43) and Figure 6. The theoretical and experimental values agreed very well. The bar signs designate nondimensional quantities which are define as

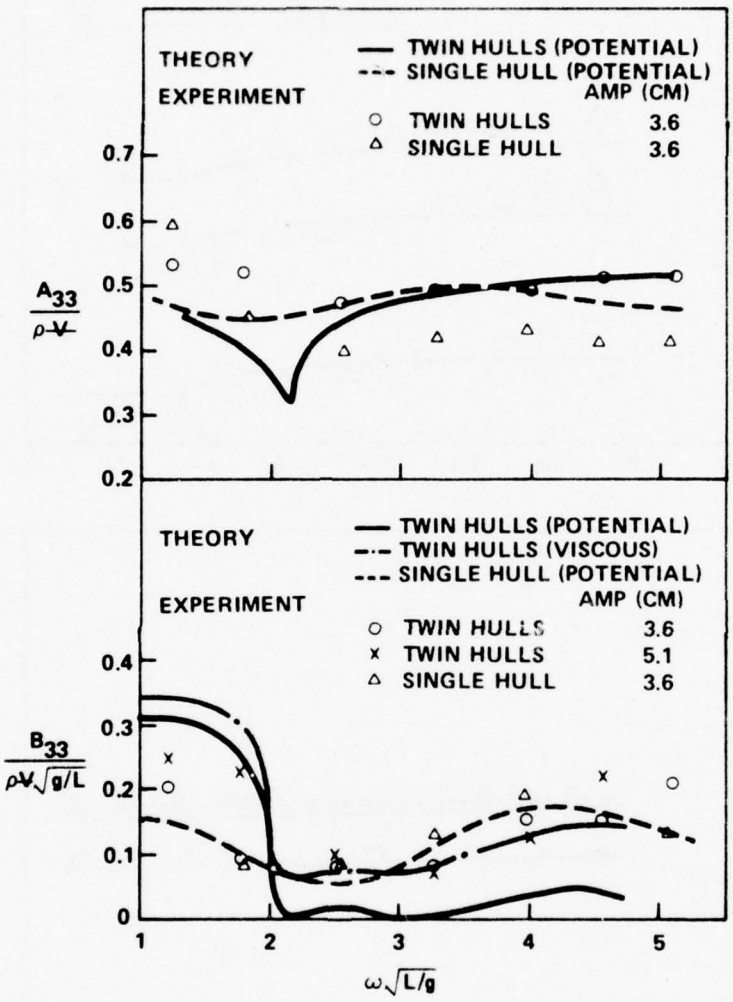

Figure 10 – Heave Added Mass and Damping Coefficients of SWATH 1 at Fn = 0

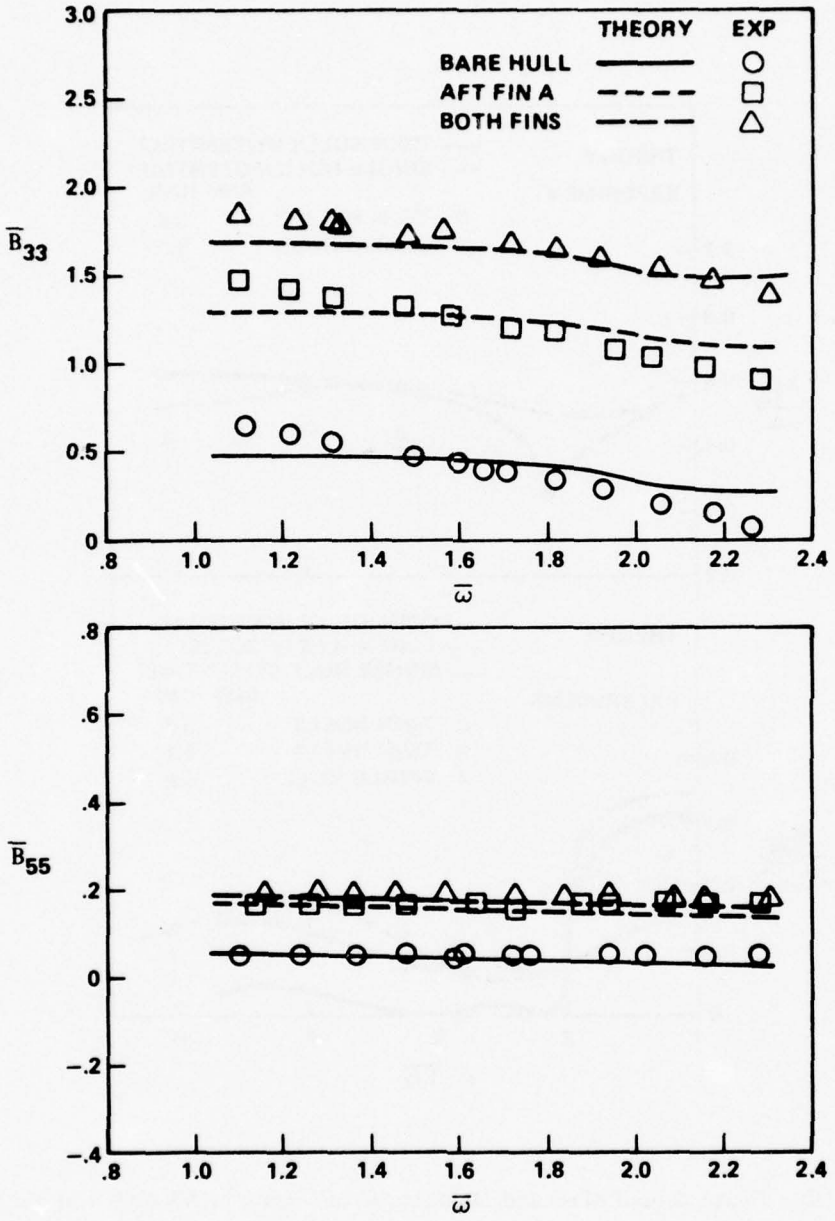

Figure 11 – Heave and Pitch Damping Coefficients of SWATH 6A at 20 Knots

$$\bar{B}_{33} = \frac{B_{33}}{\rho \nabla \sqrt{g/L}}, \bar{B}_{55} = \frac{B_{55}}{\rho \nabla L \sqrt{gL}} \text{ and } \bar{\omega} = \omega \sqrt{L/g}$$

where L is the main hull length. Comparisons of other coefficients associated with the heave-pitch motion are given in Lee and Murray.[34] Most of the trends were in good agreement for the frequency of oscillation, but some of them indicated almost constant magnitudes of difference between the two results over the range of frequencies examined in the experiment. Since there have been some unresolved uncertainties in the experimental measurements, it is difficult to judge at present whether theoretical prediction of those coefficients is unreliable. At any rate, **uncoupled damping coefficients constitute the most sensitive coefficients with** respect to peak amplitudes. The good agreement obtained for B_{33} and B_{55} is the major contributing factor that produced good agreement in the vertical plane motion shown in the subsequent figures.

Figure 12 shows the wave-exciting heave amplitudes and phases of SWATH 6A with fore-*and-aft fins versus the wave-to-ship length ratio.* The ship length is that of the main hull, i.e., 73.15 m. Agreement between theoretical and experimental results was good except the phase angles at zero speed. Similar comparisons for wave-exciting pitch moment were poor. However, for the same reasons stated previously, it is not obvious whether the theoretical prediction is poor.*

Comparisons of motion are shown in the next seven figures. Figure 13 shows the amplitudes and phases of the heave and pitch motion of SWATH 4 without fins in regular head waves at 20 knots. The results are given versus the frequency ratio ω/ω_n where ω_n (= 0.6128 rad/sec) is the natural heave frequency. It can be seen clearly from Figure 13 that SWATH ships exhibit a highly tuned response at the heave natural frequency. This highly tuned motion of SWATH ships does not usually occur for monohull surface ships, except for roll motion. The results presented in Figure 13 demonstrate the validity of the theoretical prediction of motion for the bare-hull condition. The effects of the viscous coefficients a_o and C_D in reducing the peak amplitudes can be seen by comparing Figures 3 and 13.

Figure 14a presents the amplitudes of heave, pitch, and relative vertical motion at the edge of the forward deck of SWATH 6A with fore-and-aft fins in regular head waves at 0 and 28 knots. An accurate position of the relative motion was 2.74 m from the main hull nose.

*The experimental values were consistently almost twice the theoretical values of amplitude over the range of wavelengths. If the theoretical values were wrong, the agreements shown in Figures 13, 14a, and 14b for pitch amplitudes and phases could not have been obtained.

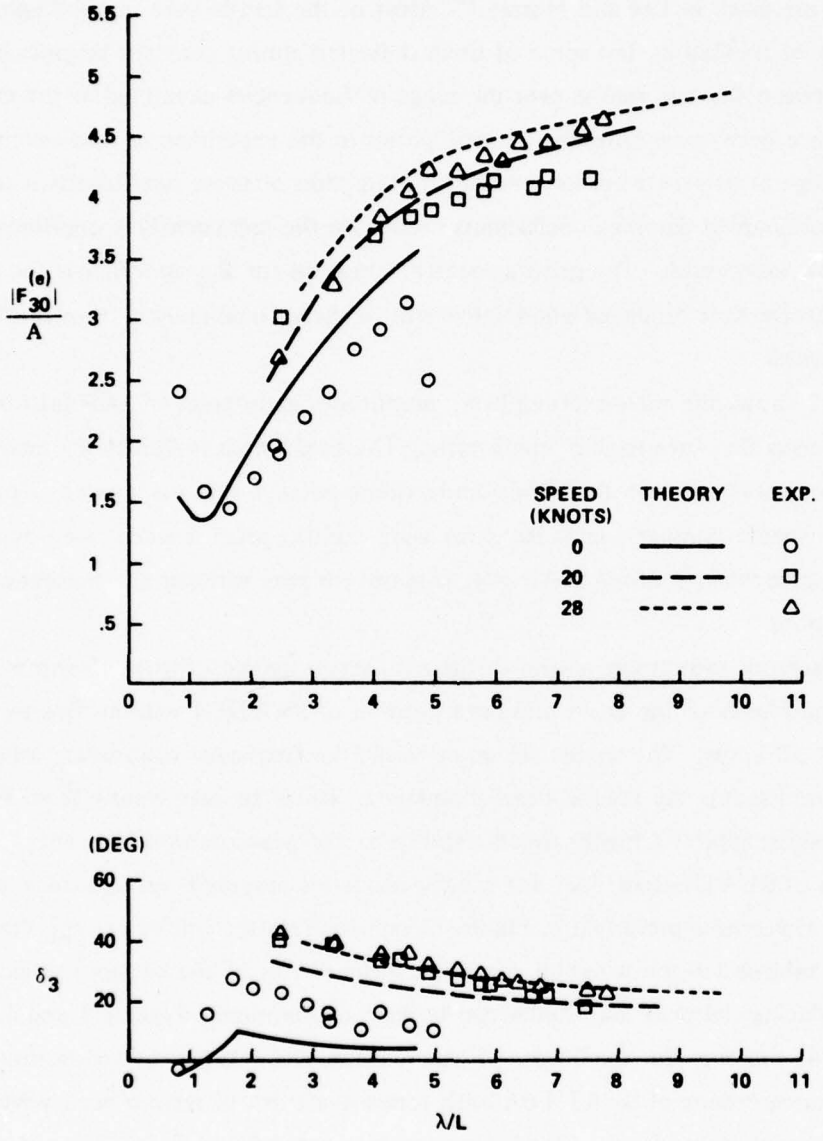

Figure 12 – Amplitudes and Phases of Wave-Exciting Heave Force on SWATH 6A in Regular Head Waves at 20 Knots

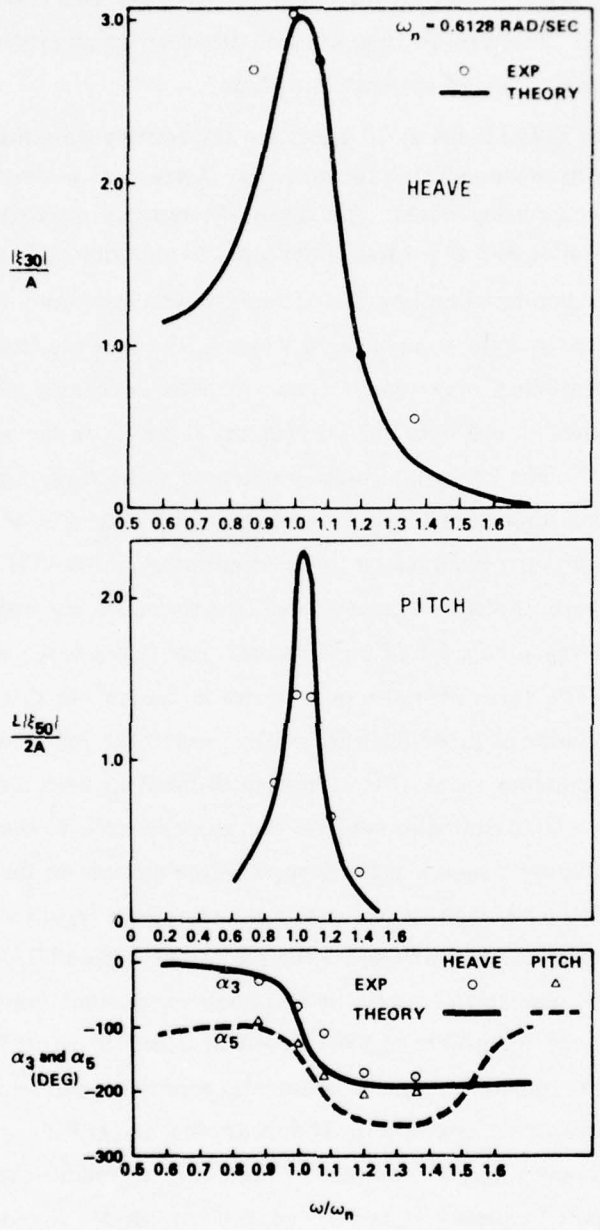

Figure 13 – Motion of SWATH 4 in Regular Head Waves at 20 Knots

Normally, the relative motion prediction is less reliable than other motions because the theory does not account for the deformation of the incoming waves caused by the diffraction by the body and by the body motion. However, agreement between the two results was very good in this case, particularly at 28 knots. It suggests that the wave deformation near the bow may not be so significant as in the case of conventional ships.

Motion amplitudes of SWATH 6A at 20 knots are respectively presented in Figures 14b and 14c for bow-quartering waves and following waves. Agreement between the two results is good in the case of bow-quartering waves. The largest discrepancy in pitch amplitude between the wave-to-ship length ratios of 3 and 4 was in the order of experimental error, i.e., about ±0.03 deg.

As expected, the prediction of motion in following waves was poor. At 20 knots, the wavelength which gave zero encountering frequency was 0.93 times the length of the ship. When the encountering frequency is extremely small, the hydrodynamic coefficients obtained by the strip theory becomes invalid since the strip theory is based on the assumption of high frequency of oscillation.[20] The large amplitudes predicted by the theory near $\lambda/L = 1.0$ are considered to be errors resulting from the shortcomings of the strip theory for small encountering frequencies. Furthermore, as observed in the experiment, a SWATH model exhibits some instabilities in the vertical-plane mode near the zero encountering frequency. Thus it can easily be judged that any theory based on harmonic time dependence would fail to provide a realistic solution. The experimental results shown in Figure 14c should by no means be interpreted to be as reliable as those for head waves. For those following waves which can make the encountering frequency small, it is extremely difficult to keep a model at constant speed; hence an effort by the person who controls the propeller rpm to maintain a constant speed of the model can impose a significant man-made surge motion on the model. The large surge motion generated in such a manner seems to induce motions in other modes.

Although the present method of predicting the motion of a SWATH ship in following and stern-quartering waves may still be useful, it definitely needs some improvement.

Figure 15 shows the roll amplitude of SWATH 6A at 0 and 20 knots in regular beam waves. Agreement between theoretical and experimental results is good except for the peak amplitude at the roll resonance at zero speed. It appears that larger values of C_D and $C_{Di}^{(f)}$ than those used for heave and pitch motion may be necessary to reduce the peak amplitude. Except for the roll resonant frequency at zero speed, roll amplitudes were less than 1 deg for $\lambda/A > 100$. The highly tuned roll response at the zero speed disappeared at 20 knots and this was correctly predicted by the theory. The damping contributed by the fins and the viscous effects seem to be the main factors which reduced the resonant roll amplitudes.

Figure 14 Motion of SWATH 6A for Various Wave Headings and Ship Speeds

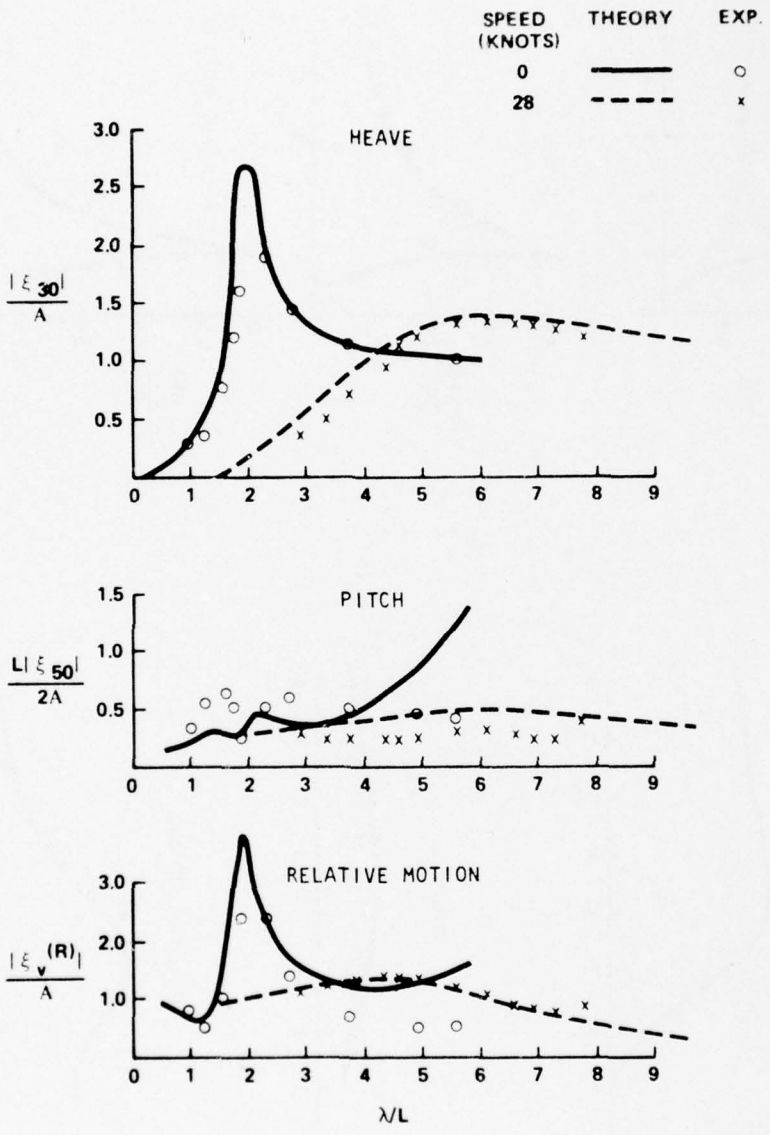

Figure 14a – In Head Waves (β = 180 Degrees) at 0 and 28 Knots

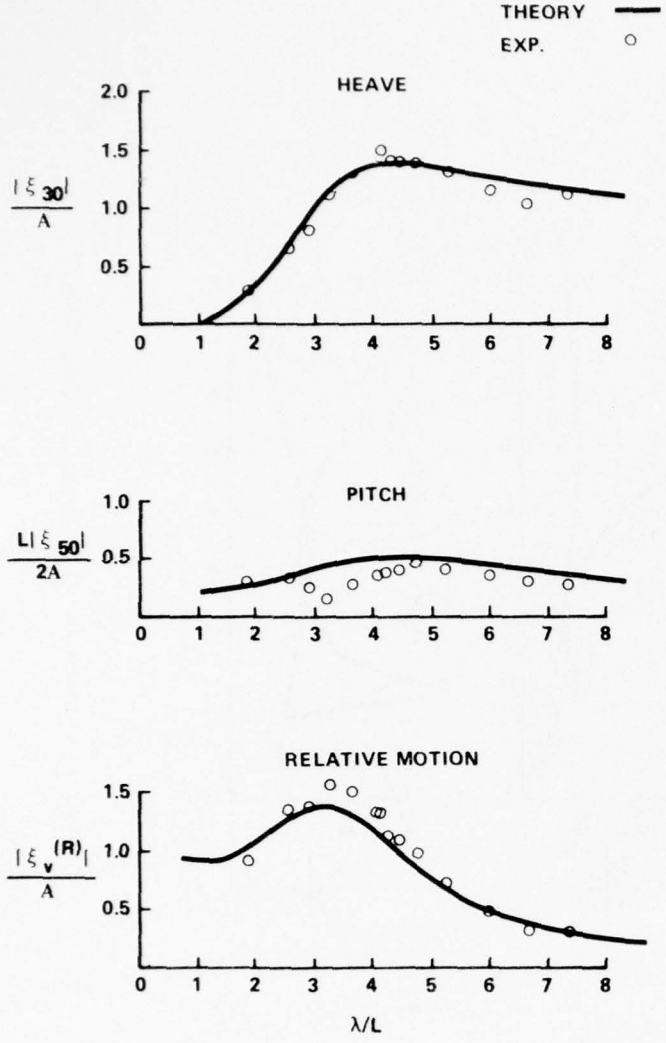

Figure 14b – In Bow Quartering Waves (β = 135 Degrees) at 20 Knots

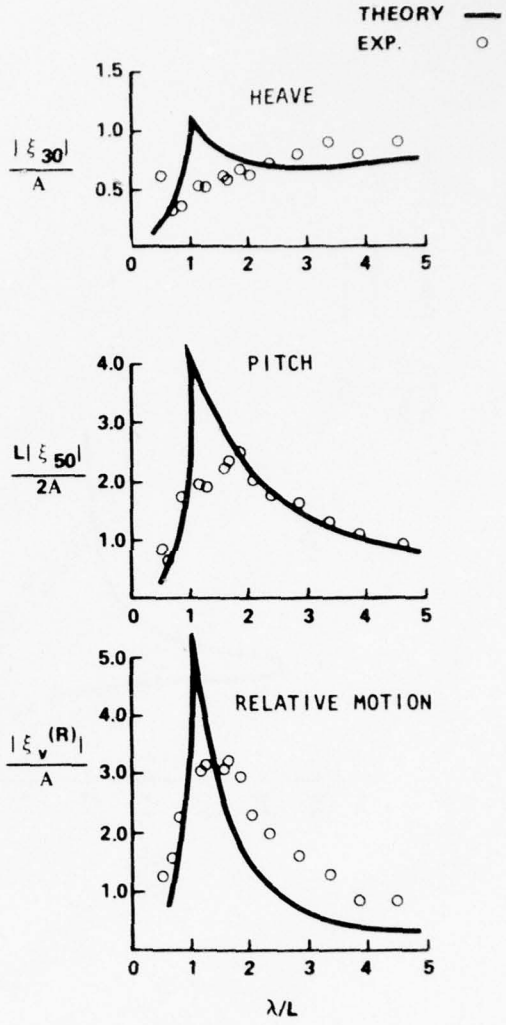

Figure 14c – In Following Waves (β = 0 Degree) at 20 Knots

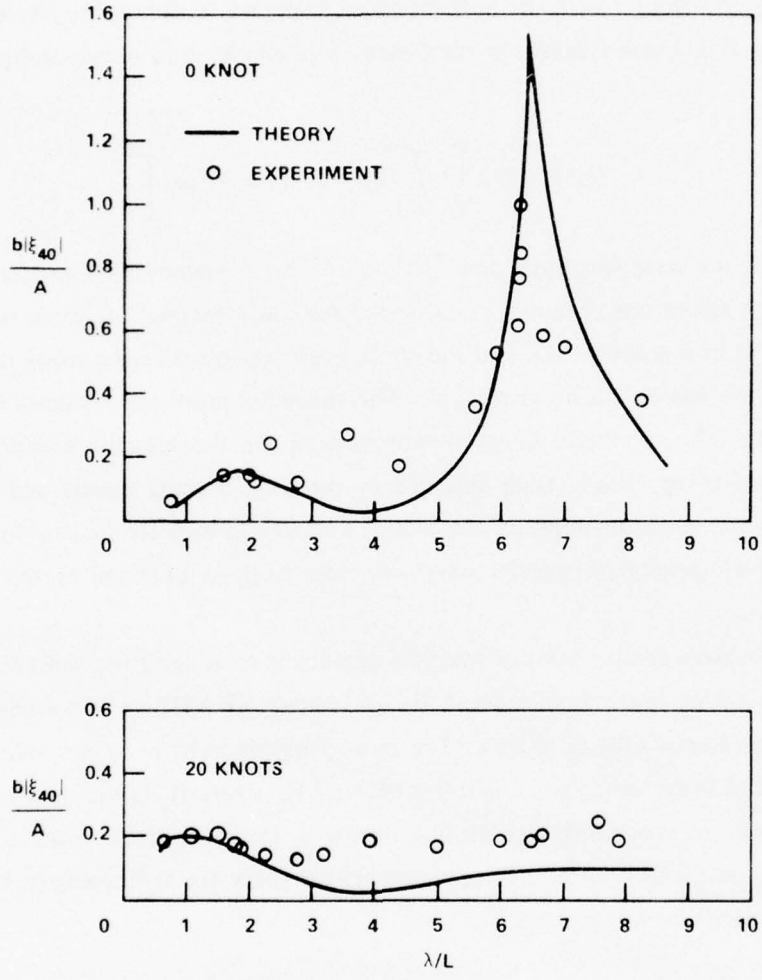

Figure 15 — Roll Amplitudes of SWATH 6A in Regular Beam Waves at 0 and 20 Knots

Figure 16 indicates the correlation of motion of a geosim of SWATH 6A with a displacement of 14,100 long tons in irregular waves. The irregular waves used for the computation were assumed to be unidirectional and propagating opposite to the ship heading. The wave spectra obtained at Station India in the North Atlantic Ocean[13] were used with the proper weighting factor for their frequency of occurrence.[14] The RAO's obtained by the present theory were used together with the aforementioned spectra to obtain the relative bow motion represented by the square symbols in the figure. The equation to obtain these values is given by

$$(\xi_v^{(R)})_s = 2\left[\int_0^\infty |\bar{\xi}_v^{(R)}|^2 S(\omega_o)\, d\omega_o\right]^{1/2} \tag{54}$$

where $S(\omega_o)$ is the wave spectrum, and $\bar{\xi}_v^{(R)} = \xi_v^{(R)}/A$ is obtained by Equation (11). The solid line in the figure was obtained by using the Pierson-Moskowitz formula (see Equation (16) for $S(\omega_o)$) in Equation (54), and the circle mark was obtained by using the wave spectrum employed for the towing basin experiment. The triangular mark was obtained entirely from the experiment. The agreement between experimental and theoretical values when an identical spectrum is used is very good. Data obtained by the Station India spectra and the Pierson-Moskowitz spectrum formula are included merely to indicate that motion data obtained by using the basin-generated irregular waves are close to those obtained by the other two methods.

Figure 17 shows the probability that the significant values and the most probable extreme values of the heave amplitude of the 14,100-ton SWATH 6A will be exceeded during operation in the North Atlantic Ocean. The most probable extreme values were obtained from Equation (19) by letting $\delta = 1$ and $T = 68 - 1.4\, H_s$ where H_s is the significant waveheight in feet. This way of presenting such motion results as slamming, deck wetness, and vertical accelerations is deemed useful in a comparative design study for seakeeping qualities of two or more candidate hull forms.

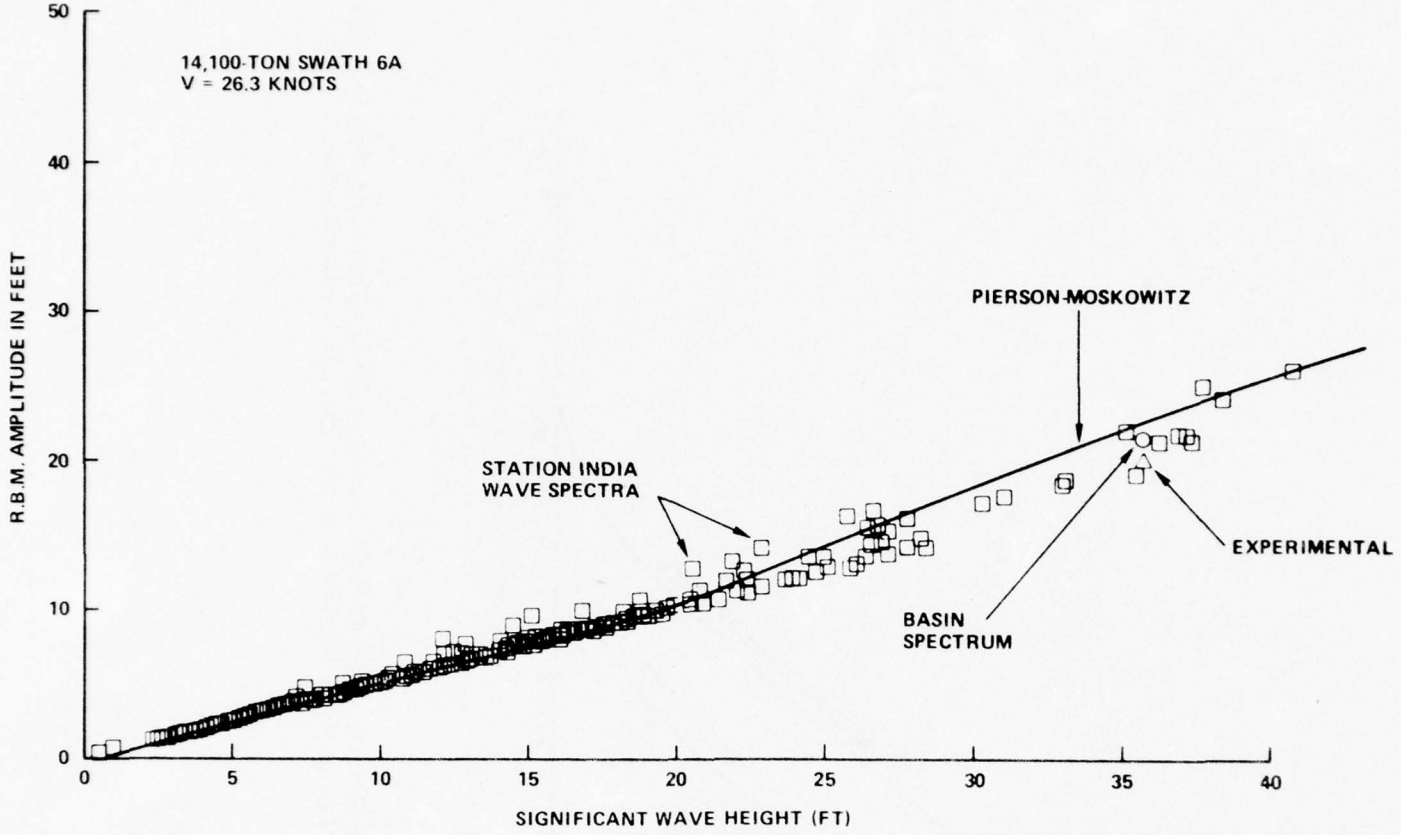

Figure 16 — Significant Relative Bow Motion Amplitudes for SWATH 6A in Irregular Waves at 26.3 Knots

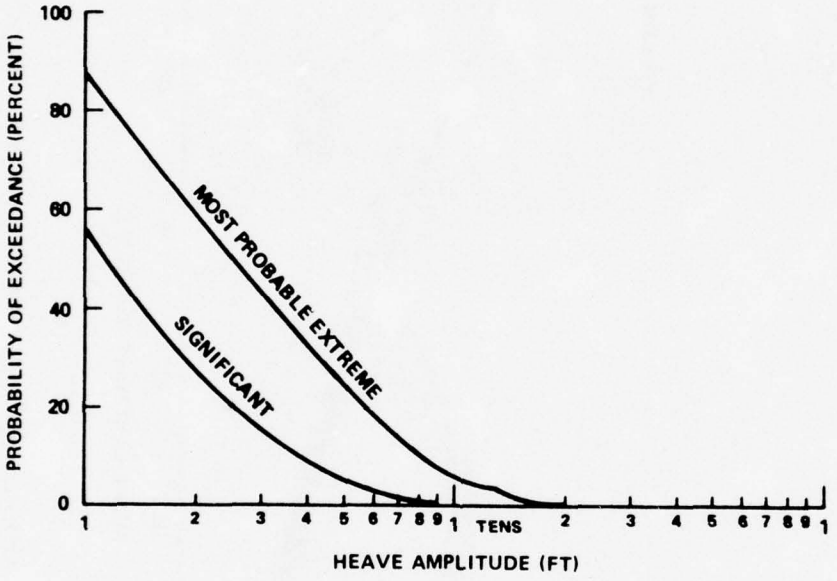

Figure 17 – Probability of SWATH 6A Exceeding the Significant and Most Probable Extreme Values of Heave Amplitude at 26.3 Knots in the North Atlantic Ocean

SUMMARY AND CONCLUSIONS

This report presents a theoretical method for predicting the motion of small-waterplane-area, twin-hull (SWATH) ships in waves. The method divides equations of motion into three independent groups; equations for surge motion alone, equations for coupled heave and pitch motion, and equations for coupled sway, roll, and yaw motion. The equations are based on the linear frequency response of a ship to harmonic wave excitation. The reference frame of the measure of the oscillatory motion of a ship is a Cartesian coordinate system translating on the calm-water plane parallel to the mean heading of the ship with a constant mean speed. When the ship is at rest in calm water, the origin of the coordinate system is located on the free surface directly above or below the ship longitudinal center of gravity.

The hydrodynamic coefficients associated with the equations of motion are assumed to consist of three parts. The first part is obtained under the potential-flow assumption (see Appendix A). The basic ingredient of this part comes from the solution of two-dimensional boundary-value problem for oscillating twin cylinders in a free surface.[17] The expression for the hydrodynamic coefficients contributed by the first part is given in Table 1.

The second part is obtained by an empirical method derived from the cross-flow approach to a slender body at a moderate angle of incidence in a uniform flow.[24] A psuedo-steady-state assumption is invoked to apply the method to an oscillatory body. Two coefficients involved in the cross-flow approach are the viscous-lift coefficient a_0 which is associated with the forward velocity of the ship and the cross-flow drag coefficient C_D which is independent of the forward speed.

An equivalent linearization method is used to include the cross-flow drag term as a linear damping term in the equations of motion. This necessitates an iterative solution of the equations of motion until a reasonable convergence of the solution is obtained.

The third part is that contributed by the stabilizing fins, if any. This part is obtained by using the method developed by Pitts et al.[28] The analysis accounts for the lift induced by the fin on the body and vice versa.

Theoretical predictions were verified by comparing them with available results from model experiments. The sectional added mass and damping coefficients of a SWATH cross section, the three-dimensional hydrodynamic coefficients associated with heave and pitch motion, and the wave-exciting heave force were checked. The predicted motions of two SWATH models were compared with model experimental data to examine the effects of fins, wave-heading angle, ship forward velocity, and wavelength. The predicted motion in irregular waves was also compared with model experimental data.

From the present study, the following conclusions have been drawn:

1. The linear frequency response theory can be applied for predicting motions of SWATH ships in waves.

2. The strip theory used in deriving the hydrodynamic coefficients is acceptable as an approximation in predicting motions for SWATH ships.

3. The effects of viscous damping on SWATH motions can be predicted by combining the cross-flow approach with strip theory. In a strict theoretical sense, an extension of the equilinearization method to predict motion in irregular waves (as presently used) cannot be justified; however, for practical purposes, the present approach is recommended until a more rigorous and practical means is developed.

4. The present method of predicting the effects of stabilizing fins on the motion of a SWATH ship in waves seems to be acceptable despite neglect of such seemingly important effects as free surface, unsteadiness, and downwash on the aft fins by the forward fins.

5. Prediction of SWATH motion in following waves is an area which needs improvement of both theory and model experimental techniques. This is particularly important if future plans call for equipping SWATH's with controllable fins to maintain good seakeeping quality in following waves.

ACKNOWLEDGMENTS

The author appreciates the assistance of Ms. Katherine McCreight in handling some of the computer programming that led to the theoretical predictions presented in this report. Thanks are also extended to those whose experimental studies were used for comparison purposes.

The author gratefully acknowledges the support of Ms. Margaret Ochi, Mr. D.S. Cieslowski, and the SWATH Program staff of the Systems Development Department at DTNSRDC during the course of this study.

APPENDIX A
DETERMINATION OF HYDRODYNAMIC COEFFICIENTS UNDER POTENTIAL-FLOW ASSUMPTION

If we assume that the fluid surrounding a catamaran has irrotational motion, we can introduce a velocity potential $\Phi(x, y, z, t)$ in the fluid region. The velocity potential should satisfy, in addition to the Laplace equation, the following boundary conditions

$$\left(\frac{\partial}{\partial t} - U\frac{\partial}{\partial x}\right)^2 \Phi(x, y, z, t) + g\Phi_z = 0 \quad \text{on } z = 0 \tag{55}$$

where g is the gravitational acceleraton,

$$\nabla\Phi \cdot \underline{n} = V_n \quad \text{on } S_o \tag{56}$$

where $\underline{n}$ is the unit normal vector on the body surface pointing into the body, V_n is the normal component of the velocity of the body surface, and S_o is the mean position of the body,

$$\Phi_z(x, y, -\infty, t) = 0 \tag{57}$$

and a physically appropriate far-field condition for $(x^2 + y^2)^{1/2} \to \infty$ to make the problem well posed.

Assuming that the flow disturbance is a small perturbation from uniform flow, we can express Φ in the form

$$\Phi = -Ux + \phi_s(x, y, z) + \phi_o(x, y, z)\, e^{-j\omega t} \tag{58}$$

Here U is the forward velocity of the ship, ϕ_s is the steady potential representing the wave-making disturbance due to the forward velocity, and $\phi_o = \phi_{oc} + j\phi_{os}$ is the potential associated with the oscillatory fluid disturbance. We can further divide ϕ_o with three distinct origins of the oscillatory fluid disturbance as

$$\phi_o = \phi_I + \phi_D + \phi_M \tag{59}$$

The incoming wave potential ϕ_I is given by

$$\phi_I = -\frac{jgA}{\omega_o} e^{K_o(z + jx\cos\beta - jy\sin\beta)} \tag{60}$$

Here β is the wave-heading angle with respect to the positive x-axis, ω_o is the wave frequency, K_o is the wave number given by ω_o^2/g, and A is the wave amplitude. The wave diffraction is

represented by ϕ_D and the fluid disturbance caused by the motion of the body in initially calm water is represented by ϕ_M. Within a linear approximation to the solution of the velocity potential, we can let

$$\phi_M = \sum_{k=1}^{6} \xi_{ko} \phi_k \tag{61}$$

where ϕ_k is another set of velocity potentials, and ξ_{ko}, k = 1, 2, . . . , 6 are the complex amplitudes of the displacement of the body from its mean position in surge, sway, heave, roll, pitch, and yaw modes, respectively. The pressure at any point of the hull is obtained from the Bernoulli equation by

$$p = \frac{\rho}{2} U^2 - \rho \left(\Phi_t + g z(t) + \frac{1}{2} | \nabla \Phi |^2 \right)$$

At this point, we will establish the following conditions: (1) the motion of the body is small and so the pressure at a point on the body surface at any instant can be obtained via the Taylor expansion of the pressure at the mean position of the body; (2) the terms $O(\phi_s^2, \phi_s\phi_o, \phi_o^2, \xi_{ko}\phi_s, \xi_{ko}\phi_D, \xi_{ko}^2)$ will be discarded in the evaluation of pressure; (3) only those components of the pressure which have harmonic time dependence will be considered; and (4) the static-pressure component and the component which contributes to the static restoring force or moment of the body will not be included in the evaluation of pressure.

With the foregoing conditions, the complex amplitude of the pressure at a point on the body surface can be expressed by

$$\begin{aligned} p &= \rho \left(j\omega + U \frac{\partial}{\partial x} \right) \phi_o \\ &= \rho \left(j\omega + U \frac{\partial}{\partial x} \right) \left(\phi_I + \phi_D + \sum_{k=1}^{6} \xi_{ko} \phi_k \right) \end{aligned} \tag{62}$$

evaluated at the mean position of the body.

Integration of the pressure over the wetted surface of a ship should yield the hydrodynamic forces and moments. Thus, we have

$$\begin{aligned} F_i^{(H)} &= \iint_{S_o} p \, n_i \, ds \\ &= \rho \iint_{S_o} n_i \left(j\omega + U \frac{\partial}{\partial x} \right) \left(\phi_I + \phi_D + \sum_{k=1}^{6} \xi_{ko} \phi_k \right) ds \end{aligned}$$

for i = 1, 2, 3, 4, 5, 6, where n_1, n_2, and n_3 are respectively the x-, y-, and z-components of the unit normal vector and $n_4 = yn_3 - zn_2$, $n_5 = zn_1 - xn_3$, $n_6 = xn_2 - yn_1$.

We can further **decompose the hydrodynamic force into two parts, i.e.,**

$$F_i^{(H)} = F_i^{(e)} + F_i^{(m)}$$

where

$$F_i^{(e)} = \text{wave-excited force}$$

$$= \rho \iint_{S_o} n_i \left(j\omega + U \frac{\partial}{\partial x} \right) (\phi_I + \phi_D) \, ds \tag{63}$$

and

$$F_i^{(m)} = \text{motion-excited force}$$

$$= \rho \sum_{k=1}^{6} \xi_{ko} \iint_{S_o} n_i \left(j\omega + U \frac{\partial}{\partial x} \right) \phi_k \, ds \tag{64}$$

Applying the results of Ogilvie and Tuck[20] to the simplified case in this work, and with the use of the Kronecker delta function δ_{ij}, we can show for any differentiable scalar function ϕ that

$$\iint_S n_i \phi_x \, dx = \iint_S (n_3 \delta_{i5} - n_2 \delta_{i6}) \phi \, ds - \int_{C(x)} n_i \phi \, d\ell \tag{65}$$

where S is the immersed hull surface forward of the cross section at x, and C(x) is the line integral along the contours of the cross section. Utilization of Equation (65) in Equation (63) yields

$$F_i^{(e)} = \rho \iint_{S_o} n_i \left(j\omega + U \frac{\partial}{\partial x} \right) (\phi_I + \phi_D) \, ds$$

$$= \rho \iint_{S_o} j n_i \, (\omega + U K_o \cos\beta) \phi_I \, ds$$

$$+ \rho \iint_{S_o} (j\omega n_i + U n_3 \delta_{i5} - U n_2 \delta_{i6}) \phi_D \, ds \tag{66}$$

where the line integral at the stern section is neglected.

Within the accuracy of the order of approximation in this work and together with a slenderness assumption for each hull of the ship, i.e., $n_1 = o(n_2 \text{ or } n_3)$, we can derive from Equation (56) and (59)

$$\frac{\partial \phi_M}{\partial n} = -j\omega (\underline{\xi}_o + \underline{\alpha}_o \times \underline{r}) \cdot \underline{n} - U (\underline{\alpha}_o \times \underline{e}_1) \cdot \underline{n} \quad \text{on } S_o \tag{67}$$

where

$$\underline{\xi}_o = (\xi_{1o}, \xi_{2o}, \xi_{3o})$$

$$\underline{\alpha}_o = (\xi_{4o}, \xi_{5o}, \xi_{6o})$$

$$\underline{r} = (x, y, z)$$

and $\underline{e}_1$ is the unit vector in the x-direction. The original derivation of Equation (67) without the slenderness assumption was derived by Timman and Newman.[35] Substitution of Equation (61) into Equation (67) yields

$$\frac{\partial \phi_i}{\partial n} = -j\omega n_i + U n_3 \delta_{i5} - U n_2 \delta_{i6} \tag{68}$$

on S_o for i = 2, 3, 4, 5, 6. From Equation (68), we can deduce the following relations:

$$\phi_5 = -\left(x + \frac{U}{j\omega}\right) \phi_3 \tag{69}$$

$$\phi_6 = \left(x + \frac{U}{j\omega}\right) \phi_2 \tag{70}$$

in which approximations $n_5 \simeq x\, n_3$ and $n_6 \simeq x\, n_2$ were used.

Using Equation (68) and the relation

$$\omega + U K_o \cos\beta = \omega_o$$

in Equation (66), we get

$$F_i^{(e)} = j\rho\omega_o \iint_{S_o} n_i \phi_I \, ds$$

$$- \rho \iint_{S_o} \left(\phi_{in} + \frac{2U}{j\omega} \phi_{3n} \delta_{i5} - \frac{2U}{j\omega} \phi_{2n} \delta_{i6}\right) \phi_D \, ds$$

[35] Timman, R. and J.N. Newman, "The Coupled Damping Coefficients of a Symmetric Ship," J. Ship Res., Vol. 5, No. 4, pp. 1-7 (1962).

Since

$$\iint_{S_o} \phi_{in}\, \phi_D \, ds = \iint_{S_o} \phi_{Dn}\, \phi_i \, ds$$

by the Green theorem and

$$\phi_{In} = -\phi_{Dn} \quad \text{on } S_o$$

from the kinematic boundary condition, we can show that

$$F_i^{(e)} = \rho \iint_{S_o} \left[j\omega_o\, n_i + \left(\phi_i + \frac{2U}{j\omega}\, \phi_3\, \delta_{i5} - \frac{2U}{j\omega}\, \phi_2\, \delta_{i6} \right) \frac{\partial}{\partial n} \right] \phi_I \, ds \tag{71}$$

Since we have assumed that $n_1 = o(n_2 \text{ or } n_3)$, it follows from Equation (67) that $\phi_1 = O(n_1) = o(\phi_i,\ i = 2, 3, \ldots, 6)$. Hence, we let

$$F_1^{(e)} = j\rho\, \omega_o \iint_{S_o} n_1\, \phi_I \, ds$$

The above procedure for eliminating the diffraction potential ϕ_D from the expression for the wave-exciting force and moment was first shown by Haskind[36] for zero speed and was later extended by Newman[37] for the case of forward speeds. It is referred to as the Haskind-Newman relation.

Similarly, we can derive

$$F_i^{(m)} = \rho \sum_{k=2}^{6} \xi_{ko} \iint_{S_o} (j\omega\, n_i + U\, n_3\, \delta_{i5} - U\, n_2\, \delta_{i6})\, \phi_k \, ds$$

$$= -\rho \sum_{k=2}^{6} \xi_{ko} \iint_{S_o} \left(\phi_{in} + \frac{2U}{j\omega}\, \phi_{3n}\, \delta_{i5} - \frac{2U}{j\omega}\, \phi_{2n}\, \delta_{i6} \right) \phi_k \, ds \tag{72}$$

If we express $F_i^{(m)}$ in the form

$$F_i^{(m)} = \sum_{k=2}^{6} \xi_{ko}\, (\omega^2 A_{ik} + j\omega B_{ik})$$

---

[36] Haskind, M.D., "The Exciting Forces and Wetting of Ships in Waves," Isvestia Akademic Nauk SSSR, Otdelenie Teknicheskikh Nauk, No. 7 (1957); David Taylor Model Basin Translation 307 (1962).

[37] Newman, J.N., "The Exciting Forces on a Moving Body in Waves," J. Ship Res., Vol. 9, No. 3, pp. 190-199 (1965).

where A_{ik} are the so-called added mass quantities, and B_{ik} are the damping quantities, we find from Equation (72) that

$$A_{ik} = Re_j\left[-\frac{\rho}{\omega^2}\iint_{S_o}\left(\phi_{in} + \frac{2U}{j\omega}\phi_{3n}\,\delta_{i5} - \frac{2U}{j\omega}\phi_{2n}\,\delta_{i6}\right)\phi_k\,ds\right] \tag{73}$$

$$B_{ik} = Im_j\left[-\frac{\rho}{\omega}\iint_{S_o}\left(\phi_{in} + \frac{2U}{j\omega}\phi_{3n}\,\delta_{i5} - \frac{2U}{j\omega}\phi_{2n}\,\delta_{i6}\right)\phi_k\,ds\right] \tag{74}$$

To be consistent with earlier approximation, we let

$$A_{1k} = B_{1k} = 0 \quad \text{for } k = 1, 2, \ldots, 6. \tag{75}$$

We can assume that there is no coupling between the motions on the horizontal and vertical planes for slender ships, so that

$$A_{ik} = B_{ik} = 0$$

for the following combinations of i and k

$$i = 2, 4, 6 \quad \text{for } k = 3, 5$$

and

$$i = 3, 5 \qquad \text{for } k = 2, 4, 6$$

As has been seen previously, the hydrodynamic coefficients appearing in the equations of motion can be obtained if solutions of the velocity potentials ϕ_i ($i = 2, \ldots\ldots, 6$) are known. In the solution of ϕ_i, the flow around each transverse section is assumed to be two dimensional, and thus the variable x enters as a parameter in the expressions for ϕ_i. We then have

$$A_{ik} = Re_j\left[-\frac{\rho}{\omega^2}\int_L dx\int_{C(x)}\left(\phi'_{iN}(y, z; x) + \frac{2U}{j\omega}\phi'_{3N}\,\delta_{i5} - \frac{2U}{j\omega}\phi'_{2N}\,\delta_{i6}\right)\phi'_k\,d\ell\right] \tag{76}$$

$$B_{ik} = Im_j\left[-\frac{\rho}{\omega}\int_L dx\int_{C(x)}\left(\phi'_{iN} + \frac{2U}{j\omega}\phi'_{3N}\,\delta_{i5} - \frac{2U}{j\omega}\phi'_{2N}\,\delta_{i6}\right)\phi'_k\,d\ell\right] \tag{77}$$

where ϕ'_i is the two-dimensional velocity potential function; the subscript N means the normal derivative in the y-z plane only, $\int_L$ is the ship lengthwise integral and $\int_{C(x)}$ is the contourwise integral at section x.

APPENDIX B
APPROXIMATION OF DOWNWASH EFFECTS ON TWIN SLENDER BODIES BY FORWARD FINS

A SWATH ship is assumed to be replaced by the main hulls without the vertical struts and placed in a uniform flow in unbounded fluid with a small angle of attack.

Downwash effects by the forward fins of a SWATH ship will be examined by assuming a horseshoe vortex model. The vortex line eminating from the fin is assumed to be located at a distance of $\pi/4$ times the span of the fin from the body-fin juncture at the trailing edge; this is based on the assumption of elliptic circulation distribution along the span of the fin. This vortex line is assumed to be parallel to the body axis; the other vortex line inside the body is the reflected image of the former about a circular cylinder which is assumed to represent a main hull of the SWATH ship.

Based on these assumptions, Pitts et al.[28] derived the following two lift-curve slopes:

$$(C_{L\alpha})_{T(V)} = i \frac{(C_{L\alpha})_{W1} (C_{L\alpha})_{W2} K_{W(B)} C_2}{4\pi (f_1 - r_1)} \tag{78}$$

$$(C_{L\alpha})_{B(V)} = -(C_{L\alpha})_{W1} K_{W(B)} \left\{ \frac{f_1 + r_1}{f_1} - \frac{(f_1^2 - r_1^2)}{(f_1 - r_1) f_1} \right\} \tag{79}$$

where the subscripts T(V) and B(V) respectively refer to the induced lift due to the trailing vortices on the tail fin and on the body after the forward fin. In these equations, i is the tail interference factor, C_2 is the average chord of the aft fin, f_1 is the transverse distance from the body axis to the vortax line outside the body, r_1 and r_2 are respectively the radii of the body at which the forward and the aft fins are attached, $(C_{L\alpha})_{W1}$ and $(C_{L\alpha})_{W2}$ are the lift-curve slope of the forward and the aft fins as defined by Equation (42), and $K_{W(B)}$ is as defined by Equation (40).

For SWATH 6A, we have (see Table 5) $(C_{L\alpha})_{W1} = 2.18$, $(C_{L\alpha})_{W2} = 2.0$, $K_{W(B)} = 1.37$, $C_2 = 4.48$ m, $f_1 = 4.24$ m, $r_1 = 2.29$ m, $r_2 = 2.01$ m, and $i = -1.08$ which is obtained from Chart 7 in Pitts et al.[28] Substitution of these values into Equations (78) and (79) yields

$$(C_{L\alpha})_{T(V)} = -1.18$$

$$(C_{L\alpha})_{B(V)} = 0.39$$

Since the total lift due to the trailing vortices from the forward fin is obtained[28] by

$$L_{(V)} = [(C_{L\alpha})_{T(V)} + (C_{L\alpha})_{B(V)}] \frac{\rho}{2} U^2 A_1^{(f)}$$

the additional lift-curve slope to be assigned to the aft fin is obtained by

$$(C_{L\alpha})_{(V)} = [(C_{L\alpha})_{T(V)} + (C_{L\alpha})_{B(V)}] \frac{A_1^{(f)}}{A_2^{(f)}}$$

$$= (-1.18 + 0.39) \frac{8.05}{24.04} = -0.26 \,(8.1\% \text{ of } C_{L\alpha 2})$$

which corresponds to less than 10 percent of the lift-curve slope without the downwash effect.

Another downwash effect which is contributed by the Magnus effect on the body induced by the trailing vortices and the transverse flow velocity due to a mutual blockage effect between the two hulls. This effect will be examined next.

The average circulation per unit span Γ on the forward fin is obtained by

$$\Gamma = \frac{U A_1^{(f)} C_{L\alpha 1} \alpha}{2(f_1 - r_1)} \tag{80}$$

If we denote the transverse flow velocity on one hull by $v(x)$, then the vertical lift L and pitch moment M_p induced by the Magnus effect are given by

$$L = \rho \Gamma \int_{x_a}^{\ell_1} v(x)\, dx \tag{81}$$

$$M_p = \rho \Gamma \int_{x_a}^{\ell_1} x\, v(x)\, dx \tag{82}$$

where ℓ_1 and $x_a < o$ are respectively the x-coordinates from the center of gravity to the quarter-chord point of the forward fin and the rear end of the body.

The transverse flow velocity between twin bodies can be obtained from the solution of the problem for a slender body moving near a wall.[38] That is,

$$v(x) = \frac{U A'(x)}{4\pi \sqrt{b^2 - r^2(x)}} \tag{83}$$

[38] Newman, J.N., "The Force and Moment on a Slender Body of Revolution Moving near a Wall," David Taylor Model Basin Report 2127 (1965).

Here b is one-half the distance between the axis of the two bodies, $r(x)$ is the radius of the cross section at x, and $A(x)$ is the cross-sectional area.

Substitution of Equation (80) and (83) into (81) and (82) gives

$$L = \frac{1}{2}\rho U \Gamma \int_{x_a}^{\ell_1} \frac{r\, r'(x)}{\sqrt{b^2 - r^2}}\, dx$$

$$= \frac{\rho U^2 A_1^{(f)} C_{L\alpha 1}}{4(f_1 - r_1)} \alpha \left(b - \sqrt{b^2 - r_1^2}\right) \tag{84}$$

where $r_1 = r(\ell_1)$, and

$$M_p = -\frac{1}{2}\rho U \Gamma \int_{x_a}^{\ell_1} \frac{x\, r\, r'}{\sqrt{b^2 - r^2}}\, dx$$

$$= \frac{\rho U^2 A_1^{(f)} C_{L\alpha 1}}{4(f_1 - r_1)} \alpha \left(\ell_1 \sqrt{b^2 - r_1^2} - x_a\, b\right.$$

$$- \frac{\rho U^2 A_1^{(f)} C_{L\alpha 1}}{4(f_1 - r_1)} \alpha \int_{x_a}^{\ell_1} \sqrt{b^2 - r^2(x)}\, dx \tag{85}$$

The integral $\int_{x_a}^{\ell_1} \sqrt{b^2 - r^2(x)}\, dx$ can be approximated for a slender body by

$$\int_{x_a}^{\ell_1} \sqrt{b^2 - r^2}\, dx = b \int_{x_a}^{\ell_1} \sqrt{1 - \left(\frac{r}{b}\right)^2}\, dx$$

$$\simeq b \int_{x_a}^{\ell_1} \left\{1 - \frac{1}{2}\left(\frac{r}{b}\right)^2 + \ldots\right\} dx = b(\ell_1 - x_a) - \frac{\forall}{2b\pi} \tag{86}$$

where $\forall$ is the volume of the body after $x = \ell_1$.

Substitution of Equation (86) into (85) yields

$$M_p = -\frac{\rho U^2 A_1^{(f)} C_{L\alpha 1}}{4(f_1 - r_1)} \alpha \left\{\ell_1 \sqrt{b^2 - r_1^2} \quad - b\ell_1 - \frac{\forall}{2b\pi}\right\} \tag{87}$$

A sample computation will now be made for SWATH 6A. The lift and moment generated on the body by the trailing vortices will be considered to be borne by the forward and aft fins. The additional lift on the fins will be represented as the additional lift-curve slope to each fin. Thus,

$$\frac{\rho U^2 A_1^{(f)}}{4(f_1 - r_1)} C_{L\alpha 1} \left(b - \sqrt{b^2 - r_1^2} \right) \alpha$$

$$= \frac{\rho}{2} U^2 (A_1^{(f)} C'_{L\alpha 1} + A_2^{(f)} C'_{L\alpha 2}) \alpha \tag{88}$$

$$\frac{\rho U^2 A_1^{(f)}}{4(f_1 - r_1)} C_{L\alpha 1} \left\{ \ell_1 \sqrt{b^2 - r_1^2} \quad - \ell_1 b + \frac{\forall}{2b\pi} \right\}$$

$$= \frac{\rho}{2} U^2 (A_1^{(f)} \ell_1 C'_{L\alpha 1} + A_2^{(f)} \ell_2 C'_{L\alpha 2}) \tag{89}$$

Here subscripts 1 and 2 respectively indicate the forward and aft fins, $C'_{L\alpha 1}$ and $C'_{L\alpha 2}$ are the additional lift-curve slopes to be determined, and $\ell_2 < o$ is the x-coordinate of the quarter-chord point of the aft fin. From Equations (88) and (89), $C'_{L\alpha 1}$ and $C'_{L\alpha 2}$ are obtained by

$$C'_{L\alpha 1} = - \frac{C_{L\alpha 1}}{4(f_1 - r_1)(\ell_1 - \ell_2)} \left\{ b(\ell_1 - \ell_2) \left(-1 + \sqrt{1 - \left(\frac{r_1}{b} \right)^2} \right) + \frac{\forall}{2b\pi} \right\} \tag{90}$$

$$C'_{L\alpha 2} = \frac{A_1^{(f)} \forall C_{L\alpha 1}}{4b\pi (f_1 - r_1)(\ell_1 - \ell_2) A_2^{(f)}} \tag{91}$$

The values necessary for the computation are shown below.

$A_1^{(f)} = 8.05\ m^2$ $\qquad$ $A_2^{(f)} = 24.04\ m^2$

$f_1 = 4.24\ m$ $\qquad$ $b = 11.43\ m$

$\ell_1 = 18.27\ m$ $\qquad$ $\ell_2 = 26.75\ m$

$C_{L\alpha 1} = 4.38/rad$ $\qquad$ $C_{L\alpha 2} = 3.2/rad$

$r_1 = 2.29\ m$ $\qquad$ $\forall = 1020.82\ m^3$

The foregoing values substituted into Equations (90) and (91) give

$$C'_{L\alpha 1} = -0.047 \ (1\% \text{ of } C_{L\alpha 1})$$

$$C'_{L\alpha 2} = 0.119 \ (3.7\% \text{ of } C_{L\alpha 2})$$

As can be seen from the above, the downwash effects on the body by the trailing vortices are negligible. Although the results shown here are applicable only to SWATH 6A under various assumptions, it is felt that the downwash effects by the forward fins of a SWATH ship may not be significant.

REFERENCES

1. Lang, T.G. and D.T. Higdon, *"S^3 Semi-Submerged Ship Concept and Dynamic Characteristics,"* AIAA/SNAME/USN Advanced Marine Vehicles Meeting, Annapolis, Maryland (Jul 1972).

2. Leopold, R. et al., *"The Low Water Plane Multi-Hull Principles, Status, and Plans,"* AIAA/SNAME/USN Advanced Marine Vehicles Meeting, Annapolis, Maryland (Jul 1972).

3. Hawkins, S. and T. Sarchin, *"The Small Waterplane-Area Twin Hull (SWATH) Program – A Status Report,"* AIAA/SNAME Advanced Marine Vehicles Meeting, San Diego, California (Jul 1974).

4. Motora, S. and T. Koyama, *"Wave-Excitationless Ship Forms,"* 6th Naval Hydrodynamic Symposium, Washington, D.C.; proceedings published by the Office of Naval Research, pp. 383-411 (1966).

5. Salvesen, N. et al., *"Ship Motion and Sea Loads,"* Trans. SNAME, Vol. 78, pp. 250-287 (1970).

6. Pien, P.C. and C.M. Lee, *"Motion and Resistance of a Low-Waterplane Catamaran,"* 9th Naval Hydrodynamic Symposium, Paris, France; proceedings published by the Office of Naval Research, pp. 463-545 (1972).

7. McCreight, K.K. and C.M. Lee, *"Manual for Mono-Hull or Twin-Hull Ship Motion Prediction Computer Program,"* DTNSRDC Report SPD-686-02 (1976).

8. Cummins, W.E., *"The Impulse Response Function and Ship Motions,"* Schiffstechnik, Vol. 9, pp. 101-109 (1962); reprinted as DTMB Report 1661.

9. St. Denis, M. and W.J. Pierson, *"On the Motion of Ships in Confused Seas,"* Trans. SNAME, Vol. 61, pp. 280-357 (1953).

10. Pierson, W.J. and L. Moskowitz, *"A Proposed Spectral Form for Fully Developed Wind Seas, Based on the Similarity Theory of S.A. Kitaigarodskii,"* J. Geophys. Res., Vol. 69, No. 24, pp. 5181-5190 (1964).

11. Bretschneider, C.L., *"Wave Variability and Wave Spectra for Wind-Generated Gravity Waves,"* Beach Erosion Board, U.S. Army Corps of Engineers TM 118 (1959).

12. Hadler, J.B. et al., *"Ocean Catamaran Seakeeping Design, Based on the Experiences of USNS HAYES,"* Trans. SNAME, Vol. 82, pp. 126-161 (1974).

13. Miles, M., *"Wave Spectra Estimated from a Stratified Sample of 323 North Atlantic Wave Records,"* National Research Council, Division of Mechanical Engineering Report LTR-SH-118 (1971).

14. Hogben, N. and F.E. Lamb, *"Ocean Wave Statistics,"* H.M. Stationery Office, London (1967).

15. Pierson, W.J., *"The Theory and Applications of Ocean Wave Measuring Systems at and below the Sea Surfaces, on the Land from Aircraft, and from Space Craft,"* NASA Contractors Report NASA CR-2646 (1976).

16. Ochi, M.K., *"On Prediction of Extreme Values,"* J. Ship Res., Vol. 17, No. 1, pp. 29-37 (1973).

17. Lee, C.M. et. al., *"Added Mass and Damping Coefficients of Heaving Twin Cylinders in a Free Surface,"* NSRDC Report 3695 (1971).

18. John, F., *"On the Motion of Floating Bodies: II. Simple Harmonic Motions,"* Commun. Pure Appl. Math., Vol. 13, pp. 45-101 (1950).

19. Ohmatsu, S., *"On the Irregular Frequencies in the Theory of Oscillating Bodies in a Free Surface,"* Ship Research Institute of Japan Report 48 (1975).

20. Ogilvie, T.F. and E.O. Tuck, *"Rational Strip Theory of Ship Motions; Part I,"* University of Michigan, College of Engineering Report 013 (1969).

21. Faltinsen, O., *"Numerical Investigation of the Ogilvie-Tuck Formulas for Added Mass and Damping Coefficients,"* J. Ship Res., Vol. 18, pp. 73-84 (1974).

22. Kim, Ki-Han, *"Determination of Damping Coefficients of SWATH Catamaran Using Thin Ship Theory,"* Mass. Inst. Technol., Dept. Ocean Eng. Report 75-4 (1975).

23. Frank, W., *"Oscillation of Cylinders in or below the Free Surface of Deep Fluids,"* NSRDC Report 2375 (1967).

24. Thwaites, B. (Editor), *"Incompressible Aerodynamics,"* Oxford University Press, pp. 405-421 (1960).

25. Allen, H.J. and E.E. Perkins, *"A Study of Effects of Viscousity on Flow over Slender Inclined Bodies of Revolution,"* NACA Report 1048 (1951).

26. Lee, C.M. and M. Martin, *"Determination of Size of Stabilizing Fins for Small Waterplane Area, Twin-Hull Ships,"* DTNSRDC Report 4495 (1974).

27. Kallio, J.A. and J.J. Ricci, *"Seaworthiness Characteristics of a Small Waterplane Area Twin-Hull (SWATH IV) Part II,"* DTNSRDC Report SPD 620-02 (1976).

28. Pitts, W.C., J.N. Nielsen, and G.E. Kaattari, *"Lift and Center of Pressure of Wing-Body-Tail Combinations at Subsonic, Transonic, and Supersonic Speeds,"* NACA Report 1307 (1959).

29. Spreiter, J.R., *"The Aerodynamic Forces on Slender Plane- and Cruciform-Wing and Body Combinations,"* NACA Report 962 (1950).

30. Morikawa, G., *"Supersonic Wing-Body Lift,"* J. Aeron. Sci., Vol. 18, No. 4, pp. 217-228 (1951).

31. Whicker, L.F. and L.F. Fehlner, *"Free-Stream Characteristics of a Family of Low-Aspect-Ratio, All-Movable Control Surfaces for Application to Ship Design,"* David Taylor Model Basin Report 933 (1958).

32. Ashley, H. and W.P. Rodden, *"Wing-Body Aerodynamic Interaction,"* Ann. Rev. Fluid Mech., Vol. 4 (1972).

33. Lawrence, H.R. and E.H. Gerber, *"The Aerodynamic Forces on Low Aspect Ratio Wings Oscillating in an Incompressible Flow,"* J. Aeron. Sci., Vol. 19, No. 11, pp. 769-781 (1952).

34. Lee, C.M. and L.O. Murray, *"Experimental Investigation of Hydrodynamic Coefficients of a Small Waterplane Area, Twin-Hull Model (SWATH 6A),"* DTNSRDC Report (in preparation).

35. Timman, R. and J.N. Newman, *"The Coupled Damping Coefficients of a Symmetric Ship,"* J. Ship Res., Vol. 5, No. 4, pp. 1-7 (1962).

36. Haskind, M.D., *"The Exciting Forces and Wetting of Ships in Waves,"* Isvestia Akademic Nauk SSSR, Otdelenie Teknicheskikh Nauk, No. 7 (1957); David Taylor Model Basin Translation 307 (1962).

37. Newman, J.N., *"The Exciting Forces on a Moving Body in Waves,"* J. Ship Res., Vol. 9, No. 3, pp. 190-199 (1965).

38. Newman, J.N., *"The Force and Moment on a Slender Body of Revolution Moving near a Wall,"* David Taylor Model Basin Report 2127 (1965).

INITIAL DISTRIBUTION

Copies	
1	WES
1	CHONR/438 Cooper
2	NRL 1 Code 2027 1 Code 2627
1	ONR/Boston
1	ONR/Chicago
1	ONR/Pasadena
1	ONR/San Francisco
1	NORDA
1	NOO/Lib (Naval Oceanographic Office)
5	USNA 1 Tech Lib 1 Nav Sys Eng Dept 1 Jewell 1 Bhattacheryya 1 Calisal
4	NAVPGSCOL 1 Library 1 T. Sarpkaya 1 Thaler 1 Garrison
1	NADC
1	NELC/Lib
3	NUC, San Diego 1 Library 1 Lang 1 Higdon
1	NCSL/712 D. Humphreys
1	NCEL/Code 131
1	NSWC, Dahlgren
1	NUSC/Lib
7	NAVSEA 1 SEA 03221 1 SEA 032 1 SEA 03512/Peirce 1 SEA 037 3 SEA 09G32
1	NAVFAC/Code 032C

Copies	
1	NAVSHIPYD PTSMH/Lib
1	NAVSHIPYD PHILA/Lib
1	NAVSHIPYD NORVA/Lib
1	NAVSHIPYD CHASN/Lib
1	NAVSHIPYD LBEACH/Lib
2	NAVSHIPYD MARE 1 Library 1 Code 250
1	NAVSHIPYD BREM/Lib
1	NAVSHIPYD PEARL/Code 202.32
10	NAVSEC 1 SEC 6034B 1 SEC 6110.01 1 SEC 6114 1 SEC 6114P 1 SEC 6120 1 SEC 6136 1 SEC 6136/Covich 1 SEC 6114D 1 SEC 6120E 1 SEC 6136/Goldstein
1	NAVSEC, NORVA/6660.03 Blount
12	DDC
1	AFOSR/NAM
1	AFFOL/FYS, J. Olsen
1	NSF/Eng Lib
1	LC/Sci & Tech
1	DOT/Lib TAD-491.1
2	MMA 1 Capt McClean 1 Library
1	NBS/Klebanoff
1	MARAD/Lib
5	U. of Cal/Dept Naval Arch, Berkely 1 Eng Library 1 Webster 1 Paulling 1 Wehausen

Copies	
2	U. of Cal, San Diego
	1 A.T. Ellis
	1 Scripps Inst Lib
2	CIT
	1 Aero Lib
	1 T.Y. Wu
1	City College, Wave Hill/Pierson
1	Catholic U. of Amer/Civil & Mech Eng
1	Colorado State U./Eng Res Cen
1	U. of Connecticut/Scottron
1	Cornell U./Sears
2	Florida Atlantic U.
	1 Tech Lib
	1 S. Dunne
1	U. of Hawaii/St. Denis
1	U. of Illinois/J. Robertson
3	U. of Iowa
	1 Library
	1 Landweber
	1 Kennedy
1	John Hopkins U./Phillips
1	Kansas State U./Nesmith
1	U. of Kansas/Civil Eng Lib
1	Lehigh U./Fritz Eng Lab Lib
6	MIT
	1 Library
	1 Yeung
	1 Mandel
	1 Abkowitz
	1 Newman
	1 Oakley
4	U. of Mich/NAME
	1 Library
	1 Ogilivie
	1 Beck
	1 Daoud
2	U. of Notre Dame
	1 Eng Lib
	1 Strandhagen
2	New York U./Courant Inst
	1 A. Peters
	1 J. Stoker

Copies	
1	Penn State/Arl/B. Parkin
1	Princeton U./Mellor
6	SIT
	1 Library
	1 Breslin
	1 Savitsky
	1 Dalzell
	1 Fridsma
	1 Kim
1	U. of Texas/Arl Lib
1	Utah State U./Jeppson
2	Southwest Res Inst
	1 Applied Mech Rev
	1 Abramson
2	Stanford U.
	1 Eng Lib
	1 R. Street
1	Stanford Res Inst/Lib
2	U. of Washington
	1 Eng Lib
	1 Mech Eng/Adee
3	Webb Inst
	1 Library
	1 Lewis
	1 Ward
1	Woods Hole/Ocean Eng
1	Worchester Pl/Tech Lib
1	SNAME/Tech Lib
1	Bethlehem Steel/Sparrows Point
1	Bethlehem Steel/New York/Lib
1	Bolt, Beranek & Newman/Lib
1	Exxon, NY/Design Div, Tank Dept
1	General Dynamics, EB/Boatwright
1	Gibbs & Cox/Tech Info
5	Hydronautics
	1 Library
	1 E. Miller
	1 A. Goodman
	1 V. Johnson
	1 C.C. Hsu

Copies	
2	Lockheed, Sunnyvale
	1 Potash
	1 Chung
2	McDonnell Douglas, Long Beach
	1 J. Hess
	1 T. Cebeci
1	Newport News Shipbuilding/Lib
1	Nielsen Eng & Res
1	Oceanics
1	Rockwell International/B. Ujihara
1	Sperry Rand/Tech Lib
1	Sun Shipbuilding/Chief Naval Arch
2	American Bureau of Shipping
	1 Lib
	1 Cheng
1	Robert Taggart
1	Tracor
1	Maritime Research Information Service

CENTER DISTRIBUTION

Copies	Code	
1	1102	G.D. Elmer
1	117	R.M. Stevens
1	1170	G.R. Lamb
1	1170	S. Hawkins
1	1170	J.J. Luckard
1	1500	W.E. Cummins
1	1504	V.J. Monacella
1	1506	M.K. Ochi
1	1507	D. Cieslowski
1	1512	J.B. Hadler
1	1520	R. Wermter
1	1521	P. Pien
1	1524	Y.T. Shen
1	1524	W.C. Lin
1	1524	A.M. Reed
1	1532	G. Dobay
1	1532	M. Wilson
1	1540	W.B. Morgan
1	1552	J. McCarthy
1	1552	N. Salvesen
1	1542	B. Yim
1	1560	G. Hagen
1	1560	N. Hubble
10	1561	C.M. Lee
1	1562	M. Martin
1	1564	J. Feldman
1	1564	R.M. Curphey
1	1568	G. Cox
1	1568	E.A. Baitis
1	1568	W.R. McCreight
1	1572	M.D. Ochi
1	1572	E. Zarnick
1	1572	K.K. McCreight
1	1572	J.A. Fein
1	1576	W.E. Smith
30	5214.1	Reports Distribution
1	5221	Unclassified Library (C)
1	5221	Unclassified Library (A)